



Libraries and Learning Services

# University of Auckland Research Repository, ResearchSpace

## Copyright Statement

The digital copy of this thesis is protected by the Copyright Act 1994 (New Zealand).

This thesis may be consulted by you, provided you comply with the provisions of the Act and the following conditions of use:

- Any use you make of these documents or images must be for research or private study purposes only, and you may not make them available to any other person.
- Authors control the copyright of their thesis. You will recognize the author's right to be identified as the author of this thesis, and due acknowledgement will be made to the author where appropriate.
- You will obtain the author's permission before publishing any material from their thesis.

## General copyright and disclaimer

In addition to the above conditions, authors give their consent for the digital copy of their work to be used subject to the conditions specified on the [Library Thesis Consent Form](#) and [Deposit Licence](#).

# Transport of Bacteria in Column for *in situ* Bioremediation Application

---

*Effect of dissolved surfactant and microbubble on bacterial mobility  
in sand*

**Wei Tao**

*A thesis submitted in fulfillment of the requirements for the degree of Doctor of Philosophy in  
Engineering, The University of Auckland, 2018*

## Abstract

The absence of bacteria capable of degrading pollutants and the shortage of oxygen in contaminated soil have been identified as key factors that can limit the efficiency of *in situ* bioremediation. Inoculating contaminated soils with exogenous bacteria and oxygen purging are common approaches for stimulating *in situ* bioremediation. The use of surfactant and microbubble offers a way of addressing these limitations by promoting bacteria transport while at the same time providing oxygen. This study investigates the effect of surfactant solution and surfactant microbubble on bacteria transport in sand columns with the aim of understanding the factors and mechanisms that affect bacteria transport in soil. This study also introduces an innovative measurement probe, the optrode, for *in situ* monitoring of bacteria distribution. Rhamnolipid and tergitol were used as surfactant in this study, and *Pseudomonas putida* (a hydrophilic bacterium) and *Rhodococcus erythropolis* (a hydrophobic bacterium) were the chosen bacteria.

The different types of surfactant altered bacterial hydrophobicity to differing extents but had an equivalent effect on the hydrophobicity of sand particles. In the presence of surfactant solution, a higher proportion of hydrophilic *P. putida* (76.7%) was eluted out of the column compared to the hydrophobic *R. erythropolis* (60.3%). Both rhamnolipid and tergitol enhanced the transport of both bacterial strains. However, the larger enhancement in bacteria transport observed for rhamnolipid was attributed to increased Lifshitz-van der Waals and acid-base (LW-AB) interaction energies between bacteria and sand particles. A continuous supply of microbubbles was found able to transport bacteria into the soil using a smaller amount of surfactant. In comparison to a propeller mixer, microbubbles generated by a flat spinning disc mixer were more stable and could elute a greater proportion of bacteria. Microbubbles of rhamnolipid eluted a greater percentage of the injected bacteria compared to tergitol, because rhamnolipid microbubbles showed more stability and higher affinity for bacteria. Hydrophilic *P. putida* was more likely to be transported with microbubble than hydrophobic *R. erythropolis* due to the favourable adhesion of hydrophobic *R. erythropolis* to sand particles. Bacterial transport increased considerably in porous media with higher porosity. Bacteria transport in

columns was monitored using both *ex situ* measurement with a microplate photometer and *in situ* measurement with the optrode. The optrode measurement demonstrated that sample collection, which is necessary for measurement with conventional *ex situ* approaches, could affect the local bacterial transport in sand columns. In columns with *ex situ* sampling, optrode measurements differed from the *ex situ* concentrations, with the breakthrough curves for optrode showing smaller bacterial concentrations and a larger lag than those obtained via *ex situ* measurements. However, when the optrode and *ex situ* measurements were conducted in independent columns, their concentrations and breakthrough curves were almost identical. The transport parameters obtained by fitting the breakthrough curves showed that estimates from the optrode data were more consistent with less error.

This study provides very useful information on bacteria transport with surfactant solutions and microbubbles in sand columns simulating soil environment. It has demonstrated that optimizing parameters including surfactant type and form, and bacteria strain can contribute to enhanced bacteria transport when surfactant solution and microbubble are used as the bacteria carrier during soil bioremediation. This study also validates the operation of an innovative technique, the optrode, for real time monitoring of bacteria transport without the need to take bacterial samples.

## Co-Authorship Form

This form is to accompany the submission of any PhD that contains published or unpublished co-authored work. **Please include one copy of this form for each co-authored work.** Completed forms should be included in all copies of your thesis submitted for examination and library deposit (including digital deposit), following your thesis Acknowledgements. Co-authored works may be included in a thesis if the candidate has written all or the majority of the text and had their contribution confirmed by all co-authors as not less than 65%.

Please indicate the chapter/section/pages of this thesis that are extracted from a co-authored work and give the title and publication details or details of submission of the co-authored work.

Chapter 3 is from this paper

Effect of Rhamnolipid and Tergitol Surfactant on the Transport of Rhodococcus erythropolis and Pseudomonas putida in Saturated Sand Column

Nature of contribution by PhD candidate	undertaking experiment, analysing data and writing the draft of text
Extent of contribution by PhD candidate (%)	80%

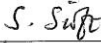
### CO-AUTHORS

Name	Nature of Contribution
Naresh Singhal	Supervisor and reviewer
Simon Swift	Supervisor and reviewer
Yantao Song	Provide advice on experimental design and reviewer

### Certification by Co-Authors

The undersigned hereby certify that:

- ❖ the above statement correctly reflects the nature and extent of the PhD candidate's contribution to this work, and the nature of the contribution of each of the co-authors; and
- ❖ that the candidate wrote all or the majority of the text.

Name	Signature	Date
Naresh Singhal		17 July 2017
Simon Swift		14 July 2017
Yantao Song		12/7/2017

## Co-Authorship Form

This form is to accompany the submission of any PhD that contains published or unpublished co-authored work. **Please include one copy of this form for each co-authored work.** Completed forms should be included in all copies of your thesis submitted for examination and library deposit (including digital deposit), following your thesis Acknowledgements. Co-authored works may be included in a thesis if the candidate has written all or the majority of the text and had their contribution confirmed by all co-authors as not less than 65%.

Please indicate the chapter/section/pages of this thesis that are extracted from a co-authored work and give the title and publication details or details of submission of the co-authored work.

Chapter 4 is from the paper

Upward Transport of *Rhodococcus erythropolis* and *Pseudomonas putida* with Continuously Injected Microbubble in Sand Column: the Role of Microbubble Generation Method, Surfactant Type, Bacterial Hydrophobicity and the Porosity of Sand Column

Nature of contribution by PhD candidate	undertaking experiment, analysing data and writing the draft of the text
---	--

Extent of contribution by PhD candidate (%)	80%
---	-----

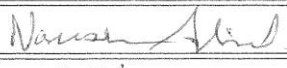
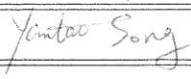
### CO-AUTHORS

Name	Nature of Contribution
Naresh Singhal	Supervisor and reviewer
Simon Swift	Supervisor and reviewer
Yantao Song	Provide advice on experimental design and reviewer

### Certification by Co-Authors

The undersigned hereby certify that:

- ❖ the above statement correctly reflects the nature and extent of the PhD candidate's contribution to this work, and the nature of the contribution of each of the co-authors; and
- ❖ that the candidate wrote all or the majority of the text.

Name	Signature	Date
Naresh Singhal		16 July 2017
Simon Swift		14 July 2017
Yantao Song		12/7/17

## Co-Authorship Form

This form is to accompany the submission of any PhD that contains published or unpublished co-authored work. **Please include one copy of this form for each co-authored work.** Completed forms should be included in all copies of your thesis submitted for examination and library deposit (including digital deposit), following your thesis Acknowledgements. Co-authored works may be included in a thesis if the candidate has written all or the majority of the text and had their contribution confirmed by all co-authors as not less than 65%.

Please indicate the chapter/section/pages of this thesis that are extracted from a co-authored work and give the title and publication details or details of submission of the co-authored work.	
Chapter 5 is from the paper: Employing a Novel Optical Biosensor for in situ Monitoring of Bacteria Transport in Saturated Column in Varying Physicochemical Conditions	
Nature of contribution by PhD candidate	undertaking experiment, analysing data and writing the draft of text
Extent of contribution by PhD candidate (%)	80%

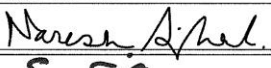
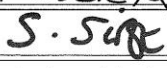
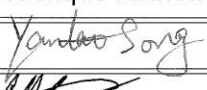
### CO-AUTHORS

Name	Nature of Contribution
Naresh Singhal	Supervisor and reviewer
Simon Swift	Supervisor and reviewer
Frédérique Vanholsbeeck	Supervisor and reviewer
Yantao Song	Provide advice on experiment design and reviewer
Cushla McGoverin	Provide technical advice on the optrode and protocol of optrode intensity extraction and reviewer

### Certification by Co-Authors

The undersigned hereby certify that:

- ❖ the above statement correctly reflects the nature and extent of the PhD candidate's contribution to this work, and the nature of the contribution of each of the co-authors; and
- ❖ that the candidate wrote all or the majority of the text.

Name	Signature	Date
Naresh Singhal		12 July 2017
Simon Swift		11 JUL 2017
Frédérique Vanholsbeeck	Frédérique Vanholsbeeck <small>Digitally signed by Frédérique Vanholsbeeck DN: cn=Frédérique Vanholsbeeck, o=The University of Auckland, ou=The Physics Department, email=f.vanholsbeeck@auckland.ac.nz, c=NZ Date: 2017.07.10 01:23:29 +1200</small>	
Yantao Song		12/07/2017
Cushla McGoverin		11/07/2017

## **Acknowledgments**

I am very grateful to the China Scholarship Council (CSC) for providing the financial support for this PhD study. I would also like to express my sincere appreciation and thanks to my supervisor, A/P. Naresh Singhal for his guidance, supervision, and encouragement throughout my entire doctoral programme. I would also like to sincerely thank my co-supervisor A/P Simon Swift for his technical guidance and important and insightful advice on this project. I am fortunate to have them as supervisors.

I would like to thank my friend and technical officer Dr. Yantao Song. She gave me a lot of help in the process of experimental design and method, and also provided me with professional advice. Her constant involvement and encouragement were extremely helpful for my PhD project. Furthermore, I would also like to thank my lecturers, Frederique Vanholsbeeck and Dr. Cushla McGoverin, for their technical help and knowledge on the optrode and data analysis. My thanks also go to laboratory officers, Deborah Prendergast and Mike Goldthorpe, for offering laboratory resources for my project during the closure of PC1.

I would like to thank all my friends for their support, understanding and companionship. Especially I would like to thank Kun Wang, Febelyn Reguyal, Mali Ding and Jishan Liu. They made my graduate studies enjoyable and gave me continuous support when I went through hard times. I am also very grateful to the Environmental Engineering and Microbiology and Infectious Disease research group members for their support and collaboration in reshaping my PhD project.

Finally and most importantly, I would like to thank my parents and sister for their never-ending support and understanding.

# Table of Contents

Abstract.....	i
Acknowledgments.....	vi
Table of Contents.....	vii
List of Figures.....	x
List of Tables.....	xii
List of Acronyms.....	iii
Chapter 1. General Introduction.....	1
1.1. Key Factors Influencing the Efficiency of in situ Bioremediation.....	1
1.2. Transport of Bacteria.....	3
1.3. Bacteria Transport with Microbubble.....	4
1.4. Monitoring Bacteria Transport in Soil.....	5
1.5. Research Hypotheses.....	5
1.6. Research Objectives.....	6
1.7. Thesis Outline.....	6
Chapter 2. Literature Review.....	9
2.1. Introduction.....	9
2.2. Bacteria Transport in Soil.....	9
2.2.1. Bacterial Properties.....	10
2.2.2. Surfactant.....	12
2.3. Microbubble.....	17
2.3.1. General Properties.....	17
2.3.2. Microbubble Applications in Bioremediation.....	18
2.3.3. Parameters that Affect the Efficiency of Microbubble as Bacteria Carrier.....	21
2.4. Approaches for Monitoring Bacterial Distribution.....	22
2.4.1. Traditional Approaches for Environmental Monitoring of Bacterial Activates.....	23
2.4.2. In situ Approaches for Environmental Monitoring of Bacterial Activates.....	23
2.4.3. The Optrode System.....	25
2.5. Approaches for Bacteria Transport in Porous Media.....	26
2.5.1. The Extended DVLO Approach.....	26
2.5.2. The Thermodynamic Approach.....	27
2.6. Model Simulation for Bacteria Transport.....	29
Chapter 3. Effect of Rhamnolipid and Tergitol Surfactant on the Transport of <i>Rhodococcus erythropolis</i> and <i>Pseudomonas putida</i> in Saturated Sand Columns.....	32
Abstract.....	33
3.1. Introduction.....	35
3.2. Materials and Method.....	37
3.2.1. Materials.....	37
3.2.2. Interaction Energy Calculation and Surface Tension Parameters Measurement.....	39
3.2.3. Column Set-up and Bacteria Transport.....	40
3.2.4. Mathematical Modeling.....	41
3.3. Results and Discussions.....	42
3.3.1. The Modification of Surfactant on the Surface Tension Parameters of Bacteria and Sand Particles.....	42
3.3.2. Comparison of the Transport of <i>R. erythropolis</i> and <i>P. putida</i> KT2442 in the Absence of Surfactant Solution.....	43
3.3.3. The Effect of surfactant Solution on the Transport of <i>R. erythropolis</i> and <i>P. putida</i> KT2442 Cells.....	45
3.3.4. Discussions.....	49
3.4. Conclusion.....	53
Acknowledgments.....	53
Chapter 4. Upward Transport of <i>Rhodococcus erythropolis</i> and <i>Pseudomonas putida</i> with Continuously Injected Microbubble in Sand Column: the Role of Microbubble Generation Method, Surfactant Type, Bacterial	

Hydrophobicity and the Porosity of Sand Column.....	54
Abstract.....	55
4.1. Introduction.....	57
4.2. Materials and Method.....	59
4.2.1. Surfactants Selection.....	59
4.2.2. Microbubble Generation and Tests.....	60
4.2.3. Bacterial Strains and Incubation Condition.....	61
4.2.4. Column Set-up.....	62
4.2.5. Bacteria Transport in Columns.....	63
4.2.6. Calculation and Visualization of Microbubble-bacteria Interaction.....	64
4.3. Results and Discussions.....	66
4.3.1. Microbubble Stability and Bacterial Drainage from Microbubble.....	66
4.3.2. Comparison of Bacteria Transport in Surfactant Microbubble and Surfactant Solution.....	70
4.3.3. The Effect of Microbubble Generating Method, Surfactant Type, Bacterial Hydrophobicity and Sand Media Porosity on Bacteria Transport with Continuously Injected Microbubble.....	71
4.3.4. Discussions.....	78
4.4. Conclusion.....	81
Acknowledgments.....	82
Chapter 5. Employing a Novel Optical Biosensor for in situ Monitoring of Bacteria Transport in Saturated Column in Varying Physicochemical Conditions.....	83
Abstract.....	84
5.1. Introduction.....	86
5.2. Materials and Methods.....	88
5.2.1. Material .....	88
5.2.2. Bacterial Preparation.....	88
5.2.3. The Optrode Detection System.....	90
5.2.4. Calibration of the Optrode Intensity to Bacterial Concentration.....	91
5.2.5. Column Preparation and Column Experiments.....	92
5.2.6. Interaction Energy Calculation and Surface Tension Parameters Measurement.....	93
5.2.7. Data Analysis.....	94
5.3. Results and Discussions.....	96
5.3.1. In situ versus ex situ Measurements.....	96
5.3.2. Optrode Monitored Hydrophilic and Hydrophobic Bacteria Transport under Varying Physicochemical Conditions.....	97
5.3.3. Discussions.....	102
5.4. Conclusion.....	104
Acknowledgments.....	105
Chapter 6. Conclusions, Implications, and Recommendations for Future Research.....	106
6.1. Conclusions and Implications for Bioremediation.....	106
6.2. Recommendations for Future Research.....	108
Appendix.....	110
Appendix Information for Chapter 3.....	114
Appendix Information for Chapter 5.....	117
Bibliography.....	123

## List of Figures

Figure 2-1 Schematic diagram of contact angle .....	11
Figure 2-2 General structure of surfactant.....	13
Figure 2-3 Schematic diagram of micelles presents in water and on water/solid interfaces .....	13
Figure 2-4 Microbubble structure .....	17
Figure 2-5 Schematic illustration of the use of microbubble to remediate contaminated soil .....	19
Figure 2-6 Basic scheme of a biosensor .....	24
Figure 2-7 The optrode and computer setup .....	26
Figure 2-8 Relationship between contact angle and the different interfacial tensions.....	28
Figure 3-1 Column set up for the up flow pumping experiments .....	41
Figure 3-2 The aggregation of bacteria in water and rhamnolipid solution. ....	45
Figure 3-3 Comparison of the observed and fitted breakthrough curves of <i>R. erythropolis</i> in water and surfactant solution.....	48
Figure 3-4 Comparison of the observed and fitted breakthrough curves of <i>P. putida</i> KT2442 in water and surfactant solution.....	48
Figure 3-5 The changes in $\Delta G_{adh}$ between bacteria and sand particles with the addition of rhamnolipid and tergitol.....	51
Figure 3-6 The correlation of the percentage of bacteria that was eluted out of columns and the averaged first order decay to $\Delta G_{adh}$ .....	52
Figure 3-7 The relation between bacterial surface tension parameters with the interaction between bacteria and sand particles. ....	53
Figure 4-1 Column set up for up flow pumping experiments .....	66
Figure 4-2 Microbubble structure,(Sebba, 1987) .....	66
Figure 4-3 Effect of the generation method and bacteria on the half-time of microbubble.....	68
Figure 4-4 The distribution of <i>R. erythropolis</i> and <i>P. putida</i> KT2442 in rhamnolipid and tergitol microbubble over a range of time between 0 to 20 minutes.....	69
Figure 4-5 Comparison of BTCs of <i>P. putida</i> KT 2442 transport with surfactant microbubble (empty symbols) and surfactant solution (solid symbols).....	71
Table 4-1 The percentage of bacteria that was eluted out of the column, .....	74
Figure 4-6 Comparison of the observed breakthrough curves of <i>R. erythropolis</i> and <i>P. putida</i> KT2442 that were transport with rhamnolipid and tergitol microbubbles that were generated by the propeller mixer.....	75
Figure 4-7 Comparison of the observed breakthrough curves of <i>R. erythropolis</i> and <i>P. putida</i> KT2442 that were transport with rhamnolipid and tergitol microbubbles that were generated by the flat spinning disc mixer.....	76
Figure 4-8 Comparison of high and low permeable columns on the transport of <i>P. putida</i> with rhamnolipid microbubble. ....	77
Table 4-2 The dispersion coefficient in BTCs of bacteria transport with microbubble.....	77
Figure 4-9 Fluorescence image of bacteria in the presence of rhamnolipid microbubble.A: <i>R. e ythropolis</i> ; B: <i>P. putida</i> KT2442.....	81
Figure 5-1 Schematic diagram of optical fibre detection system for column study .....	91
Figure 5-2 Optical fibre probe .....	92
Figure 5-3 Comparison of the observed and fitted breakthrough curves of <i>P. putida</i> KT2442 in water that were obtained by <i>ex situ</i> measurements (A), the optrode with sampling for <i>ex situ</i> measurements (B) and the optrode without sampling for <i>ex situ</i> measurements (C).....	99

Figure 5-4 Comparison of the observed and fitted breakthrough curves of *P. putida* KT2442 in rhamnolipid that were obtained by *ex situ* measurements (A), the optrode with sampling for *ex situ* measurements (B) and the optrode without sampling for *ex situ* measurements (C). .....99

Figure 5-5 Comparison of the observed and fitted breakthrough curves of *R. erythropolis*-pTEC23 td Tomato in water that were obtained by *ex situ* measurements (A), the optrode with sampling for *ex situ* measurements (B) and the optrode without sampling for *ex situ* measurements (C). .....100

Figure 5-6 Comparison of the observed and fitted breakthrough curves of *R. erythropolis*-pTEC23 td Tomato in rhamnolipid that were obtained by *ex situ* measurements (A), the optrode with sampling for *ex situ* measurements (B) and the optrode without sampling for *ex situ* measurements (C). .....100

Figure 5-7 The value of  $\Delta G_{adh}$  between bacteria and sand particles with the addition of rhamnolipid .....104

## List of Tables

Table 2-1 The properties of rhamnolipid biosurfactant and tergitol .....	15
Table 2-2 Impact of surfactant on soil.....	16
Table 2-3 The list of probe liquids can be used as diagnostic liquid .....	28
Table 3-1 Surface Tension Parameters $\gamma^{LW}$ (LW apolar component), $\gamma^-$ (electron donor), $\gamma^+$ (electron acceptor) and free energy of aggregation ( $\Delta G$ ) ( $\text{mJ}/\text{m}^2$ ) .....	43
Table 3-2 Comparison of the transport parameters that was fitted from BTCs of <i>R. erythropolis</i> and <i>P. putida</i> KT2442 by the equilibrium equation of CXTFIT in STANMOD. ....	49
Table 4-1 The percentage of bacteria that was eluted out of the column .....	74
Table 4-2 The dispersion coefficient in BTCs of bacteria transport with microbubble, $\text{cm}^2/\text{min}$ .....	77
Table 4-3 The adhesion energy of bacteria to microbubble film and sand particles.....	81
Table 5-1 Summary the properties of <i>P. putida</i> KT2442 and <i>R. erythropolis</i> .....	93
Table 5-2 Transport parameters in BTCs of <i>P. putida</i> KT2442-GFP and <i>R. erythropolis</i> -pTEC23 td Tomato that were monitored by <i>ex situ</i> measurements and the optrode .....	101

## List of Acronyms

BTC	Breakthrough curve
CDE	Convection-dispersion equation
CGA	Colloidal gas aphanes
LW	Lifshitz-van der Waals
AB	Acid-Base
CMC	Critical micelle concentration
GMO	Genetically modified microorganisms
GFP	Green fluorescence protein
PTEC23 td Tomato	Red fluorescent protein Tomato
SNR	Signal-to-noise ratio
TS	Tryptic soy

## **Chapter 1. General Introduction**

This chapter briefly reviews the key factors that can affect the efficiency and application of *in situ* bioremediation, and highlights the importance of introducing exogenous bacteria and oxygen. Factors that influence bacteria transport are discussed and, in particular, the effect of surfactant on bacterial hydrophobicity to emphasize the importance of employing different types of surfactant solution for promoting transport of different bacteria. Further, this chapter also outlines the parameters affecting the efficiency of bacteria transport and identifies knowledge gaps in relation to the use of continuously injected microbubble suspension as a bacterial carrier. Techniques for monitoring bacteria distribution in the soil are reviewed, with emphasis on the importance of *in situ* monitoring of bacteria transport. Finally, the hypothesis, objectives, and outline for this thesis are presented.

### **1.1. Key Factors Influencing the Efficiency of *in situ* Bioremediation**

Bioremediation, which is the degradation of hazardous contaminants to less toxic by-products (Mueller et al., 1996), has emerged as an alternative technology for removing pollutants in the soil environment. Soil bioremediation can be *ex situ* and *in situ* (Stringfellow and Alvarez-Cohen, 1999). *Ex situ* bioremediation involves applying a treatment technique to the contaminated soil that has been removed from the contaminated site (Stringfellow and Alvarez-Cohen, 1999). *In situ* bioremediation is designed to treat the contaminated soil and groundwater in place, with minimum disturbance to the contaminated site (Melnik et al., 2015; Stringfellow and Alvarez-Cohen, 1999; Wang et al., 2012). Compared with *ex situ* bioremediation, *in situ* bioremediation is a relatively cost-effective and environmentally friendly treatment (Mohan et al., 2006). However, *in situ* bioremediation requires a relatively long treatment time, and the following factors can negatively affect the efficiency of the process: the low bioavailability of contaminants (Abalos et al., 2004; Scullion, 2006; Semple et al., 2007; Spasojević et al., 2015); the absence of bacteria able to degrade pollutants in contaminated soil (Romantschuk et al., 2000; Scullion, 2006; Van Hamme, 2004); oxygen supply (Choi et al., 2009; Park et al., 2009; Pinyakong et al., 2000; M. Ripley et al., 2002); the properties of the sediments (Kwok and Loh, 2003;

Reddy and Saichek, 2003; Scullion, 2006); and a lack of nutrients. Among these factors, the low bioavailability of pollutants, the absence of certain bacteria, and the oxygen-deficient soil have been identified as key influences on the efficiency of *in situ* bioremediation.

Bioavailability defines whether a compound “is freely available to cross an organism’s (cellular) membrane from the medium the organism inhabits at a given point of time” (Semple et al., 2004; Semple et al., 2007). The use of surfactants to enhance bioavailability of pollutants and stimulate the degradation of pollutants has gain increasing attention (Johnsen et al., 2005; Tiehm, 1994; Volkering et al., 1995; Zhu et al., 2013). However, merely increasing the bioavailability of contaminants is not sufficient to enhance bioremediation and further could pose threat to groundwater if these pollutants are not degraded in the soil.

The presence of bacteria is another important factor that can affect the efficiency of *in situ* bioremediation. Indigenous bacteria are ubiquitous in the natural soil environment. For example, several PAHs-degrading bacteria species (e.g. *Pseudomonas aeruginosa*, *Pseudomonas fluorescens*, *Mycobacterium* spp., *Haemophilus* spp., *Rhodococcus* spp., and *Paenibacillus* spp.) have been identified from the PAHs contaminated soil (Aitken et al., 1998; Dean et al., 2001; Dennis and Zylstra, 2004; Lang et al., 2016; Leneva et al., 2009; Stringfellow and Aitken, 1995; Trzesicka-Mlynarz and Ward, 1995; Yang et al., 2014; Zhao et al., 2009). However, the small numbers and less active nature of the indigenous bacteria can result in a prolonged pollutant removal process, despite the highly diverse microbial communities are present in the soil environment. Introducing exogenous pollutant-degrading bacteria is an approach commonly used to expand the population of indigenous bacteria for *in situ* bioremediation. It is crucial that the exogenous bacteria can move or be transported to the contaminated soil to stimulate the degradation of pollutants. The low mobility of bacteria (Q. Li and Logan, 1999; Martin et al., 1996) in the soil under natural conditions is another challenge that needs to be addressed when introducing exogenous bacteria to contaminated sites. As a result, methods for promoting the transport of bacteria in contaminated soil are also explored.

## Chapter 1. General Introduction

The mere presence of bacteria with the capacity for bioremediation is not always sufficient for enhanced *in situ* bioremediation in oxygen-deficient contaminated sites. Although organic pollutants (such as PAHs) can be degraded under both aerobic and anaerobic condition (Philp et al., 2005; M. Ripley et al., 2002; Romantschuk et al., 2000; Vidali, 2001), aerobic biodegradation generally offers a more cost-effective and complete degradation route than anaerobic degradation (M. Ripley et al., 2002; Ripley et al., 2000; Romantschuk et al., 2000). However, the naturally available dissolved oxygen is quickly consumed when organic pollutants are released into the soil, and the degradation process slowed accordingly. Several technologies have been developed to address oxygen deficiency through supplying contaminated soil with extra air during *in situ* bioremediation, including air-sparging (Bouwer and Zehnder, 1993; USACE, 1997) and bioventing (Leeson and Hincee, 1996). However, the implementation of such methods is limited to certain situations (Vidali, 2001). Considering their small numbers and the less active nature of indigenous bacteria, combined with a lack of oxygen in contaminated sites, a cost-effective solution could be to provide both bacteria and oxygen to contaminated soil.

### **1.2. Transport of Bacteria**

The transport of bacteria is affected by many factors: fluid velocity (Hendry et al., 1999); the chemistry of solution, including pH and ionic strength (Bradford et al., 2002; Gang Chen et al., 2004; Gexin Chen and Walker, 2007; Gang Chen and Zhu, 2004; Xiao-Hong et al., 2010); the cell size of the bacteria and properties of the cell surface (Abu-Lail and Camesano, 2003; Dong et al., 2002; Gannon et al., 1991; Q. Li and Logan, 1999; Tsuneda et al., 2003); and the properties of the soil particles (H. Bai et al., 2016; Bradford et al., 2002) and surfactants (Abu-Lail and Camesano, 2003; H. Bai et al., 2016; Gexin Chen and Walker, 2007; Gang Chen and Zhu, 2004; Tsuneda et al., 2003; Zhong et al., 2016). Among these factors, the hydrophobicity of bacteria and soil/sediment particles, and the use of surfactants have drawn increasing attention in studies of bacteria transport in soil/sediment. Compared to hydrophobic strains of bacteria, hydrophilic bacteria are less likely to attach to soil particles and penetrate through the column more easily (Gang Chen and Zhu, 2004; Huysman and Verstraete, 1993). With regard to the

hydrophobicity of soil/sediment particles, bacteria show less affinity to a more hydrophilic surface (Gang Chen and Strevett, 2001; Zhong et al., 2016). The addition of surfactant solutions has been found to promote bacteria transport by modifying the interaction between bacteria and the soil (G. Bai et al., 1997; Gang Chen et al., 2004; Gang Chen and Zhu, 2004; Zhong et al., 2016), however, no data were observed in these studies regarding the comparison of the anionic surfactant and nonionic surfactant. In another study, different types of surfactant have different extent effect on modifying bacterial hydrophobicity. For example, anionic rhamnolipid surfactants made hydrophobic *R. erythropolis* 3586 less hydrophobic and hydrophilic *P. putida* 852 less hydrophilic (Feng et al., 2013a). Similar results were obtained when adding nonionic tergitol, but a different extent of modification was observed. Therefore, the effect of anionic vs. nonionic surfactant modification of the bacterial surface on microbial transport in saturated columns will be further investigated in this thesis.

### **1.3. Bacteria Transport with Microbubble**

Bubbles with diameters ranging from 10 to 100 micrometers are known as microbubbles (Sebba, 1985). Microbubbles have emerged as a potential vehicle of bacteria and oxygen for *in situ* bioremediation because their unique properties such as small size (Jauregi et al., 2000), large interfacial area (Jauregi and Varley, 1999; Parker, 1989), relatively high stability, and the fact that particles can adsorb to the microbubble surfaces (Wan and Wilson, 1994). In experiments using pulse injected microbubble to deliver bacteria to soil, it was demonstrated that microbubbles are a more efficient vehicle than surfactant solution because microbubble reduced the usage of surfactant solution (Andrew Jackson et al., 1998). However, the efficiency of microbubbles as particle carriers can be affected by parameters such as microbubble stability, the soil pore size, and hydrophobicity of the particles. For example, the effectiveness of microbubbles as particle carriers increases with the increasing of microbubble stability and pore size of soil (Desai and Banat, 1997; Ding et al., 2013; Shen et al., 2011; Wan et al., 2001). Hydrophobic bacteria are known to have a stronger affinity to gas-liquid interfaces (M. Ripley et al., 2002; Wan et al., 1994) than hydrophilic bacteria. In experiments using artificial sand column, microbubbles stimulated the aerobic biodegradation of organic pollutants (Kristen B Jenkins et al.,

1993; D. Michelsen et al., 1984; Catherine N Mulligan and Farzad Eftekhari, 2003; Park et al., 2009; Rothmel et al., 1998), and a greater degradation of pollutant was achieved at the bottom of the column where a higher concentration of gas was obtained (Park et al., 2009). It is thought continuous injection of microbubbles could potentially provide more oxygen to contaminated sites than pulse injection of microbubbles. Accordingly, the transport of bacteria using continuously supplied microbubble suspension will be investigated in this thesis.

#### **1.4. Monitoring Bacteria Transport in Soil**

*In situ* monitoring of bacteria transport offers a rapid, real-time and cost-effective method for quantifying the transport of microorganisms in the soil. The development of biosensor microorganisms and biosensor techniques has provided ways of achieving *in situ* monitoring of bacteria transport. Fluorescence optical systems which are based on biosensors have been introduced in environmental monitoring to identify particular pollutants, and to measure degradation of pollutants and growth activity of microorganisms (Dorn et al., 2005; Heitzer et al., 1994; Ivask et al., 2007; Yolcubal et al., 2000). However, there is little published data using fluorescence as an *in situ* monitoring method to study the transport of bacteria. A time-resolved fibre-optic spectroscopic probe system (the optrode) has been developed at the University of Auckland. The optrode has been used to identify and quantify fluorescently labeled microorganisms in batch experiments (Hewitt et al., 2012) and enumerate acridine orange-stained *Escherichia coli* in liquid media rapidly (Guo et al., 2017). In this thesis, the potential of using the optrode to measure bacteria transport in soil columns will be investigated.

#### **1.5. Research Hypotheses**

The following hypotheses are presented in this study:

1. Bacterial hydrophobicity is an important factor determining bacteria transport in soil.
2. Surfactant type can modify bacterial hydrophobicity to different extents and the transport of bacteria will be accordingly.

3. Continuously injected microbubble suspension can deliver bacteria to the soil.
4. Parameters such as the method of microbubble generation, surfactant types, bacteria hydrophobicity and the porosity of the column can influence the effectiveness of continuously supplied microbubble suspension as bacteria carrier.
5. The optrode can overcome complex conditions in soil thereby monitoring and quantifying bacteria transport.

## 1.6. Research Objectives

The overall aim of this study is to better understand the distribution of bacteria in the soil with surfactant alone and in combination with microbubble suspension, for the purpose of optimizing the introduction of bacteria for effective *in situ* bioremediation. The specific objectives of this study are:

1. To study the effect of anionic and nonionic surfactant solution on the transport of bacteria with different surface properties in saturated sand columns to find the most suitable match between surfactant type and bacteria type for delivering bacteria cells to contaminated sites for the purpose of *in situ* bioremediation.
2. To investigate the efficiency of continuously supplied microbubble suspension in the delivery of bacteria for *in situ* bioremediation under various conditions: method of microbubble generation, surfactant type, hydrophobicity of the bacteria and porosity of the column.
3. To quantify the transport of fluorescence labeled microorganisms (hydrophilic and hydrophobic) in the sand columns using the optrode to monitor the effect of rhamnolipid biosurfactant on bacteria transport

## 1.7. Thesis Outline

This thesis consists of three draft journal manuscripts to be submitted for publication. As a result, the repetition of some materials was unavoidable. The thesis outline is presented below.

## Chapter 1. General Introduction

Chapter 1 has provided a general review of the challenges of *in situ* bioremediation and this study's particular interest in the transport of bacteria in the soil for the purpose of *in situ* bioremediation. The research hypotheses, research objectives, and thesis outline are also presented.

Chapter 2 gives an overview of bacterial properties, and the properties of surfactant and microbubbles and how these properties affect transport behaviour of bacteria in the soil. Monitoring methods including the optrode are also reviewed. The principal theories and models used for describing bacteria transport are also presented.

Chapter 3 describes the transport of hydrophobic *Rhodococcus erythropolis* and hydrophilic *Pseudomonas putida* in saturated sand columns. The modifying effect of surfactant solution on the properties of bacteria and sand particles are also outlined. Bacteria transport in the presence and absence of surfactant solutions is investigated, and the parameters of transport compared and interpreted in terms of the interaction energy.

Chapter 4 tests the ability of continuously injected microbubble to deliver hydrophobic *Rhodococcus erythropolis* and hydrophilic *Pseudomonas putida* in the columns. The stability and drainage of microbubble suspension are described. The efficiency of continuously injected microbubble and surfactant solution in delivering bacteria in the columns are compared. The effectiveness of continuously supplied microbubbles as bacteria carrier is investigated under different parameters, including the method of microbubble generation, surfactant type, bacterial hydrophobicity and the porosity inside the column. The interaction energy interprets the percentage of total injected bacteria that is eluted out of the columns.

Chapter 5 compares the results obtained from *ex situ* measurements and the optrode using two experiment protocols (conducted with and without sampling for *ex situ* measurements). The analysis of the bacteria transport observed by the optrode without sampling for *ex situ* measurements is also presented.

Chapter 1. General Introduction

Chapter 6 summarizes the study's findings, discusses implications for stimulating *in situ* bioremediation, and makes recommendations for future research.

## Chapter 2. Literature Review

### 2.1. Introduction

In this literature review, I consider studies published in five key areas:

- 1) The impact of bacterial properties and surfactant solution on bacteria transport in the soil, including the properties of bacteria, properties of surfactant solution and the interaction between the surfactant, bacteria and soil.
- 2) The potential of microbubble suspensions as bacterial carriers in the soil, including the properties of surfactant microbubbles and their advantaged and limitations for application in bioremediation.
- 3) Traditional and *in situ* methods for monitoring bacteria transport.
- 4) Models for calculating LW-AB interaction between bacteria and sand particles.
- 5) Modeling of bacteria transport in the soil.

### 2.2. Bacteria Transport in Soil

Indigenous bacterial strains can adapt to the presence of a pollutant and degrade pollutant (Atlas and Bartha, 1981; Leahy and Colwell, 1990), however the process is usually very slow. In soil with insufficient or non-detectable numbers of indigenous bacteria that available to degrade pollutants, it is necessary to inoculate contaminated sites with exogenous bacteria to expand the bacteria population and promote the efficiency of *in situ* bioremediation. Knowledge of bacterial distribution in the soil is necessary for developing efficient *in situ* bioremediation strategies when applying exogenous bacteria to contaminated sites. The transport of bacteria in the soil is affected by many factors: fluid velocity (Hendry et al., 1999), pH (Bradford et al., 2002; Gang Chen et al., 2004; Gexin Chen and Walker, 2007; Gang Chen and Zhu, 2004; Xiao-Hong et al., 2010), ionic strength (Bradford et al., 2002; Gang Chen et al., 2004; Gexin Chen and Walker, 2007; Gang Chen and Zhu, 2004; Xiao-Hong et al., 2010), bacterial

surface properties and size (H. Bai et al., 2016; Bradford et al., 2004; Bradford et al., 2003; Gannon et al., 1991; Herzig et al., 1970; Sakthivadivel, 1968, 1969; van Loosdrecht et al., 1989), properties of the soil (H. Bai et al., 2016; Bradford et al., 2002) and surfactants (Abu-Lail and Camesano, 2003; H. Bai et al., 2016; Gexin Chen and Walker, 2007; Gang Chen and Zhu, 2004; Tsuneda et al., 2003; Zhong et al., 2016).

Among these factors, the properties of bacteria and surfactant affect the attachment of bacteria to the surface of soil particles.

### **2.2.1. Bacterial Properties**

Bacteria can be classified as Gram-negative and Gram-positive, according to the bacterial cell wall architecture (Beveridge, 1981; Prescott et al., 2005). Bacterial surface properties such as hydrophobicity and surface charge can affect the transport of bacteria in soil (H. Bai et al., 2016; Gannon et al., 1991; van Loosdrecht et al., 1989). Bacterial radius can also affect transport of bacteria in soil (Bradford et al., 2004; Bradford et al., 2003; Fontes et al., 1991; Herzig et al., 1970; Sakthivadivel, 1968, 1969).

#### **1) Bacteria surface hydrophobicity**

Bacterial surface hydrophobicity measures the macroscopic property of cell, to which is various surface biomolecules surface biomolecules contribute, including different lipopolysaccharides and surface proteins, as well as surface appendages (Dickinson, 2006). Bacterial surface hydrophobicity is typically used to explain non-specific interactions, including the cell's adhesion to non-biological surfaces that commonly exist in both environmental and engineering processes. Bacterial surface hydrophobicity is one of the most important factors affecting bacterial adhesion to surfaces such as solid surfaces and air-water interfaces (H. Bai et al., 2016). If applied to soil hydrophilic bacteria will penetrate further than hydrophobic bacteria before attaching to a soil particle, but once attached, are re-suspended at a slow rate (McCaulou et al., 1994).

In gas-liquid systems, bacteria tend to adsorb onto gas-liquid interfaces, with hydrophobic bacteria having a greater tendency to do so compared to hydrophilic bacteria (M. Ripley et al., 2002; Wan et al., 1994). Cell surface hydrophobicity can be measured in different ways, including by the microbial adhesion to hydrocarbons (MATH) assay (Rosenberg, 1984) and water contact angle measurement (Bos, Van der Mei, et al., 1999). The MATH method is based on the differential partitioning of bacteria between aqueous and organic solvent layers. It is simply a ratio based on the assumption that hydrophilic bacteria will remain in aqueous phase and hydrophobic bacteria transfer to hydrophobic phase. The water contact angle ( $\theta_{\text{water}}$ ) measurement on bacterial lawns has become a more acceptable method for providing a mean value to quantify bacteria cell surface hydrophobicity (Bos, Van der Mei, et al., 1999; Feng et al., 2013a). It is the tangent (angle) of a water drop to a solid surface at the base, as shown in Figure 2-1. The water contact angle of hydrophilic bacteria is regarded as less than 45 °, and vice versa (Daffonchio et al., 1995; Grotenhuis et al., 1992).

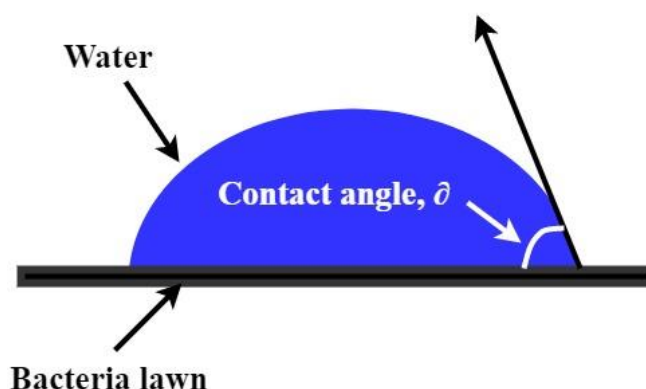


Figure 2-1 Schematic diagram of contact angle

## 2) Bacterial surface charge and bacterial radius

Bacterial surface charge is not only determined by bacterial species but also affected by growth medium, bacterial age and bacteria surface structure (Gilbert et al., 1991; Hogt et al., 1986). The surface charge can be expressed as the zeta potential or electrophoretic mobility. Some studies have found that bacterial surface charge can affect the adhesion of bacteria to soil (H. Bai et al., 2016; Gilbert et al., 1991; Subramani and Hoek, 2008). For example, the adhesion of electro-neutral *Staphylococcus epidermidis* to soil increased when its surface electronegativity was increased, but the

adhesion of electro-negative *Escherichia coli* to soil decreased with increasing surface electronegativity (Gilbert et al., 1991). However, other studies report that the adhesion of bacteria to different surfaces is not significantly affected by the bacteria cell surface (Abbott et al., 1983; Hogg et al., 1985). As the role of surface charge on bacteria adhesion has not been definitively established (Dickinson, 2006). This study will focus on the effect of bacterial hydrophobicity on bacteria transport. The ratio of the bacterial size to soil particle size is another crucial parameter in determining the staining of bacteria in porous media. Colloid filtration theory is employed to quantify the effect of the size of bacteria and porous media on bacteria transport. In this theory, all particles are assumed to be spheres and cell shape in terms of width and length will affect the transport of bacteria through porous media. Cell filtration is thought to play a significant role in determining bacteria transport in soil when the ratio of cell diameter to porous media is greater than 0.05 (Bradford et al., 2004; Bradford et al., 2003; Herzig et al., 1970; Sakthivadivel, 1968, 1969).

### 2.2.2. Surfactant

#### 1) Surfactant and biosurfactant

Surfactants are surface active agents that have both a hydrophobic and a hydrophilic moiety (Figure 2-2). Figure 2-3 is a schematic of the principal forms of surfactants in water and at a solid surface based on the *critical micelle concentration* (CMC). When surfactants are dissolved in water at a concentration lower than the CMC, only single molecules are present in the water solution. When the surfactant concentration in water is higher than CMC, surfactants form aggregates which are known as *micelles*. In a micelle, the hydrophilic moieties face out into the water to maximize their contact with water, while the hydrophobic moieties face into the interior to minimize their contact with water. Figure 2-3 also demonstrates the adsorption of surfactants at the solid-water interface. When the surfactant concentration is less than CMC, the surfactant randomly adsorbs on the solid surface to form a *surfactant monomer*. When the surfactant concentration increases beyond CMC, the functional groups of the surfactant adsorb on the solid phase and form single (*hemimicelle*) or double (*admicelles*) layers

on solid interfaces. As a result, these layers can modify the solid surface and hence the interaction between the bacteria and the solid surface (Gang Chen et al., 2004).

Surfactants can be classified into four groups – anionic (negative charge), nonionic (no charge), cationic (positive charge) and zwitterionic (both negative and positive), according to their hydrophilic charge. They can also be classified as either a synthetic surfactant or a biosurfactant, according to how they are synthesized. Synthetic surfactants are chemically manufactured surfactants that can cause secondary pollution and inhibit bacterial growth due to their chemical nature (Hartmann, 1966; Rothmel et al., 1998; Tiehm, 1994). Biosurfactants have emerged as alternatives to synthetic surfactants owing to their low ecological toxicity and biodegradable nature (Abalos et al., 2004; Nitschke et al., 2005; Rebello et al., 2014).

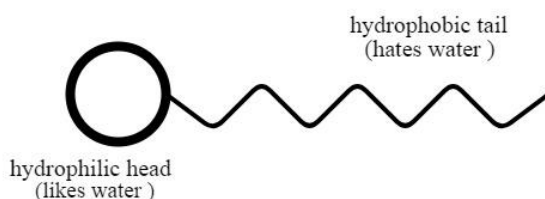


Figure 2-2 General structure of surfactant

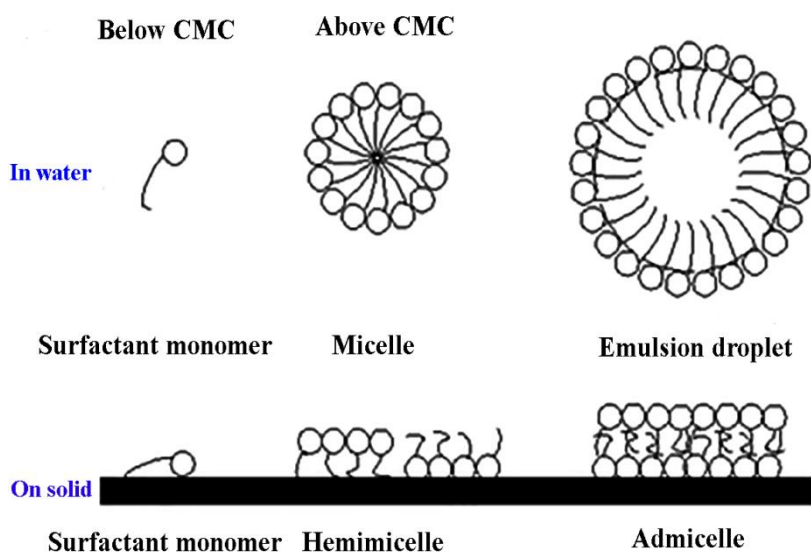
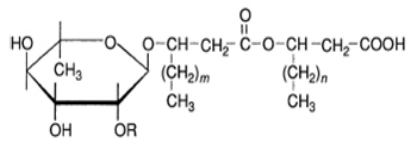
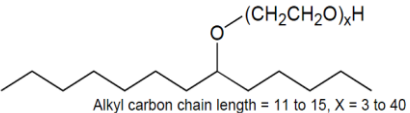


Figure 2-3 Schematic diagram of micelles presents in water and on water/solid interfaces

Rhamnolipid is also one of the most closely studied biosurfactants for bioremediation purpose (Abalos et al., 2004; Avramova et al., 2008; Dean et al., 2001; Noordman and Janssen, 2002; K.-H. Shin et al., 2008; K. H. Shin et al., 2004; Zhang et al., 1997; Zhang and Miller, 1992; Zhu et al., 2013). It is a rhamnose-containing glycolipid surfactant that is primarily produced by *Pseudomonas aeruginosa* (Desai and Banat, 1997). Rhamnolipids are produced as mixtures in various proportions. Monorhamnolipids (R1) and dirhamnolipids (R2) are the two most common forms of rhamnolipids produced by *Pseudomonas aeruginosa* during cultivation in a liquid culture containing glucose or glycerol (Soberón-Chávez et al., 2005). R1 has a single rhamnose group whereas R2 comprises two rhamnose groups joined by an ether bridge. The hydrophilic head group of rhamnolipid molecules comprise the rhamnose and free carboxyl groups, whereas the hydrophobic tails are made up of two hydrocarbon chains. The general structures of the rhamnolipid compounds (R1 and R2) are depicted in Table 2-1 (Maier, 2003). Due to protonation of the carboxyl groups, rhamnolipids behave as anionic surfactants at pH greater than 4.0, with their  $pK_a$  equal to 5.6 (Champion et al., 1995; Ishigami et al., 1987).

TERGITOL™ 15-S-12 surfactants are secondary alcohol ethoxylates. They are transparent, colorless liquids with a mild odor. This series of amphiphilic molecules consists of a secondary alcohol hydrophobic (oil soluble) component with varying numbers of ethylene-oxide (ethoxylate) units making up the hydrophilic (water soluble) component. The water-soluble ethoxylate chain ranges from 3 to 40 ethylene oxide units. The final number in the product name indicates the number of ethylene oxide units in the ethoxylate chain (Table 2-1). Rhamnolipid and tergitol were selected for this study because they are readily biodegradable and environmentally friendly (J.-L. Li and Chen, 2009) as well as showing little toxicity to bacteria (J.-L. Li and Chen, 2009; Rothmel et al., 1998; Zhang et al., 1997; Zhu et al., 2013).

**Table 2-1 The properties of rhamnolipid biosurfactant and tergitol**

Name	Structure	Charge	MW(g/mol)	CMC(mg/L)
Rhamnolipid		Anionic	500	40
Tergitol	 <p>Alkyl carbon chain length = 11 to 15, X = 3 to 40</p>	Nonionic	738	100

Rhamnolipid structure: R=H for R1 and R=rhamnose for R2; m and n values vary

## 2) Impact of surfactant on bacteria transport in soil

Some studies have shown that the surface hydrophobicity of bacteria and soil play an important role in determining the transport of bacteria in soil (H. Bai et al., 2016; Gang Chen et al., 2004; Vu et al., 2015). Surfactants can enhance the transport of bacteria in the soil (Gang Chen et al., 2004; Gang Chen and Zhu, 2004; Vu et al., 2015; Zhong et al., 2016) by modifying their respective surface hydrophobicity.

### a) Modification of bacterial hydrophobicity by surfactant

Dissolved surfactant solution tends to change the properties of the bacterial cell surface when in contact with certain species of bacteria. In one study, tergitol reduced the hydrophilic property of some *Sphingomonas* species, gram-negative bacteria, by altering their cell surface to the extent they became hydrophobic (Brown and Jaffé, 2006). In another study rhamnolipid and tergitol altered the hydrophobicity of hydrophobic *R. erythropolis* 3586 and hydrophilic *P. putida* 852, but hydrophilic bacteria remained hydrophilic, and hydrophobic bacteria remained hydrophobic (Feng et al., 2013a). However, compared with tergitol, rhamnolipid had a greater impact on altering the hydrophobicity of both bacteria strains (Feng et al., 2013a). The adsorption kinetics of synthetic surfactants and rhamnolipid biosurfactant on *Pseudomonas aeruginosa* cells follow the second-order law (Yuan et al., 2007). Surface free energy theory is a useful tool for quantifying the bacterial surface hydrophobicity (Gang Chen et al., 2004; Feng et al., 2013a; Jeong et al., 2000).

### b) Modification of soil by surfactant

Surfactants attach on the surface of sand particles due to their amphiphilic nature. The adsorbed surfactants form a stable coating around the sand particles, which form the stationary phase in porous media, and affect the mass transfer of solutes between the adsorbed phase and the micelle phase in bulk fluid (Ko et al., 1998). The addition of pollutant can change the physical, chemical and biological properties of soil (Kuhnt, 1993), as shown in Table 2-2. The presence of anionic surfactant has a significant impact on sand's hydraulic properties, including increasing the solid-liquid contact angle, soil dispersion and soil penetration coefficient, which in turn causes a decrease in the capillary rise and so penetrability of water in soil (Abu-Zreig et al., 2003).

**Table 2-2 Impact of surfactant on soil**

Soil parameters	Potential effects
	Cause stability or instability of soil phase
Physics	Improvement or worsening of soil–water balance
	Acceleration of soil erosion
	Washout of nutrients and pollutants
Chemistry	Altered reactivity and composition of the soil solution
	Blocking of exchange surfaces and reduction of exchange capacity
Biology	Higher persistence of organic pollutants
	Influence on soil fertility
	Alteration of microbial population and activity

Surfactants (e.g. pentaethylene glycol monododecyl ether, decaethylene glycol monododecyl ether, and rhamnolipid) promote bacteria transport in porous media (G. Bai et al., 1997; Gang Chen et al., 2004; Gang Chen and Zhu, 2004; Zhong et al., 2016). In one study, rhamnolipid modified the interaction between bacteria and silica sand ,thereby reducing the retention of *Lactobacillus casei* and *Streptococcus mitis* on the sand (Gang Chen et al., 2004). Further, the addition of rhamnolipid alters bacteria hydrophobicity, hence hydrophobic interactions between cells and solid surface, to enhance bacteria transport (Zhong et al., 2016). However, to date no study has compared the effect of different types of surfactant (anionic vs. anionic) on bacteria (hydrophobic and hydrophilic) transport. Accordingly, the results from this study could shed light on suitable matches between bacteria and

surfactant particularly when inoculating contaminated sites with exogenous bacteria for *in situ* bioremediation.

### 2.3. Microbubble

A surfactant microbubble, or colloidal gas aphron (CGA), is a surfactant bound gas bubble with a diameter ranging from 10 to 100  $\mu\text{m}$  (Sebba, 1985). The structure of single microbubble was first proposed by Sebba (1987) (Figure 2-4). A microbubble suspension comprises a large number of minute spherical gas bubbles encapsulated in a soapy liquid film in an aqueous surfactant solution.

#### 2.3.1. General Properties

Surfactant microbubbles are considered potential vehicles for delivering bacteria and oxygen for bioremediation in oxygen-deficient environments (Choi et al., 2009). Microbubble suspensions provide larger interfacial areas (Jauregi and Varley, 1999; Parker, 1989), relatively high stability, are easily dissociated from the bulk liquid, and have water-like flow properties (Jauregi et al., 1997; Save and Pangarkar, 1994; Sebba, 1971). The application of microbubbles in bioremediation depends on the microbubble dispersion properties, such as bubble structure, stability (Desai and Banat, 1997; Ding et al., 2013; Shen et al., 2011), size, and gas hold-up (C.-W. Huang and Chang, 2000).

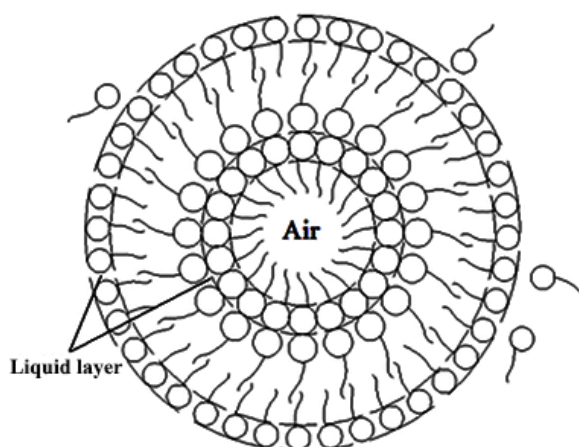


Figure 2-4 Microbubble structure

### **1) Stability**

With regard to bioremediation, a stable microbubble could enable soil penetration, thus delivering bacteria, oxygen, and nutrients, and hence metabolizing pollutants. The stability of microbubble refers to its ability to resist collapse and can be quantified as the time required for half of the microbubble to collapse (half-time). Microbubble stability depends on the surfactant type, the concentration of surfactant micelles, and the presence of dissolved or suspended solutes in the solution and the method for generating microbubbles (Feng et al., 2009; Shen et al., 2011). Anionic surfactant microbubble dispersion (rhamnolipid) is more stable than nonionic surfactant microbubble dispersion (Feng et al., 2009; Matsushita et al., 1992; Shen et al., 2011). For example at pH ~7, the microbubbles of rhamnolipid has a half-time of 461 seconds, which is greater than the half-time of tergitol microbubbles (383 seconds) (Feng et al., 2009). The method used to generate microbubble including the mixer and stirring speed also affects the stability of microbubble (Feng et al., 2009; Jauregi et al., 1997; Sebba, 1985). For example, microbubbles that were generated by a flat spinning disc mixer have a half-time of 466 seconds compared to 325 seconds using a propeller mixer (unpublished studies at the University of Auckland).

### **2) Gas hold-up**

In microbubbles, the gas hold-up is defined as the volume fraction of gas to the total volume of microbubbles. The gas volume is equal to the difference between the total volume of microbubble and the final liquid volume. Gas hold-up could potentially be used to quantify the capacity of the microbubble to carry oxygen for bioremediation. Microbubble dispersion normally displays a gas hold-up ability ranging from 50% to 70% (Feng et al., 2009; Sebba, 1987; Subramaniam et al., 1990).

#### **2.3.2. Microbubble Applications in Bioremediation**

Microbubble dispersion has been studied for its potential in bioremediation of soil; for example by removing pollutants, penetrating heterogeneous media, and carrying and dispersing oxygen, nutrients,

and bacteria (Figure 2-5). These applications in bioremediation make good use of the unique properties of the microbubbles : their (1) small size (Jauregi et al., 2000), (2) large interfacial areas (Jauregi and Varley, 1999; Parker, 1989), (3) relatively high stability, (4) and the fact that particles can adsorb on the microbubble surfaces (Wan and Wilson, 1994).

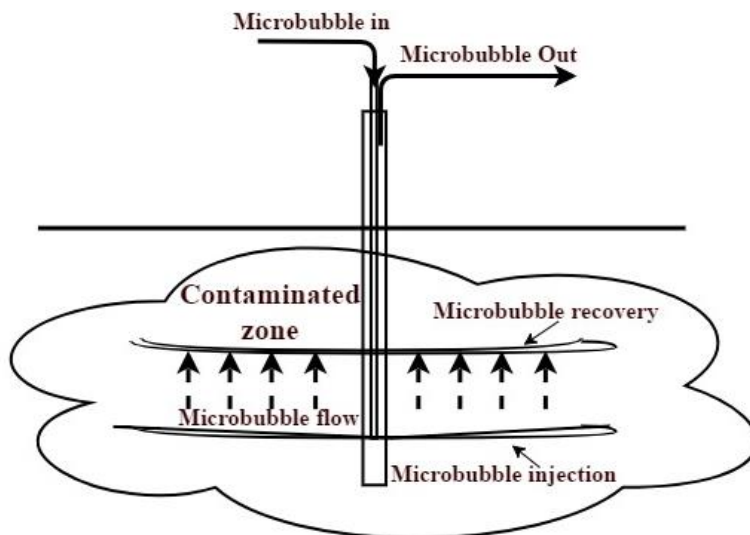


Figure 2-5 Schematic illustration of the use of microbubble to remediate contaminated soil (Kilbane et al., 1997)

### 1) Pollutant removal

Microbubbles have the potential to physically remove pollutants, like oily waste and nonaqueous phase liquids, in contaminated sites (Dipak Roy et al., 1995; D. Roy et al., 1995; Roy et al., 1994; Ussawarujikulchai et al., 2008). As the microbubble collapses to gas and then liquid phase after travelling a short distance in the soil, the released gas may carry the volatile oily waste and float upwards, thereby enhancing the removal of oily waste. Microbubbles were found more effective in flushing oily waste when compared with a conventional surfactant solution and with water, likely due to the phase separation of the microbubble during transport in the soil (Roy et al., 1994). For example, when using the same concentration and volumes of Triton SP-series surfactant solution, 36% of n-pentadecane was removed by using foam with a gas proportion of 83%, compared 26% removal by surfactant solution (C.-W. Huang and Chang, 2000). Under the same conditions, the removal rate of n-pentadecane increased from 36% to 74% when the proportion of gas in the foam was increased from 83%

to 91% (C.-W. Huang and Chang, 2000). This application of foam in pollutant removal lowers the interfacial tension between pollutant and the flushing liquid, as well as provides viscous forces for flushing of pollutants.

## **2) Carrying oxygen and bacteria**

Foam can penetrate the low-permeability zones and flow uniformly through heterogeneous media as a result of its plug-flow behaviour in soil (2008a; Mamun et al., 2002; 2001). Due to this behaviour, it may be possible for microbubbles to penetrate the liquid-impermeable heterogeneous areas of soil to deliver oxygen and bacteria to trapped hydrophobic pollutants.

### **a) Oxygen delivery**

The application of microbubbles to carry oxygen has gained intense research focus as a way of stimulating *in situ* bioremediation. Microbubble suspensions have been shown to promote the aerobic degradation of organic pollutants such as phenol (D. L. Michelsen et al., 1984), p-xylene (K B Jenkins et al., 1993) and pentachlorophenol (C N Mulligan and F Eftekhari, 2003) in artificial sandy columns by delivering oxygen. A bench-scale column study compared the degradation of phenanthrene by *Burkholderia cepacia* RPH1 (Park et al., 2009) achieved by purging with microbubbles and solution. After 21 days, approximately 30% of phenanthrene was removed in the columns with microbubble, while no degradation of phenanthrene was observed in columns when pumping the same concentration of surfactant solution (Park et al., 2009). This study found that the gas phase concentration at the bottom of the column was about 84% and its value decreased increasing column depth, to around 10% at the top of the columns. Consequently, the relative residual of phenanthrene decreased from 80% to 40% at the bottom of the columns after 21 days, while it had increased slightly at the top of columns (Park et al., 2009). These studies suggest that the more gas introduced to contaminated soil, the greater the level of pollutant biodegradation achieved.

## **b) Bacteria delivery**

Bioremediation will potentially be stimulated if the microbubble suspensions can deliver both bacteria and oxygen to contaminated soil. The pulse injection of microbubbles into a column was used to investigate the efficiency of microbubbles in delivering bacteria. Compared to surfactant solutions, microbubbles enhanced bacteria transport in soil columns (1998; Park et al., 2009). For example, after using 2.5 pore volumes of surfactant solution, the density of bacteria in the effluent obtained in the microbubble treatment was around 2 orders of magnitude higher than the bacterial density in the effluent that was treated with the same surfactant solution [89]. In other words, compared to surfactant solution treatment, microbubble treatment would reduce the amount of surfactant solution that was required to deliver the same number of bacteria. Another advantage of bacteria transport by microbubble is that a uniform distribution of bacteria throughout column can be achieved when using microbubble as the vehicle (Park et al., 2009).

### **2.3.3. Parameters that Affect the Efficiency of Microbubble as Bacteria Carrier**

The potential effectiveness of microbubble as bacteria/microsphere carriers is influenced by a few parameters, including microbubble stability, pore size of soil and the hydrophobicity of the bacteria/nanoparticles. Microbubbles generated from anionic surfactant (e.g. sodium lauryl ether sulfate and sodium dodecyl sulfate) are more stable than those generated using nonionic tergitol (e.g. Tween 20 and Triton X-100) (Ding et al., 2013; Shen et al., 2011). In column experiments, the anionic surfactant microbubble suspension demonstrates slightly better ability for carrying nanoparticles than microbubbles of nonionic surfactant (Ding et al., 2013; Shen et al., 2011). According to *Kozeny's* equation, the pore size of soil is dependent on the soil particle size and the porosity of soil (Skorokhod et al., 1988). When delivering nanoparticles to the column, microbubble dispersion is more efficient in columns with coarse pore size (ranges from 0.18~0.51 mm) than in columns with finer pore size (ranges from 0.09~0.18 mm) [70]. In contrast, one study found that microbubbles were better able to penetrate columns with finer sand (ranges from 0.10~0.20 mm) than sand with coarse pore size

(0.20~0.57 mm) (Su et al., 2014). Bacteria transport by microbubbles is reliant on the adhesion tendency of bacterial suspension to sand particles and air-water interfaces. The preferential sorption of bacteria to the air-liquid interfaces rather than the solid water interfaces can contribute to the enhancement of transport and dispersion of bacteria (M. B. Ripley et al., 2002; Wan and Wilson, 1994). Both hydrophilic and hydrophobic bacteria show preferential sorption onto gas-water interfaces over solid-water interfaces (Wan and Wilson, 1994). Bacterial hydrophobicity is another important factor that can affect the adhesion tendency. For example, hydrophobic bacteria have a stronger affinity to soil particles than hydrophilic bacteria (Gang Chen and Zhu, 2004; Huysman and Verstraete, 1993). Hydrophobic bacteria also have a greater adhesion tendency to gas-liquid interfaces than do hydrophilic bacteria (M. Ripley et al., 2002; Wan et al., 1994).

In the applications using microbubble as the carrier for bacteria and oxygen, microbubble was introduced either before or after a water/surfactant pulse. These studies also suggested that the more gas introduced to contaminated soil, the better pollutant biodegradation potentially achieved. Continuously supplied microbubble could potentially provide more gas, and therefore greatly enhance the cost effectiveness of microbubble delivery of bacteria for *in situ* bioremediation.

### **2.4. Approaches for Monitoring Bacterial Distribution**

Developments in molecular biology have allowed molecular biologists to design genetically modified microorganisms (GMO) as biosensor microorganisms (Belkin, 2003; Hewitt et al., 2012; Paul et al., 2005; Urgun-Demirtas et al., 2006). Biosensor microorganisms are genetically engineered bacteria that can synthesize reporter (fluorescent or bioluminescent) proteins to respond to the presence of chemicals or physiological stresses. A wide range of fluorescent (blue, cyan, green, yellow, orange, red and far red) or bioluminescent proteins have been employed to develop biosensor microorganisms (Hewitt et al., 2012; Jansson, 2003; Shaner et al., 2005). In laboratory studies simulating soil conditions for the purpose of *in situ* bioremediation, the rapid production of fluorescence or bioluminescence by

biosensor microorganisms enables their activity to be quantified, in terms of their distribution, and concentration in a rapid manner (Ron, 2007; Singh and Ward, 2004).

### **2.4.1. Traditional Approaches for Environmental Monitoring of Bacterial Activates**

Traditional approaches for monitoring the transport behaviour of bacteria in the soil involve collecting liquid samples from the effluent or from a sampling port (Lang et al., 2016; Unc and Goss, 2003; Zhong et al., 2016). Liquid samples are been analyzed in the laboratory using quantitative methods, such as total viable counts on agar plates, epifluorescence microscopy and microscopic fluorescence counts and flow cytometry (Banning et al., 2002; Maraha et al., 2004), to detect bacterial concentration. However, these approaches are challenged by some constraints such as the difficulty of detecting the attached bacteria, the time-consuming sampling (Tian et al., 2003), transportation and analysis processes, and it is also limited by sample size. There is therefore a growing demand for quantifying the transport of microorganisms in the soil in a rapid, real-time and cost-effective manner.

### **2.4.2. *In situ* Approaches for Environmental Monitoring of Bacterial Activates**

#### **1) Biosensor**

With the development of advanced measurement technologies, *in situ* methods for quantifying bacterial concentration are becoming increasingly accepted. One of the *in situ* methods which overcome the constraints of traditional monitoring approaches by using an appropriately designed biosensor. Biosensors (Figure 2-6) are defined as devices that detect chemical compounds through electrical, thermal or optical signals, using specific biochemical reactions mediated by sensing elements including isolated enzymes, immune systems, tissues, DNA, receptors organelles or microorganisms (D'souza, 2001; Davis et al., 1995; McNaught and McNaught, 1997). Among these sensing elements, microorganisms (e.g. algae, bacteria, and yeast) have emerged as a suitable biological sensing element due to their being easier and cheaper to popularize, and more tolerant to environmental conditions (D'souza, 2001; Davis et al., 1995).

Microbial biosensors can be classified into three groups: electrochemical, microbial fuel cell and optical. Electrochemical microbial biosensors have been extensively studied and commercialized. These types of biosensors quantify or semiquantify the analyte by using a biological recognition element retained in direct spatial contact with an electrochemical transduction element (Th évenot et al., 2001). Microbial fuel cell biosensors have bio-electrochemical transducers, which convert the chemical energy into electrical energy by the metabolic activity of microorganisms (Rabaey and Verstraete, 2005). These types of biosensors can be applied for *in situ* analysis and monitoring of target chemical compounds due to altered electricity production when the compound is consumed, or toxic compounds' inhibition of metabolic pathways. Generally, optical detection measures luminescent, fluorescent, colorimetric, or other optical signals produced by the interaction of microorganisms with the analytes, and then correlate the observed optical signal with the concentration of target compounds. Optical biosensors transfer the biochemical interaction between microorganisms and the analytes into signals including luminescent, fluorescent, colorimetric, or other optical signals. This type of biosensor can correlate the observed signal with the concentration of the target chemical compounds (Dorn et al., 2005; Heitzer et al., 1994; Ivask et al., 2007; Yolcubal et al., 2000). Among these biosensors, optical biosensors have been proven to outperform other types of sensors in multi-target sensing and continuous real-time on-site monitoring (Long et al., 2013).

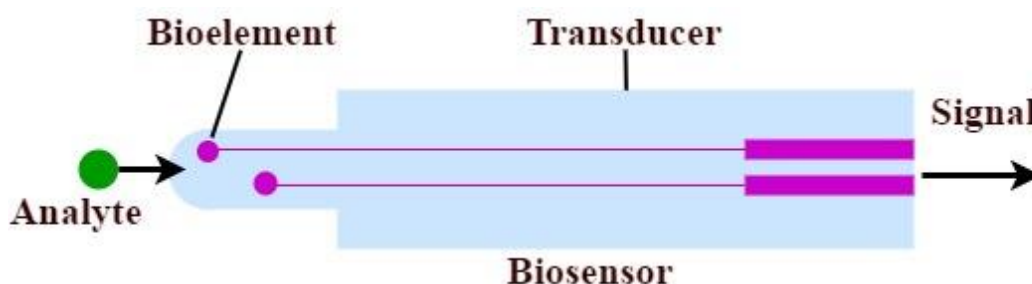


Figure 2-6 Basic scheme of a biosensor

## 2) The application of optical biosensor in monitoring bacterial activity

The use of biosensor microorganisms is a well-established approach for monitoring microorganism activity in the soil environment. Very few studies have used fluorescence optical systems that are based on biosensors for monitoring bacterial activity. The lux reporter bacterium *P. putida* RB1353 was used to detect on microbial growth activity during naphthalene degradation in porous media (Dorn et al., 2005). The same reporter organism has also been used as a remote sensor for *in situ* measurements in porous media to examine the applicability of reporter organisms (Yolcubal et al., 2000). However, to date, no data regarding bacteria transport was published using the biosensor.

### 2.4.3. The Optrode System

Since 2008, the Auckland University's Physics Department has been working on the development of a spectroscopic fibre optic system ('the optrode'). The setup for the optrode has been described previously by A. Y. H. Chen et al. (2010) and Hewitt et al. (2012), as shown in Figure 2-7. Diode pumped solid state lasers are used for excitation. The light is directed to the sample via a multimode fibre coupler, and the collected spectrum is then measured by a spectrometer. The laser mount includes a shutter to control excitation timing and duration. The optrode employs the same optical fibre to release the excitation light and collect the emission light. The spectrum is then subtracted from the background spectrum to obtain a pure fluorescence signal. The background spectrum can be measured before starting the actual measurements and then removed in the collected samples, which allows the optrode to be utilized in a diverse range of environments. A customized computer software interface enables control of the optrode for quick presentation of the measured fluorescence spectrum and signal. The optrode has shown capability for rapidly identifying and quantifying green/red fluorescent protein labelled microorganisms in batch experiments (Hewitt et al., 2012) and rapidly enumerating acridine orange-stained *Escherichia coli* in liquid media (Guo et al., 2017). The optrode is uniquely suited to take measurements from columns in the laboratory because it offers a non-destructive method and can monitor bacteria transport in columns in a rapid and real-time manner.

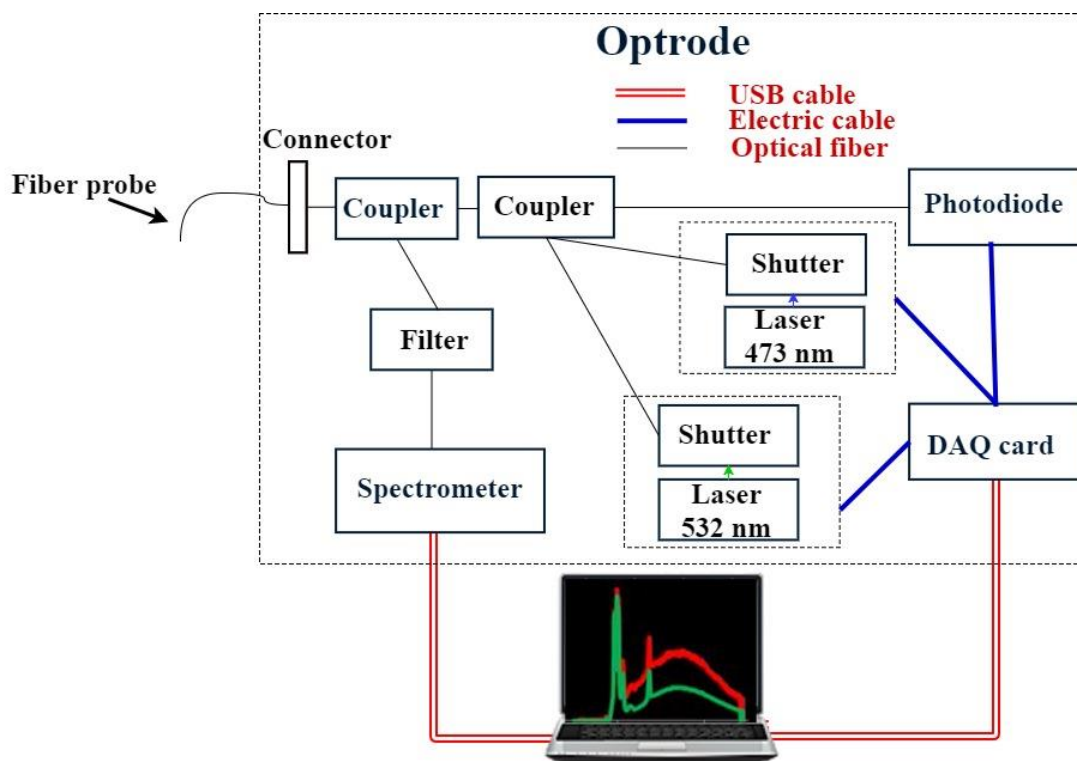


Figure 2-7 The optrode and computer setup

## 2.5. Approaches for Bacteria Transport in Porous Media

Two main approaches are known to estimate bacteria transport in soil: the extended DLVO approach and thermodynamic approach.

### 2.5.1. The Extended DVLO Approach

Derjaguin, Landau, Verveij, and Overbeek (DLVO) theory (B Derjaguin, 1993; BV Derjaguin and Landau, 1941; Werway and Overbeek, 1948) was originally developed to describe the aggregation behaviour of colloids. When applied to model the interaction of bacteria with soil particles, the cells are regarded as living colloidal particles. This theory sums electrostatic interactions and Lifshitz-van der Waals interactions as the total interaction between bacteria. Both electrostatic interactions and Lifshitz-van der Waals interactions are dependent on distance between bacteria and soil. The electrostatic interactions can be attractive or repulsive, and decrease significantly with increasing distance between the bacteria and the soil (Gang Chen and Zhu, 2004). Further, the Lifshitz-van der Waals (LW) interactions also increase with increasing distance between bacteria and soil. Acid-base (AB)

interactions were later added to DLVO theory by C. Van Oss et al. (1986) to take into account the electron donating-accepting characteristics of various materials and the results could be improved (Perni et al., 2014).

## 2.5.2. The Thermodynamic Approach

### 1) LW-AB interaction energy

At the equilibrium distance (0.157nm) (C. J. Van Oss, 2006), electrostatic interactions can be ignored, as LW-AB interactions between the electron donor and electron acceptor begin to drive bacteria adherence to sediment (Gang Chen et al., 2004). Consequently, the LW-AB interaction energy ( $\Delta G_{bls}$ ) will be applied in this study. According to this theory, if  $\Delta G_{bls}$  is negative ( $\Delta G_{bls} < 0$ ), the adhesion is favourable, and vice versa.  $\Delta G_{bls}$  is divided into two parts: the Lifshitz-van der Waals (LW) components ( $\Delta G_{bls}^{LW}$ ) and acid-base (AB) components ( $\Delta G_{bls}^{AB}$ ) of the free energy of adhesion.

$$\Delta G_{bls} = \Delta G_{bls}^{LW} + \Delta G_{bls}^{AB} \quad (2-1)$$

where subscript  $b$  denotes bacteria,  $l$  denotes liquid,  $s$  denotes solid.

The Lifshitz-van der Waals (LW) component and the acid-base (AB) component can be calculated from the interfacial tensions as follows (Absolom et al., 1983; Busscher et al., 1984; Sharma and Hanumantha Rao, 2002; C. Van Oss, 1995):

$$\Delta G_{bls}^{LW} = -2 \left( \sqrt{\gamma_b^{LW} \gamma_l^{LW}} + \sqrt{\gamma_s^{LW} \gamma_l^{LW}} - \sqrt{\gamma_b^{LW} \gamma_s^{LW}} - \gamma_l^{LW} \right) \quad (2-2)$$

$$\begin{aligned} \Delta G_{bls}^{AB} = & 2 \left( \sqrt{\gamma_l^+} (\sqrt{\gamma_b^-} + \sqrt{\gamma_s^-} - \sqrt{\gamma_l^-}) + \sqrt{\gamma_l^-} \left( \sqrt{\gamma_b^+} + \sqrt{\gamma_s^+} - \sqrt{\gamma_l^+} \right) \right. \\ & \left. - \sqrt{\gamma_b^+ \gamma_s^-} - \sqrt{\gamma_b^- \gamma_s^+} \right) \quad (2-3) \end{aligned}$$

The three unknown surface tension components,  $\gamma^{LW}$  (LW apolar component),  $\gamma^-$  (electron donor),  $\gamma^+$  (electron acceptor), in Equation 2-2 and 2-3 can be determined by using the LW-AB approach and

Yong's equation (Knox et al., 1993) and contact angle measurements (Figure 2-8) from three diagnostic liquids with known components for surface tension.

$$((1 + \cos \theta)\gamma_l = 2(\sqrt{\gamma_b^{LW}\gamma_l^{LW}} + \sqrt{\gamma_b^+\gamma_l^-} + \sqrt{\gamma_b^-\gamma_l^+}) \quad (2-4)$$

Where  $\theta$  is the contact angle, subscript  $b$  denotes bacteria,  $l$  denotes diagnostic liquid.

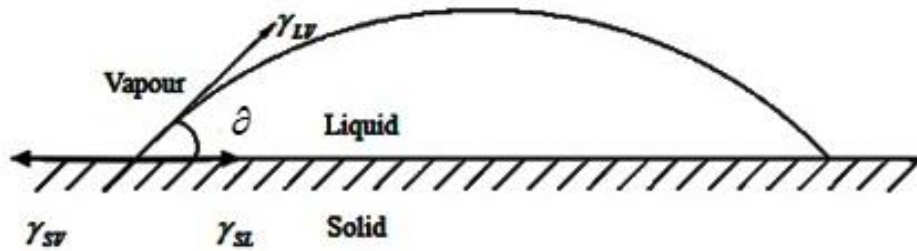


Figure 2-8 Relationship between contact angle and the different interfacial tensions

The surface tension of these probe liquids that can be used as diagnostic liquid are summarised in Table 2-3.

Table 2-3 The list of probe liquids can be used as diagnostic liquid

Diagnostic liquid	$\gamma$	$\gamma^{LW}$	$\gamma^{AB}$	$\gamma^-$	$\gamma^+$
Water	72.8	21.8	51.0	25.5	25.5
1-bromonaphthalene	44.4	44.4	0	0	0
n-octanol	27.5	27.5		0	18.0
Ethylene glycol	48.0	28.0		1.92	47.0
PEO (MW=6000)	43.0-45.9	43.0-45.9		0	58.5-64.0
Polystyrene	42	42		0	1.1
Dodecane	25.35	25.35		0	0
Tridecane	25.99	25.99		0	0
hexadecane	27.47	27.47		0	0
Nonadecane	28.59	28.59		0	0
Proteins	~26-45	~37-72		~0-5	~20-50
Formamide	58.0	39.0	19.0	39.6	3.92

## 2) Free energy of bacteria aggregation

Based on surface tension parameters, the free energy from aggregation of bacterial cells immersed in water (Van der Mei et al., 1998; C. Van Oss, 1995) indicates bacterial hydrophobicity can be calculated as:

$$\Delta G_{bwb} = -2(\sqrt{\gamma_b^{LW}} - \sqrt{\gamma_w^{LW}})^2 - 4(\sqrt{\gamma_b^+ \gamma_b^-} + \sqrt{\gamma_w^+ \gamma_w^-} - \sqrt{\gamma_b^+ \gamma_w^-} - \sqrt{\gamma_b^- \gamma_w^+}) \quad (2-5)$$

where subscript  $b$  denotes bacteria,  $w$  denotes water.

If the interaction between two bacterial cells is stronger than the interaction between the cell with water, by definition, the cell are consider to be hydrophobic since  $\Delta G_{bwb} < 0$ , and vice versa.

## 2.6. Model Simulation for Bacteria Transport

The mathematical model developed considers the transport of bacteria in columns to be the result of convection and diffusion of liquid due to the concentration gradient (Gang Chen and Zhu, 2004). Accordingly, the introduced bacteria will move through the silica sand column by convective and diffusive transport. The general equation governing one-dimensional bacteria transport is described as below (Van Genuchten and Alves, 1982):

$$\frac{\partial}{\partial x}(\theta D \frac{\partial C}{\partial x} - qC) - \frac{\partial}{\partial t}(\theta C + \rho s) = \mu_l \theta C + \mu_s \rho s - \gamma_l \theta - \gamma_s \rho \quad (2-6)$$

where  $C$  is the bacteria concentration ( $ML^3$ ),  $s$  is the adsorbed bacteria concentration ( $MM^{-1}$ ),  $\theta$  is the volumetric water content ( $M^3L^{-3}$ ),  $\rho$  ( $ML^{-3}$ ) is bulk density of the porous medium,  $x$  is the distance (L) and  $t$  is the time (T),  $\mu_l$  and  $\mu_s$  are rate constants for the first order decay in the liquid and the solid phase of the soil ( $T^{-1}$ ), respectively, and  $\gamma_l$  and  $\gamma_s$  are the rate constants for zero-order production in the two soil phase ( $ML^{-3}$  and  $T^{-1}$ ), respectively.

When only equilibrium transport is considered, the adsorption is deemed to be linear:

$$s = kC \quad (2-7)$$

where  $k$  is an empirical distribution constant ( $M^{-1}L^3$ ).

Equation (2-6) could be written as:

$$\frac{\partial}{\partial x}(\theta D \frac{\partial C}{\partial x} - qC) - \frac{\partial(\theta RC)}{\partial t} = \mu\theta C - \gamma\theta \quad (2-8)$$

where the retardation is given as:

$$R = 1 + \rho k / \theta \quad (2-9)$$

and the new rate coefficients  $\mu$  and  $\gamma$  are given as:

$$\mu = \mu_l + \mu_s \rho k / \theta \quad (2-10)$$

$$\gamma = \gamma_l + \gamma_s \rho / \theta \quad (2-11)$$

Bacteria transporting through a uniform, one-dimensional, saturated porous media, are said to be in a steady-state flow. Accordingly, the one-dimensional convection-dispersion equation (CDE) is reduced to (Van Genuchten and ALVES, 1982):

$$R \frac{\partial C}{\partial t} = D \frac{\partial^2 C}{\partial x^2} - v \frac{\partial C}{\partial x} - \mu C + \gamma \quad (2-12)$$

where  $C$  is the bacteria concentration,  $D$  is the dispersion coefficient (includes both diffusion and hydrodynamic dispersion),  $t$  is the time, and  $v$  ( $v=q/\epsilon$  ( $LT^{-1}$ )) is the average velocity inside the column.

Equation 2-12 can be solved using the CXTFIT model in STANMOD (a Windows-based software package) (Parker and Van Genuchten, 1984). This model considers the solution for the boundary value problem (the input concentration and application time), initial value problem, production value problem (Parker and Van Genuchten, 1984) and can analyze the concentration of bacteria versus time and depth in soil and can also use equilibrium and non-equilibrium transport models.

The main point of using this model is to obtain values for transport parameters such as the dispersion coefficient ( $D$ ), retardation coefficient ( $R_d$ ), and first order decay ( $\mu$ ) in one dimensional column. In homogenous porous media, the value of  $D$  would remain consistent within 100 cm (G. Huang et al., 2006). As  $R_d$  presents the interaction between the bacterial cells and sand, if there are no interaction between cell and sand particles,  $R_d$  reduces to one (Klute, 2003). The first order deposition coefficient ( $\lambda$ ) coefficient takes into account the bacterial cells entrapped on porous media, and can be used to describe the irreversible adsorption process in bacterial transport (G. Bai et al., 1997). The coefficient of determination ( $R^2$ ) is also recorded as an indicator of the goodness of fit. The value of these parameters will be obtained by fitting the obtained bacterial breakthrough curves in CXTFIT model with different initial and boundary conditions and production/degradation processes.

## **Chapter 3. Effect of Rhamnolipid and Tergitol Surfactant on the Transport of *Rhodococcus erythropolis* and *Pseudomonas putida* in Saturated Sand Columns**

To be submitted to Journal of Water Resources Research

Wei Tao<sup>a</sup>, Yantao Song<sup>a</sup>, Simon Swift<sup>b</sup> and Naresh Singhal<sup>a,\*</sup>

<sup>a</sup> Department of Civil and Environmental Engineering, <sup>b</sup> School of Medical Sciences, The University of Auckland, Private Bag 92019, Auckland 1010, New Zealand.

\*Corresponding author:

FAX: +64 9 373 7462

Phone: +64 9 923 4512

Email:n.singhal@auckland.ac.nz

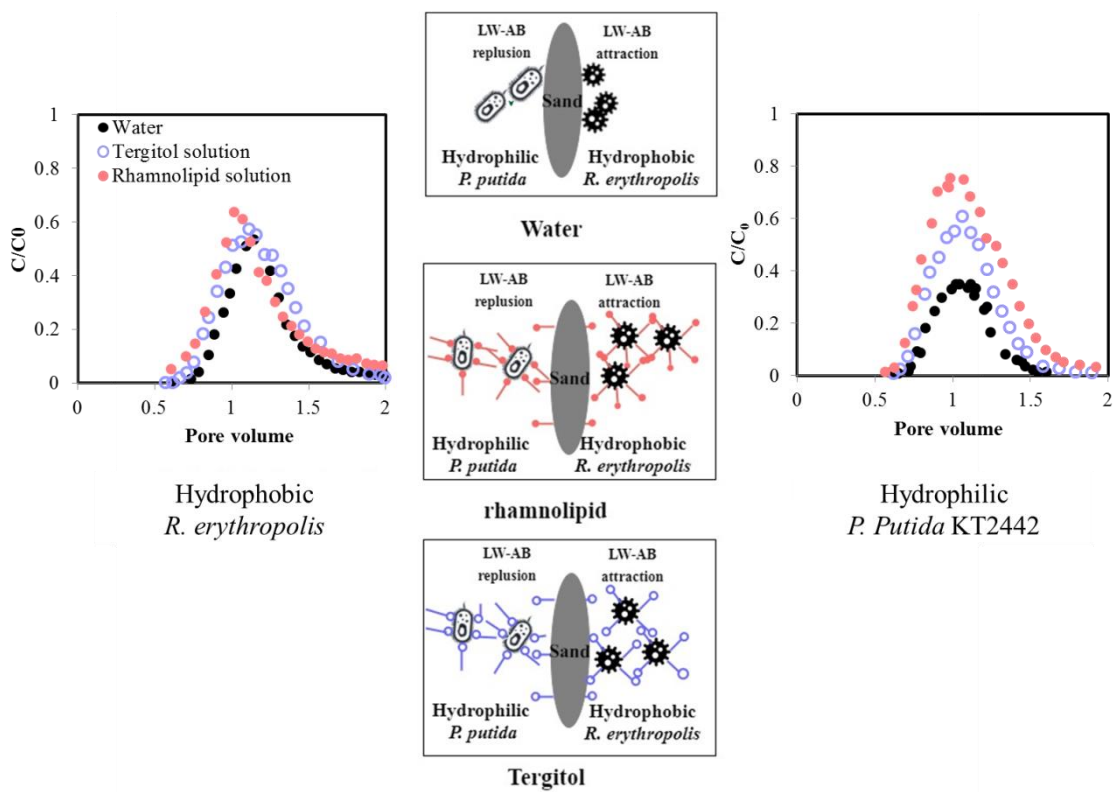
## **Abstract**

Enhanced bacteria transport in soil has been extensively studied for use of bioaugmentation processes for *in situ* bioremediation. Factors such as bacterial hydrophobicity and surfactant can affect the efficiency of bacteria transport in the soil. However, the effect of surfactant (anionic vs. nonionic) modification of the surface of bacteria cells and sand particles on microbial transport in the saturated sand columns has not been studied. This study investigated the effect of rhamnolipid and tergitol on transport behaviours of pulse injected hydrophobic *Rhodococcus erythropolis* (*R. erythropolis*) and hydrophilic *Pseudomonas putida* (*P. putida*) in a saturated sand column. The influence of the surfactant on the surface hydrophobicity of the bacteria and sand particles was also investigated. The transport of bacteria was gauged by the percentage of bacteria eluted out of the column, and the measures for transport parameters such as dispersion coefficients, retardation coefficients, and first order decay. Surfactant solutions made *R. erythropolis* and sand particles less hydrophobic while surfactant made *P. putida* less hydrophilic. Rhamnolipid and tergitol altered bacterial hydrophobicity to a different extent but had an equivalent effect on the hydrophobicity of sand particles. In the absence of surfactant solution, a higher proportion of *P. putida* (76.7%) was eluted out of the column compared to *R. erythropolis* (60.3%). Both rhamnolipid and tergitol enhanced the transport of both bacterial strains. A decrease in the values for first order decay was also observed after adding surfactant solution. The addition of surfactant increased the value of Lifshitz-van der Waals and acid-base (LW-AB) interaction energy between bacteria and sand particles. The percentage of bacteria eluted out of the column increased with increasing LW-AB interaction energy between bacteria and sand particles. The first order decay values decreased with increasing LW-AB interaction energy between bacteria and sand particles. The level of LW-AB interaction energy was related to the surface tension parameter for the bacteria. Compared to tergitol, a profound enhancement was observed for rhamnolipid, most likely due to the different LW-AB respective interaction energies between bacteria and sand particles. This study demonstrates the importance of surfactant type and bacterial hydrophobicity in bacteria transport in sand soil systems and provides insights for finding a suitable match between surfactant and bacteria,

Chapter 3. Effect of Rhamnolipid and Tergitol Surfactant on the Transport of *Rhodococcus erythropolis* and *Pseudomonas putida* in Saturated Sand Columns particularly when introducing exogenous bacteria to expand the population of indigenous bacteria in contaminated soil during bioremediation.

**Keywords:** Bacteria Transport; Anionic and nonionic surfactant; *Rhodococcus erythropolis*; *Pseudomonas putida* KT2442; LW-AB Interaction energy

**Graphical abstract**



### 3.1. Introduction

*In situ* bioremediation is relatively cost-effective and environmentally friendly compared to *ex situ* bioremediation (Mohan et al., 2006). Inoculating contaminated soils with exogenous bacteria is a common approach for stimulating *in situ* bioremediation. However, bacterial mobility can be slow, with some studies reporting that non-attaching bacteria cannot travel beyond a distance of 1 meter (Q. Li and Logan, 1999; Martin et al., 1996). Several studies have therefore focused on enhancing the mobility of bacteria within soil with the goal of promoting their access to contaminants (Gang Chen et al., 2004; Gang Chen and Zhu, 2004; Gross and Logan, 1995; Pantsyrnaya et al., 2011; Tong et al., 2010). Physical, chemical, biophysical and biochemical factors can affect the transport of bacteria in the soil. Fluid velocity (Hendry et al., 1999), and the solution's chemistry including pH and ionic strength are examples of physical and chemical parameters. Biophysical and biochemical factors include the cell size and cell surface properties of the bacteria (Abu-Lail and Camesano, 2003; Dong et al., 2002; Gannon et al., 1991; Q. Li and Logan, 1999; Tsuneda et al., 2003), and properties of the clay particles (H. Bai et al., 2016; Bradford et al., 2002) and surfactants (Abu-Lail and Camesano, 2003; H. Bai et al., 2016; Gexin Chen and Walker, 2007; Gang Chen and Zhu, 2004; Tsuneda et al., 2003; Zhong et al., 2016).

Factors such as the hydrophobicity of bacteria and soil/sediment particles, and the use of surfactants, have drawn increasing attention in the study of bacteria transport. Bacteria strains with different hydrophobicity showed different affinity to solid surfaces. For example, hydrophobic bacteria have a stronger affinity to soil particles than hydrophilic bacteria to do so (Gang Chen and Zhu, 2004; Huysman and Verstraete, 1993). Once hydrophilic bacteria have attached to the soil, they would re-suspended at a slow rate (McCaulou et al., 1994) due to their desorption rate, which could lead to a long tail in breakthrough curves (BTCs). The hydrophobicity of soil affected the affinity of bacteria. For example, bacteria tend to attach to a more hydrophobic surface (Gang Chen and Strevett, 2001; Zhong et al., 2016). The use of surfactants (e.g. pentaethylene glycol monododecyl ether (Gang Chen and Zhu, 2004), decaethylene glycol monododecyl ether (Gang Chen and Zhu, 2004) and rhamnolipid

(G. Bai et al., 1997; Gang Chen et al., 2004; Zhong et al., 2016) promoted bacteria transport in column systems. These surfactants modified the surface properties of both bacteria and soil/sand particles, thereby altering bacteria transport in the column. However, the effect of anionic and nonionic surfactant on bacteria transport is still unclear. Anionic rhamnolipid and nonionic tergitol may alter the hydrophobicity of *R. erythropolis* 3586 and hydrophilicity of *P. putida* 852 to differing extents (Feng et al., 2013a). Rhamnolipid is thought to remove the lipopolysaccharide from the surface of *P. putida* 852 (Feng et al., 2013a) and *P. aeruginosa* (Al-Tahhan et al., 2000) thereby lowering the values of surface tension parameters. The hydrophilic head of tergitol likely interacts with hydrophilic *P. putida* 852. In the treatment of *R. erythropolis* 3586 with surfactant solutions, the hydrophobic tail of the surfactant is likely to interact with hydrophobic bacteria. Although the effects of the hydrophobicity of bacteria and soil/sediment particles, and surfactant on microbial transport have been widely investigated, the comparative effects of anionic and nonionic surfactant on the hydrophobicity of bacteria and soil/sediment particles and thus on microbial transport have not been studied.

This study investigated the effect of anionic and nonionic surfactant on the transport of hydrophobic and hydrophilic bacteria in saturated sand columns. A synthetic nonionic surfactant, tergitol, was used for comparison for anionic biosurfactant rhamnolipid. Both rhamnolipid and tergitol are readily biodegradable and environmentally friendly (J.-L. Li and Chen, 2009) and show low toxicity to contaminant-degrading bacteria (J.-L. Li and Chen, 2009; Rothmel et al., 1998; Zhang et al., 1997; Zhu et al., 2013). Gram-positive *Rhodococcus erythropolis* and Gram-negative *Pseudomonas putida* were used to represent hydrophobic and hydrophilic bacterial strains in this study. Contact angle measurements were conducted to investigate the surface tension parameters of bacteria and sand particles. A pH of ~7 and ionic strength of 0.01M was used to simulate a typical soil environment. Bacteria transport was assessed by the percentage of bacteria that was eluted out of the columns, the breakthrough curves (BTCs) and the transport parameters. Bacteria transport was interpreted with the Lifshitz-van der Waals and acid-base (LW-AB) interaction between bacteria and sand particles.

## 3.2. Materials and Method

### 3.2.1. Materials

#### 1) Surfactants

Anionic rhamnolipid (JBR 210, JENEIL ® Biosurfactant Co.) was used as the biosurfactant in this work. It is a rhamnose-containing glycolipid surfactant that has been primarily produced by *Pseudomonas aeruginosa* (Desai and Banat, 1997). The synthetic nonionic surfactant Tergitol 15-S-12 (Sigma–Aldrich) was applied as the comparison for rhamnolipid biosurfactant because they had different extent of effect on the bacterial surface properties (Feng et al., 2013a). Rhamnolipid and tergitol were also chosen because they are readily biodegradable and environmentally friendly (J.-L. Li and Chen, 2009) and show low toxicity to bacteria (J.-L. Li and Chen, 2009; Rothmel et al., 1998; Zhang et al., 1997; Zhu et al., 2013). The surfactants were used at a concentration of 1000 mg/L, which is considerably larger than the critical micelle concentration (CMC) of rhamnolipid (40 mg/L) and tergitol (104 mg/L).

#### 2) Bacterial strains, incubation conditions and quantification of cell numbers

Bacteria were cultured and harvested in the same manner for each experiment. Pure strains of *Rhodococcus erythropolis* (*R. erythropolis*) (New Zealand Reference Culture Collection, ESR, Porirua, New Zealand) and *Pseudomonas putida* KT2442 (*P. putida* KT2442) (New Zealand Reference Culture Collection, Medical Section) were used in the study. These two bacterial strains were selected not only because they are commonly found in the natural soil environment, but also because of their different surface properties and ability to degrade organic pollutants (Dennis and Zylstra, 2004; Gottfried et al., 2010; Lang et al., 2016; Trzesicka-Mlynarz and Ward, 1995; Yang et al., 2014; Zhao et al., 2009). The seed stocks of the bacteria strains were prepared by mixing 0.5 mL of an overnight culture with 0.5 mL of sterile 50 % glycerol in a 1 mL sterile plastic tube, and then stored at -80 °C.

***R. erythropolis***: The water contact angle could indicate the hydrophobicity of bacterial surface: it is regarded that the water contact angle of hydrophilic bacteria is less than 45 °, vice versa. (Daffonchio et

al., 1995; Grotenhuis et al., 1992). *R. erythropolis* has a hydrophobic surface with a water contact angle of 94.7°. Its optimal growth temperature is 25~30 °C. A loopful of seed stock of *R. erythropolis* was taken and placed on tryptic soy (TS) agar plates and then incubated at 28 °C for 72 hours until visible colonies formed. To obtain enough bacterial cells, we then transferred *R. erythropolis* cells to new TS agar plates and incubated at 28 °C for 72 hours. At least four plates were prepared each time to ensure a sufficient quantity of cells could be harvested for each experiment. Bacteria cells were collected by using a moistened swab.

***P. putida* KT2442:** *P. putida* KT2442 has a water contact angle of 36.2°, indicating a hydrophilic surface. The optimal growth temperature for *P. putida* KT2442 is 25~30 °C. A loopful of the seed stock was taken and plated onto a TS agar plate, and placed in an incubator at 28 °C for 24 hours. After the bacterial cell colonies had formed, the bacterial agar plate was stored in a refrigerator at 4°C and kept for two weeks. To prepare bacteria for experiments, a colony of bacteria was taken from the agar plate and incubated overnight in 20 mL TS broth in 100 mL sterile flask at 28 °C, under constant shaking at 200 rpm. Then 20 mL of the bacteria solution was transferred to 2000 mL of fresh TS broth and incubated overnight at 28 °C, under constant shaking at 200 rpm. *P. putida* KT2442 cells were harvested by centrifugation at 8000 g for 10 minutes.

The harvested cells were washed three times with saline to remove soluble extracellular polymeric substance and finally resuspended in elute agent solution for further experiments. The initial concentration for batch and column experiment was  $3.5 \times 10^{10}$  CFU/mL and  $8.00 \times 10^9$  CFU/mL, for *P.putida* KT2442 and *R. erythropolis*, respectively. The number of bacteria was quantified by measuring the fluorescence signals of collected samples using a Perkin Elmer EnSpire 2300 multilabel plate reader and the Wallace Envision Manager software program. The details of the plate reader and CFU/mL measurements and results are provided in the appendix. A linear relationship was obtained between fluorescence intensity and CFU/mL, with a  $R^2$  value of 0.9597 (Figure A-1 in the appendix).

### 3.2.2. Interaction Energy Calculation and Surface Tension Parameters Measurement

This study only considered the LW-AB interactions between bacteria and sand particles because the addition of surfactant solution did not significantly affect the electrophoretic mobility of bacteria. The LW-AB interactions energy ( $\Delta G_{adh}$ ) can be calculated from the surface tension parameters as follows (Absolom et al., 1983; Busscher et al., 1984; Sharma and Hanumantha Rao, 2002; C. Van Oss, 1995):

$$\Delta G_{bls}^{LW} = -2\left(\sqrt{\gamma_b^{LW} \gamma_l^{LW}} + \sqrt{\gamma_s^{LW} \gamma_l^{LW}} - \sqrt{\gamma_b^{LW} \gamma_s^{LW}} - \gamma_l^{LW}\right) \quad (3-1)$$

$$\Delta G_{bls}^{AB} = 2\left(\sqrt{\gamma_l^+}(\sqrt{\gamma_b^-} + \sqrt{\gamma_s^-} - \sqrt{\gamma_l^-}) + \sqrt{\gamma_l^-}(\sqrt{\gamma_b^+} + \sqrt{\gamma_s^+} - \sqrt{\gamma_l^+}) - \sqrt{\gamma_b^+ \gamma_s^-} - \sqrt{\gamma_b^- \gamma_s^+}\right) \quad (3-2)$$

$$\Delta G_{adh} = \Delta G_{adh}^{LW} + \Delta G_{adh}^{AB} \quad (3-3)$$

where subscript  $b$  denotes bacteria,  $l$  denotes liquid,  $s$  denotes solid.

The three unknown surface free energy components,  $\gamma^{LW}$  (LW apolar component),  $\gamma^-$  (electron donor),  $\gamma^+$  (electron acceptor), in Equation 3-1 and 3-2 can be determined using the LW-AB approach and Yong's equation (Knox et al., 1993) with the contact angle measurements from three diagnostic liquids with known surface tension components. The contact angle measurement for bacteria followed the method used in a previous study (Feng et al., 2013a) where a homogenous bacterial lawn was prepared and then measured using a digital goniometer by dropping a diagnostic liquid on the bacteria lawn. Since quartz is the major component of silica sand, it also offers a homogeneous surface for estimating the surface hydrophobicity of silica sand. In this study, water contact angle and the free energy of bacteria aggregation were used to indicate the hydrophobicity of bacterial cell surfaces. Details of the contact angle measurements are provided in the appendix. Details of the calculation of the free energy of bacteria aggregation are provided in the appendix for Chapter 3.

### 3.2.3. Column Set-up and Bacteria Transport

A cylindrical stainless steel column (6.15 cm diameter (d) × 41 cm length (L)) was designed for the column experiments. The column has three aqueous sampling ports, termed Port 1, Port 2 and Port 3. Ports 1, 2 and 3 are located 3.0 cm, 15.5 cm and 30.5 cm from the bottom of the column, respectively (Figure 3-1). For each experiment, the column was packed with 1852.4 g of sterilized sand with particle size ranging from 0.0625 mm to 2 mm. The porosity ( $\theta$ ) of the packed column was 0.23 using gravimetric analysis. The column was pre-saturated by purging with 700 mL of eluent agent (e.g. water, rhamnolipid and tergitol) solution before each experiment. The purging direction was from the bottom to the top of the column as shown in Figure 3-1. After pre-saturation, 120 mL of bacterial suspension was introduced into the column at a flow rate of 3.0 mL min<sup>-1</sup>. The column was then eluted with a 700 mL solution of bacteria-free solution. Aqueous samples were collected from the three sampling ports and analyzed for bacteria transport. The effluent was collected up until the end of the experiment to determine the percentage of bacteria that was eluted out of the column. The concentration of bacteria (C) in the each sample was normalized to the initial concentration of bacteria (C<sub>0</sub>). The normalized concentration of bacteria (C/C<sub>0</sub>) was plotted against the actual pore volumes of eluent liquid agent that passed through the column, which is known as the breakthrough curve (BTC). All BTCs were averaged from two sets of experiments.

The actual pore volumes of eluent liquid agent that passed through the column at time t were calculated:

$$\text{Pore volume} = \frac{q \times t}{\pi \times \left(\frac{d}{2}\right)^2 \times L \times \theta} \quad (3-4)$$

where q is velocity in mL/min, t is time (minutes), d is the diameter of the column in cm, and  $\theta$  is the porosity of column.

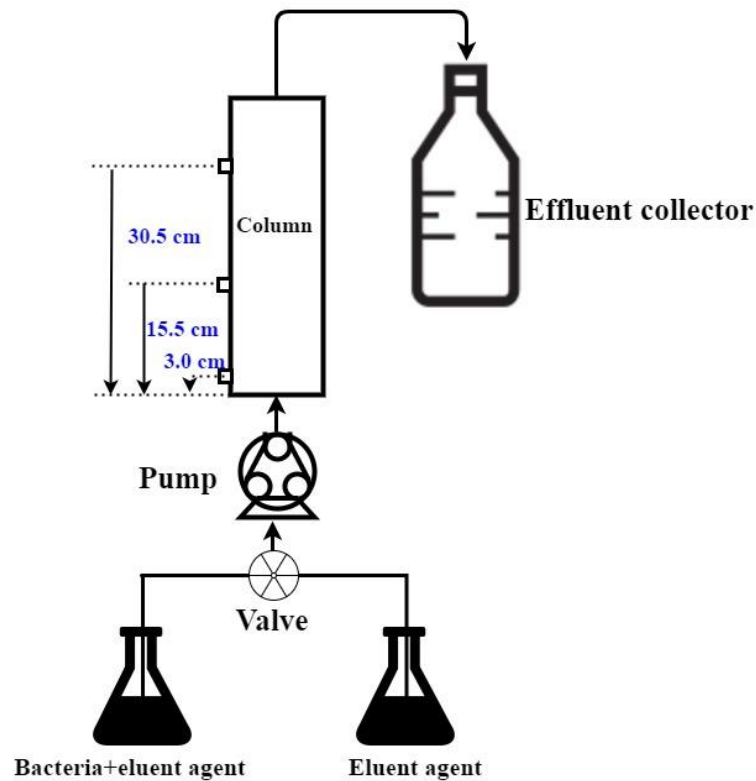


Figure 3-1 Column set up for the up flow pumping experiments

### 3.2.4. Mathematical Modeling

The mathematical model used in this study considered the transport of bacteria introduced into the column to be the result of convection and diffusion of the liquid due to the concentration gradient (Gang Chen and Zhu, 2004). We considered the bacteria to be transporting through a uniform, one-dimensional, saturated porous media, in other words at a steady-state flow, according to the one-dimensional convection-dispersion equilibrium equation (CDE) as follows (Van Genuchten and ALVES, 1982):

$$R \frac{\partial C}{\partial t} = D \frac{\partial^2 C}{\partial x^2} - v \frac{\partial C}{\partial x} - \mu C + \gamma \quad (3-5)$$

where  $C$  is the bacteria concentration,  $D$  is the dispersion coefficient (includes both diffusion and hydrodynamic dispersion),  $t$  is the time, and  $v$  ( $v=q/\epsilon$  ( $LT^{-1}$ )) is the average velocity inside the column. In this study, the equilibrium equation and nonequilibrium equation (information is provided in the appendix for Chapter 3) were solved by CXTFIT model in STANMOD (a Windows-based software package) (Parker and Van Genuchten, 1984), which has successfully predicted the adsorption and

Chapter 3. Effect of Rhamnolipid and Tergitol Surfactant on the Transport of *Rhodococcus erythropolis* and *Pseudomonas putida* in Saturated Sand Columns  
transport of *E. coli* and *P. fluorescens* (Gang Chen and Zhu, 2004). The parameters, dispersion coefficient ( $D$ ), retardation coefficient ( $R_d$ ), first order deposition coefficient ( $\mu$ ) and the coefficient of determination ( $R^2$ ), were estimated. All modeling was performed at zero initial concentration and zero production.

### 3.3. Results and Discussions

#### 3.3.1. The Modification of Surfactant on the Surface Tension Parameters of Bacteria and Sand Particles

The surface tension parameters of bacteria and sand particles were determined through contact angle measurement to understand the effect of surfactant on their respective surface hydrophobicities, as shown in Table 3-1. The ANOVA test suggests that the addition of different types of surfactant did not have a significant effect on the surface tension parameters ( $P > 0.05$ ). But, In terms of free energy of aggregation ( $\Delta G_{Iwl}$ ) that rhamnolipid and tergitol increased the value of  $\Delta G_{Iwl}$  from  $-81.6 \text{ mJ/m}^2$  to  $-56.6 \text{ mJ/m}^2$  and  $-70.2 \text{ mJ/m}^2$  (Table3-1). However, the surfactants made *P. putida* KT2442 less hydrophilic, as indicated by the decrease in the value of  $\Delta G_{Iwl}$  in the presence of rhamnolipid and tergitol, respectively (Table 3-1). Our findings are consistent with the study by Feng et al. (2013a), which found surfactant decreased the value of  $\Delta G_{Iwl}$  for hydrophilic *P. putida* 852 and reduced the value of  $\Delta G_{Iwl}$  for hydrophobic *R. erythropolis* 3586. The photomicrographs of *R. erythropolis* and *P. putida* KT2442 cell suspension in water and rhamnolipid solution provide a visual representation of the behaviours of the bacteria in the different suspension agents. Hydrophobic *R. erythropolis* cells were shown as more likely to aggregate in water (Figure 3-2A), but suspended more homogeneously in rhamnolipid solution (Figure 3-2B). No significant difference was observed for the aggregation of *P. putida* KT2442 in water and rhamnolipid solution (Figure 3-2 C and D). Table 3-1 also shows that rhamnolipid biosurfactant and tergitol increased the free energy aggregation  $\Delta G_{2w2}$  between water and quartz from  $-9.0$  to  $30.2$  and  $30.6 \text{ mJ/m}^2$ . This result is in line with observations by Chen et al. (2004) that the addition of rhamnolipid increased the surface free energy aggregation of silica sand. When comparing the effects of rhamnolipid and tergitol in modifying bacteria hydrophobicity, a greater

increase in the hydrophobicity of *R. erythropolis* was obtained with the addition of rhamnolipid, while a greater decrease in the hydrophilicity of *P. putida* KT2442 was obtained with the addition of tergitol. For quartz, different surfactant type demonstrated equivalent impact on its surface hydrophobicity. These results indicate that anionic and nonionic surfactant can modify bacterial hydrophobicity to a different extent, but have a similar modification on the hydrophobicity of sand particles.

**Table 3-1 Surface Tension Parameters  $\gamma^{LW}$  (LW apolar component),  $\gamma^-$  (electron donor),  $\gamma^+$  (electron acceptor) and free energy of aggregation ( $\Delta G$ ) (mJ/m<sup>2</sup>)**

Experimental Conditions			$\theta_{\text{water}} (^\circ)$	$\gamma^{LW}$ (mJ/m <sup>2</sup> )	$\gamma^-$ (mJ/m <sup>2</sup> )	$\gamma^+$ (mJ/m <sup>2</sup> )	$\Delta G_{I(2)w1(2)}$ (mJ/m <sup>2</sup> )
Bacteria	<i>R. erythropolis</i>	Water	94.7±0.3	34.1	0.8	0.11	-81.2
		Rhamnolipid	84.0±0.4	34.1	4.6	0.18	-56.6
		Tergitol	90.0±0.3	34.4	2.4	0.06	-70.2
	<i>P. putida</i> KT2442-GFP	Water	36.2±0.4	30.3	54.5	0.30	40.6
		Rhamnolipid	39.2±0.2	28.4	49.7	0.66	33.0
		Tergitol	39.7±0.5	38.5	38.8	0.62	15.5
Sand	Quartz	Water	46.7±1.3	38.6	22.4	2.86	-9.0
		Rhamnolipid	14.8±1.2	39.1	53.1	1.23	30.2
		Tergitol	14.1±1.6	39.6	53.4	1.15	30.6

Where subscript 1 denotos bacteria, 2 denotos sand and w denoteswater.

### 3.3.2. Comparison of the Transport of *R. erythropolis* and *P. putida* KT2442 in the Absence of Surfactant Solution

The transport of hydrophobic *R. erythropolis* and hydrophilic *P. putida* KT2442 in the absence of surfactant solution was investigated to assess the effect of the hydrophobicity of bacteria on their transport in the column (Figure 3-3A and Figure 3-4A). Firstly, 60.3 % and 76.7 % of total injected hydrophobic *R. erythropolis* and hydrophilic *P. putida* KT2442 respectively were eluted from the column. The peak height of BTCs of both bacteria strains decreased with increased travelling distance (Figure 3-3A and Figure 3-4A). The observed BTCs were fitted by nonequilibrium and equilibrium equation to further understand the bacteria transport behaviour. The value of beta ( $\beta$ ) in the nonequilibrium equation suggests that all the BTCs can fit through the equilibrium equation because

most of its value reaches 0.9999 (Table A-2 in appendix for Chapter 3). The fitted data from the equilibrium equation showed a good description of breakthrough curves with  $R^2 > 0.9270$  (Table 3-2). The fitted parameters (Table 3-2) for the hydrophobic and hydrophilic bacteria showed a similar pattern: the highest value of first order decay and the retardation was always observed at Port 1 and the values then decreased with increased travelling distance. These results are in line with those from a previous study (Gargiulo et al., 2008) where most of bacterial cells were retained close to the inlet of columns and the rate of deposition rapidly decreased with increasing in distance. The value of dispersion coefficient that was observed for the different ports was close, indicating that the column was packed at an acceptable level of homogeneity (G. Huang et al., 2006).

When comparing the fitted transport parameters, *R. erythropolis* presented a greater value for first order decay than *P. putida* KT2442 (Table 3-1). For example, the values of the first order decay ( $\mu$ ) for hydrophobic *R. erythropolis* were  $0.030 \pm 0.004$ /min,  $0.019 \pm 0.001$  /min and  $0.013 \pm 0.001$  /min respectively for Port 1, Port 2 and Port 3, while a smaller value of  $\mu$  was observed for hydrophilic *P. putida* KT2442 at each port,  $0.030 \pm 0.005$  /min,  $0.012 \pm 0.001$  /min and  $0.08 \pm 0.001$  /min for Port 1, Port 2 and Port 3, respectively. Compared to *R. erythropolis*, a greater value of retardation coefficient ( $R_d$ ) was obtained for *P. putida* KT2442 at each port. For example, *R. erythropolis* and *P. putida* KT2442 respective  $R_d$  values of  $1.08 \pm 0.03$  and  $1.73 \pm 0.06$  at Port 1. The retarded transport of hydrophilic bacteria is consistent with previous findings (McCaulou et al., 1994) that once hydrophilic bacteria were attached to the soil, they would re-suspend at a slow rate. Similarly, hydrophobic *R. erythropolis* had a smaller dispersion value with a smaller dispersion coefficient (D) than hydrophilic *P. putida* KT2442 (Table 3-2). These results indicate that hydrophilic bacteria are more likely to transport through columns.

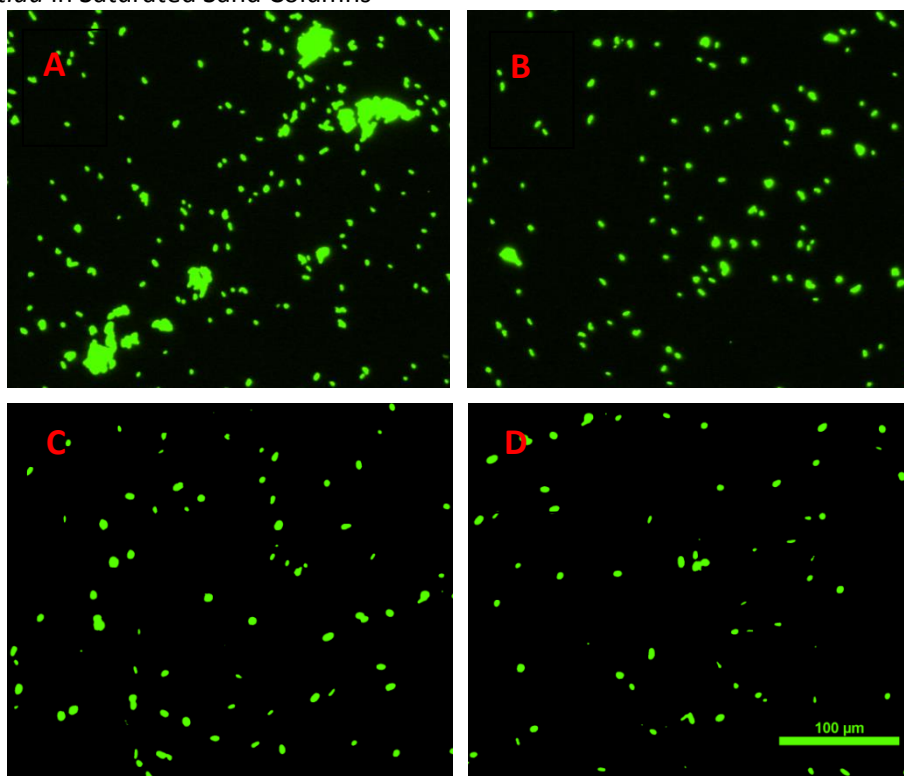


Figure 3-2 The aggregation of bacteria in water and rhamnolipid solution. A: *R. erythropolis* in water; B: *R. erythropolis* in rhamnolipid solution; C: *P. putida* KT2442 in water; D: *P. putida* KT2442 in rhamnolipid solution. Scale bar equals 100  $\mu\text{m}$

### 3.3.3. The Effect of surfactant Solution on the Transport of *R. erythropolis* and *P. putida* KT2442 Cells

Surfactants, anionic rhamnolipid and nonionic tergitol, were introduced in the column experiments to study the effect of surfactants on the transport behaviour of hydrophobic and hydrophilic bacteria. The BTCs (Figure 3-3B and C, and Figure 3-4B and C) obtained in the presence of surfactant solution present similar patterns to those for the absence of surfactant solution (Figure 3-3A and Figure 3-4A); namely, the peak height of BTCs decreased with increased travelling distance. The fitted data showed a good description of breakthrough curves with  $R^2 > 0.911$  (Table 3-2). In the presence of surfactant solution, the fitted parameters of both bacteria strains that were observed at different ports (Table 3-2) presented a similar pattern between different bacteria strains and surfatcnt types: the highest value of first order decay and the retardation is always observed at the Port 1 and their values decreased with the increase of travelling distance. This observation is simailr to the results that were obtained in the absence of surfactant solution.

**Hydrophobic *R. erythropolis*:** Rhamnolipid and tergitol solution increased the proportions of eluted *R. erythropolis* from 60.3% to 84.0% and 82.4%, respectively (Table 3-2). This observation shows that surfactants enhanced the transport of hydrophobic bacteria, which is consistent with the findings of several previous studies (G. Bai et al., 1997; Gang Chen et al., 2004; Parker and Van Genuchten, 1984; Vu et al., 2015). Moreover, in the presence of the surfactant solutions (Figure 3-3 B and C), the peak positions of BTC from Port 1 to Port 3 were higher than those in the absence of surfactant solution (Figure 3-3A). Aside from the peak position of the BTCs, a notable decrease in the value of the fitted first order deposition coefficient ( $\mu$ ) was observed with the addition of surfactant solution (Table 3-2). For example, the value of  $\mu$  decreased from  $0.030 \pm 0.005$  to  $0.010 \pm 0.003$  /min, from  $0.019 \pm 0.001$  to  $0.0001 \pm 0.001$  /min and from  $0.013 \pm 0.001$  to  $0.0001 \pm 0.0003$  /min at Port1, Port 2 and Port 3 following the introduction of rhamnolipid (Table 3-2). This result is consistent with previous findings that the addition of surfactants (e.g.  $C_{12}E_5$ ,  $C_{12}E_{10}$  and rhamnolipid) decreases the adsorption of bacteria (e.g. *E. coli*, *P. fluorescens* and *P. aeruginosa*) on sand particles (G. Bai et al., 1997; Gang Chen et al., 2004; Gang Chen and Zhu, 2004). The presence of surfactant solution also increased the dispersion coefficient (D). For example, D increased from  $0.05 \pm 0.02$  to  $0.15 \pm 0.02$  cm<sup>2</sup>/min, from  $0.20 \pm 0.04$  to  $0.24 \pm 0.02$  cm<sup>2</sup>/min and from  $0.11 \pm 0.01$  to  $0.25 \pm 0.03$  cm<sup>2</sup>/min for Port 1, 2 and 3, respectively, after the introduction of rhamnolipid (Table 3-2). An increase in retardation was observed at Port 1, where the value of the retardation coefficient ( $R_d$ ) increased from  $1.08 \pm 0.03$  to  $1.34 \pm 0.06$  and  $2.00 \pm 0.04$  in the presence of rhamnolipid and tergitol, respectively. No significant difference was found in the retardation coefficients for Port 2 and 3 with the addition of surfactant solutions (Table 3-2) (Table 3-2).

**Hydrophilic *P. putida* KT2442:** Both surfactant solutions had a similar effect on the transport behaviour of hydrophilic *P. putida* KT2442 (Figure 3-4B and C) compared to the findings for hydrophobic *R. erythropolis* (Figure 3-3B and C). The proportion of eluted bacteria increased from 76.7 % to 87.8 % and 85.7 % in the presence of rhamnolipid and tergitol, respectively. The value of  $\mu$  in BTCs decreased with the addition of surfactant solution. For example, the value of  $\mu$  decreased from  $0.030 \pm 0.005$  to  $0.007 \pm 0.004$  /min, from  $0.012 \pm 0.001$  to  $0.003 \pm 0.001$  /min and from  $0.008 \pm 0.001$  to

$0.004 \pm 0.001$  /min at Port 1, Port 2 and Port 3 after the introduction of rhamnolipid (Table 3-2). The dispersion coefficient (D) also increased with the addition of surfactant solution. For example, D increased from  $0.12 \pm 0.04$  to  $0.23 \pm 0.05$   $\text{cm}^2/\text{min}$ , from  $0.20 \pm 0.04$  to  $0.29 \pm 0.05$   $\text{cm}^2/\text{min}$  and from  $0.14 \pm 0.02$  to  $0.35 \pm 0.06$   $\text{cm}^2/\text{min}$  for Port 1, 2 and 3, respectively, after the introduction of rhamnolipid (Table 3-2). An increase in retardation was observed at Port 1, where the value of retardation coefficient ( $R_d$ ) increased from  $1.73 \pm 0.06$  to  $1.90 \pm 0.06$  and  $2.15 \pm 0.06$  in the presence of rhamnolipid and tergitol, respectively. No significant difference was found in the retardation coefficients for Port 2 and Port 3 with the addition of surfactant solutions (Table 3-2).

A comparison of the transport behaviour of hydrophobic and hydrophilic bacteria strains in the presence of surfactant solution reveals that generally the hydrophobic bacteria showed smaller values for D and  $R_d$ , and a higher  $\mu$  value than the hydrophilic bacteria, as shown in Table 3-1. Although both surfactants enhanced bacteria transport, a greater proportion of eluted bacteria was obtained in the presence of anionic rhamnolipid compared to nonionic tergitol surfactant. Smaller values for the first order decay retardation coefficient and dispersion coefficient were also observed in the presence of anionic rhamnolipid.

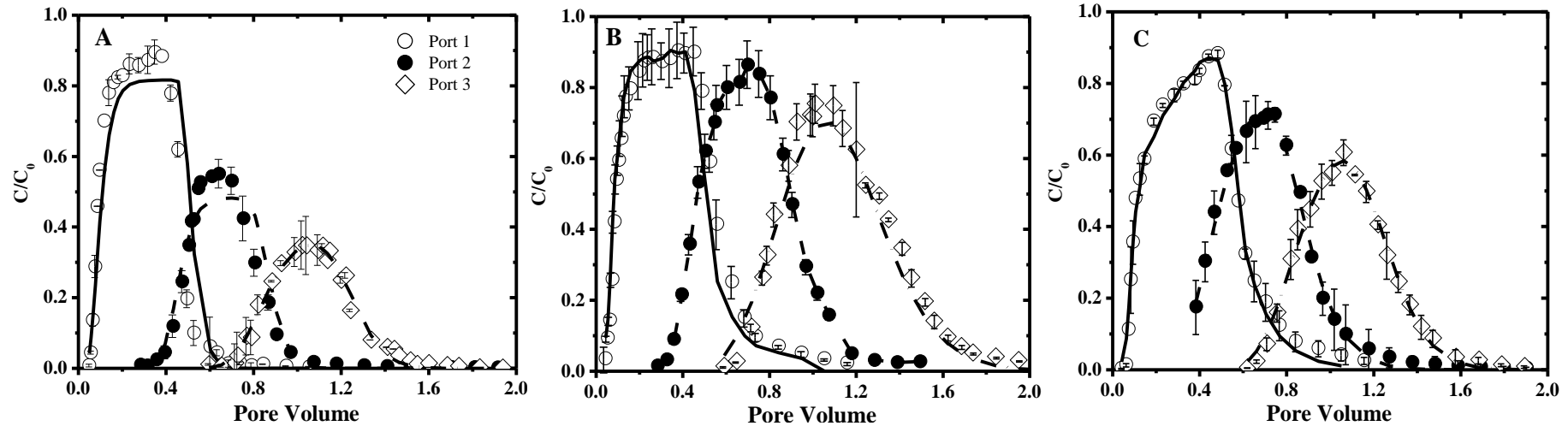


Figure 3-3 Comparison of the observed and fitted breakthrough curves of *R. erythropolis* in water and surfactant solution. A, B and C show BTCs in water, rhamnolipid solution and tergitol solution. O, ● and ◇ shows the data obtained at Port 1, Port 2 and Port 3, respectively; solid line, dash line and dash dots shows the fitted data at Port 1, Port 2 and Port 3, respectively. Symbols are averages of individual values (-) for experiments run in duplicate.

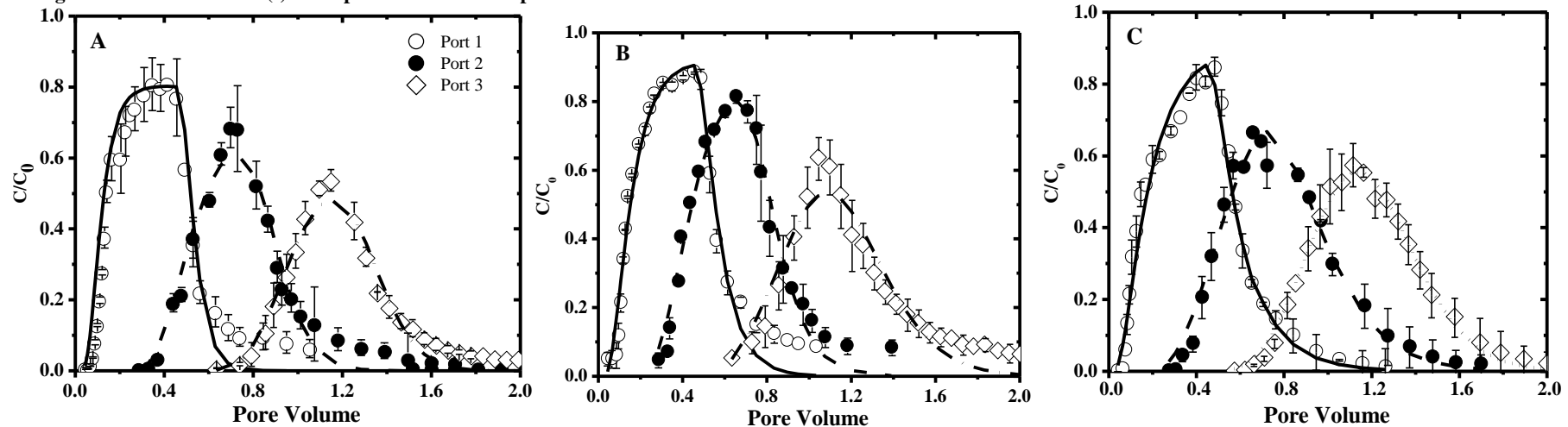


Figure 3-4 Comparison of the observed and fitted breakthrough curves of *P. putida* KT2442 in water and surfactant solution. A, B and C show BTCs in water, rhamnolipid solution and tergitol solution. O, ● and ◇ shows the data obtained at Port 1, Port 2 and Port 3, respectively; solid line, dash line and dash dots shows the fitted data at Port 1, Port 2 and Port 3, respectively. Symbols are averages of individual values (-) for experiments run in duplicate.

Chapter 3. Effect of Rhamnolipid and Tergitol Surfactant on the Transport of *Rhodococcus erythropolis* and *Pseudomonas putida* in Saturated Sand Columns

**Table 3-2 Comparison of the transport parameters that was fitted from BTCs of *R. erythropolis* and *P. putida* KT2442 by the equilibrium equation of CXTFIT in STANMOD. dispersion coefficient (D), retardation factor ( $R_d$ ), first order deposition ( $\mu$ ), the coefficient of determination ( $R^2$ ) and the proportion of bacteria that was eluted out of column**

Bacteria stains	Experiment condition	Port	D (cm <sup>2</sup> /min)	$R_d$	$\mu$ (/min)	$R^2$	The proportion of bacteria that was eluted out of column (%)
<i>R. erythropolis</i>	Water	1	0.05 ±0.02	1.08 ±0.03	0.031 ±0.004	0.961	60.3
		2	0.20 ±0.04	1.12 ±0.02	0.019 ±0.001	0.927	
		3	0.11 ±0.01	1.11 ±0.01	0.013 ±0.001	0.984	
	Rhamnolipid	1	0.25 ±0.08	1.34 ±0.06	0.010 ±0.003	0.932	84.2
		2	0.24 ±0.02	1.18 ±0.08	0.0001 ±0.001	0.990	
		3	0.25 ±0.03	1.14 ±0.01	0.0001 ±0.000	0.940	
	Tergitol	1	0.36 ±0.04	2.00 ±0.04	0.010 ±0.002	0.990	82.5
		2	0.26 ±0.02	1.22 ±0.01	0.006 ±0.004	0.995	
		3	0.19 ±0.02	1.11 ±0.01	0.005 ±0.0002	0.992	
<i>P. putida</i> KT2442	Water	1	0.14 ±0.04	1.73 ±0.06	0.030 ±0.005	0.952	76.7
		2	0.20 ±0.04	1.30 ±0.02	0.012 ±0.001	0.964	
		3	0.14 ±0.02	1.24 ±0.01	0.008 ±0.001	0.957	
	Rhamnolipid	1	0.23 ±0.05	1.90 ±0.06	0.007 ±0.004	0.960	87.8
		2	0.29 ±0.05	1.09 ±0.02	0.003 ±0.001	0.965	
		3	0.35 ±0.06	1.19 ±0.02	0.004 ±0.001	0.911	
	Tergitol	1	0.39 ±0.06	2.15 ±0.06	0.010 ±0.003	0.976	85.7
		2	0.47 ±0.06	1.41 ±0.02	0.002 ±0.001	0.975	
		3	0.30 ±0.02	1.24 ±0.01	0.003 ±0.002	0.990	

Estimated value ± standard deviation

### 3.3.4. Discussions

In this study, the filtration effect with regard to the retention of bacteria in the column was negligible because the ratio of the cell diameter to sand grain which ranged from 0.00025 to 0.032. According to Herzig et al. (1970) cell filtration by porous media is not considered to be effective when the ratio of cell diameter to porous media size is less than 0.05. The column experiments demonstrated that hydrophobic bacteria have a greater affinity to sand particles than hydrophilic bacteria in the absence of surfactant solution. This observation is consistent with previous literature reporting that more hydrophobic bacteria have a stronger affinity to soil during transport without surfactant solution (Gang

Chen et al., 2004; Gang Chen and Zhu, 2005; Gargiulo et al., 2008). The rhamnolipid and tergitol solutions made hydrophobic bacteria less hydrophobic and made hydrophilic bacteria less hydrophilic. If the hydrophobicity of bacteria is the driving force for bacteria transport, one might expect that the addition of surfactant solution would facilitate transport of hydrophobic bacteria but attenuate transport of hydrophilic bacteria. On the contrary, this study discovered that surfactant not only enhanced the transport of hydrophobic bacteria, but also hydrophilic bacteria which was not expected. This observation is in line with those of previous studies (G. Bai et al., 1997; Gang Chen et al., 2004; Gang Chen and Zhu, 2004; Zhong et al., 2016). Therefore, in the presence of surfactant solution, it is not possible to determine bacteria transport solely through bacterial hydrophobicity. As shown in Table 3-1, anionic and nonionic surfactant modified the surface properties of both bacteria and sand particles to different extents; therefore, the modification of both bacteria and sand particles should be considered. The LW-AB interactions which are based on the surface tension parameters of bacteria and sand particles may offer a possible explanation for the transport behaviour of the bacteria. The LW-AB interaction energies ( $\Delta G_{adh}$ ) were calculated to examine this hypothesis, as shown in Figure 3-5. In the absence of surfactants, the value for  $\Delta G_{adh}$  between *R. erythropolis* and sand particles was  $-34.6 \text{ mJ/m}^2$ , indicating a favorable adhesion of *R. erythropolis* to sand particles according to the definition used. Consistent with previous findings (Gang Chen et al., 2004), the addition of rhamnolipid and tergitol increased the value of  $\Delta G_{adh}$  to  $-5.9 \text{ mJ/m}^2$  and  $-10.0 \text{ mJ/m}^2$ . However, a positive value of  $\Delta G_{adh}$  ( $10.0 \text{ mJ/m}^2$ ) was obtained between hydrophilic *P.putida* KT2442 and sand particles. The value of  $\Delta G_{adh}$  increased to  $32.6 \text{ mJ/m}^2$  and  $23.7 \text{ mJ/m}^2$  with the addition of rhamnolipid and tergitol, indicating less favourable adhesion of *P.putida* KT2442 to sand particles in the presence of surfactant solutions.

Despite hydrophobic bacteria showing an attractive LW-AB interaction (negative value) with sand particles while hydrophilic bacteria showed a repulsive LW-AB interaction (positive value), surfactant increased the value of the LW-AB interaction energy thereby weakening the attraction between hydrophobic bacteria and sand particles and enhancing the repulsive LW-AB interaction between

hydrophilic bacteria and sand particles. As a result, bacteria transport was enhanced in the presence of surfactant solution.

To gain a clearer picture of the effect of  $\Delta G_{adh}$  on bacteria transport, the percentage of bacteria that was eluted out of columns and the first order decay were plotted against the value of  $\Delta G_{adh}$  (Figure 3-6). The the percentage of bacteria that was eluted out of column rises with the increase of  $\Delta G_{adh}$  while the value of the first order decay decreases with the increase of  $\Delta G_{adh}$ . These results could explain the facilitated bacteria transport found with the addition of surfactant solution. The effect of different surfactant type on the bacteria transport can be attributed to the fact that the extent of change in the value of  $\Delta G_{adh}$  is dependent on the surfactant type and the surface properties of surfactant itself. In this study, a higher value of  $\Delta G_{adh}$  was obtained in the presence of the anionic rhamnolipid compared to the corresponding value in the presence of the nonionic tergitol for both bacterial strains, as shown in Figure 3-5. Figure 3-7 shows the correlation of bacterial surface tension parameters ( $\gamma_1^{LW}$  and  $\gamma_1^-$ ) to the LW-AB interaction energy between bacteria and sand particles. An increase in the value of  $\gamma_1^{LW}$  results in a decrease in the value of  $\Delta G_{bis}^{LW}$ , while the value of  $\Delta G_{bis}^{AB}$  increases with an increase in the value of  $\gamma_1^-$ . Although no linear relationship was found due to the small sample size, these findings may help us to understand the interaction and adhesion of bacteria to solid surfaces.

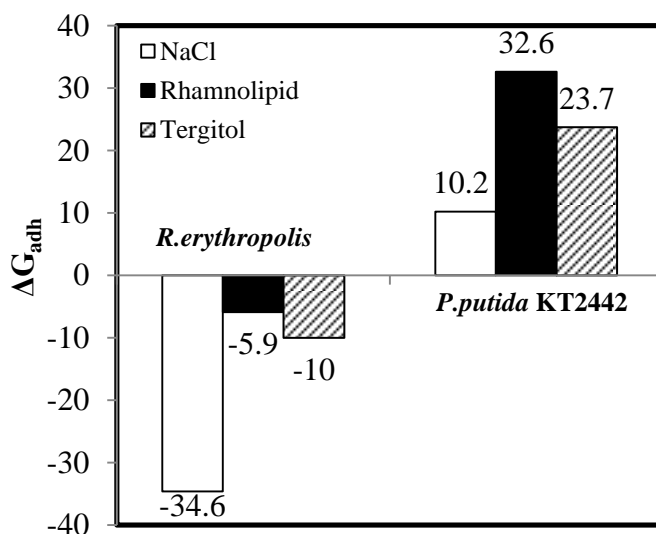


Figure 3-5 The changes in  $\Delta G_{adh}$  between bacteria and sand particles with the addition of rhamnolipid and tergitol

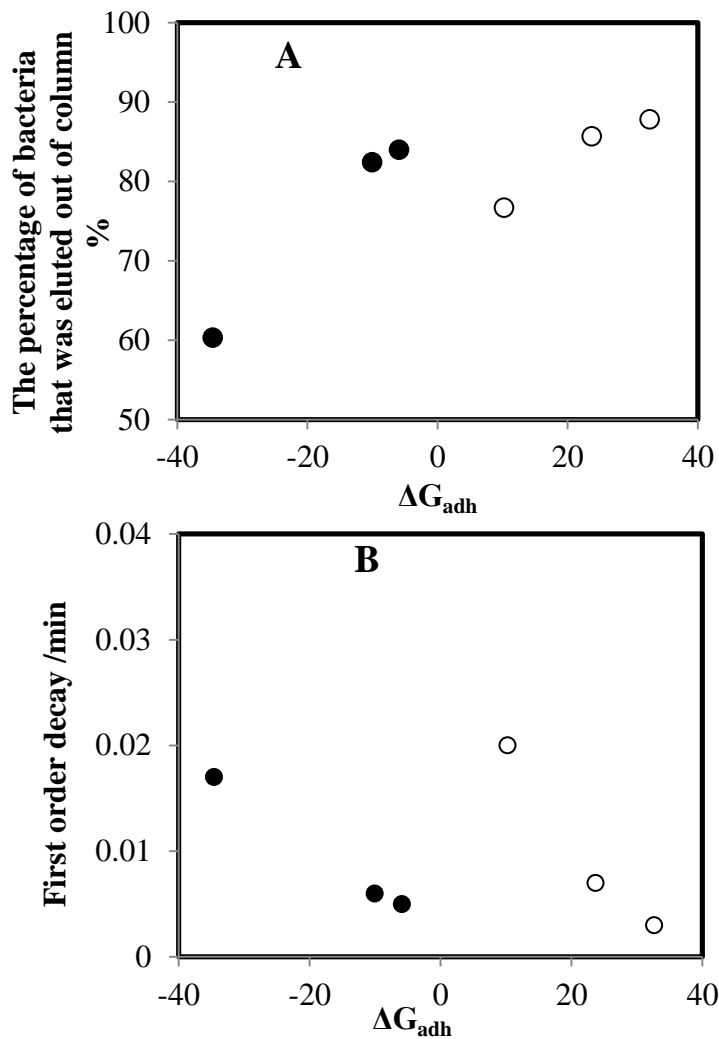
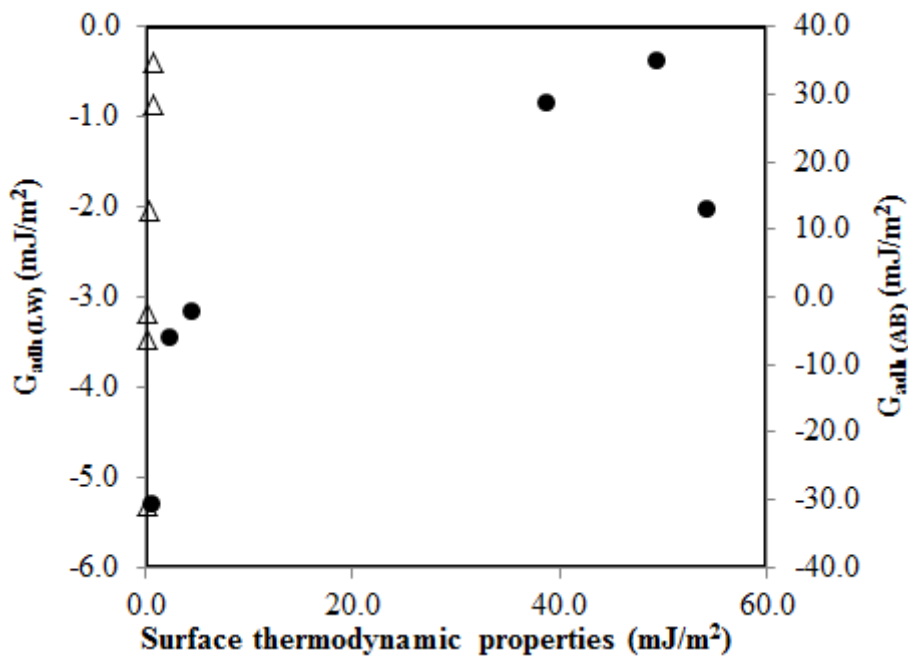


Figure 3-6 The correlation of the percentage of bacteria that was eluted out of columns and the averaged first order decay to

$\Delta G_{adh}$ . ●: *R. erythropolis*; ○: *P. putida* KT2442.



### 3.4. Conclusion

This study investigated the modification of surfactant (anionic vs. nonionic) on the surfaces hydrophobicity of bacteria (hydrophobic vs. hydrophilic) and sand particles, and the effect of these modifications on the transport behaviour of bacteria in a saturated sand column. Rhamnolipid and tergitol altered bacterial hydrophobicity to differing extents but had an equivalent effect on the hydrophobicity of sand particles. The addition of surfactant increased the LW-AB interaction energy between bacteria and sand particles. Without surfactant solution, hydrophilic bacteria are therefore more likely to transport through the column than hydrophobic bacteria. The increase in the value of LW-AB interaction energy between bacteria and sand particles enhanced the transport of both bacteria strains when using surfactants as the effluent agent. The higher value of LW-AB interaction energy in the presence of rhamnolipid compared to tergitol is shown to enhance bacteria transport differently.

This study is possibly the first document to compare and consider the modification of surfactants on both bacteria and sand particles by investigating the effect of anionic and nonionic surfactant on the transport behaviour of both hydrophobic and hydrophilic bacteria. The findings from this study could be used to shed light on ways of successfully matching bacteria with surfactants, mainly when introducing microorganisms to contaminated sites during bioremediation. As only two bacteria strains and two types of surfactant solution were used in this study, more information would be required to generalise these findings to achieve a more accurate and realistic prediction of bacterial behaviour in the soil.

### Acknowledgments

This research was supported by funding from University of Auckland (New Zealand) and China Scholarship Council (China).

**Chapter 4. Upward Transport of *Rhodococcus erythropolis* and *Pseudomonas putida* with Continuously Injected Microbubble in Sand Column: the Role of Microbubble Generation Method, Surfactant Type, Bacterial Hydrophobicity and the Porosity of Sand Column**

To be submitted to Journal of Water Resources Research

Wei Tao<sup>a</sup>, Yantao Song<sup>a</sup>, Simon Swift<sup>b</sup> and Naresh Singhal<sup>a,\*</sup>

<sup>a</sup> Department of Civil and Environmental Engineering, <sup>b</sup> School of Medical Sciences, The University of Auckland, Private Bag 92019, Auckland 1010, New Zealand.

\*Corresponding author:

FAX: +64 9 373 7462

Phone: +64 9 923 4512

Email:n.singhal@auckland.ac.nz

## **Abstract**

Delivering bacteria and oxygen to contaminated soil using pulse injected microbubbles has been studied for the purpose of stimulating aerobic biodegradation for *in situ* bioremediation. However, no study has employed continuously supplied microbubbles for delivering bacteria to the soil, which is potentially a highly promising and cost-efficient strategy for providing bacteria and oxygen. This study investigated the use of continuously injected microbubbles to deliver bacteria in artificial sand columns with a porosity of 0.23 and 0.38, respectively. Hydrophobic bacteria *Rhodococcus erythropolis* (*R. erythropolis*) and hydrophilic bacteria *Pseudomonas putida* (*P. putida*) were chosen for the study. Two types of surfactant (anionic rhamnolipid vs. nonionic tergitol) microbubbles were used as eluting agents. The preliminary batch experiments found that microbubbles that were produced by a flat spinning disc mixer are more stable than those generated by a propeller mixer. Rhamnolipid microbubbles were shown to be more stable and had greater ability to carry bacteria than tergitol microbubbles. No impact on the stability of microbubbles was observed when adding bacteria to microbubble suspension. Hydrophilic bacteria showed slightly stronger affinity to microbubbles during microbubble drainage compared to hydrophobic bacteria. Microbubbles eluted a higher percentage of bacteria out of the column than surfactant solution to do so, when the same amount of surfactant solution was used. Microbubbles that were generated by the flat spinning disc mixer eluted higher percentages of bacteria out of columns than microbubbles that were produced by the propeller mixer ones to do so. Rhamnolipid microbubbles eluted a greater proportion of the total injected bacteria than the tergitol microbubbles, because the rhamnolipid microbubbles were more stable and have greater affinity for bacteria. Hydrophilic *P. putida* was found more likely to transport with microbubbles than hydrophobic *R. erythropolis* due to the favourable adhesion of hydrophobic *R. erythropolis* to sand particles. Bacteria transport increased considerably with an increase in porosity inside the column. This information can facilitate our understanding of bacteria transport using continuously injected microbubble suspensions.

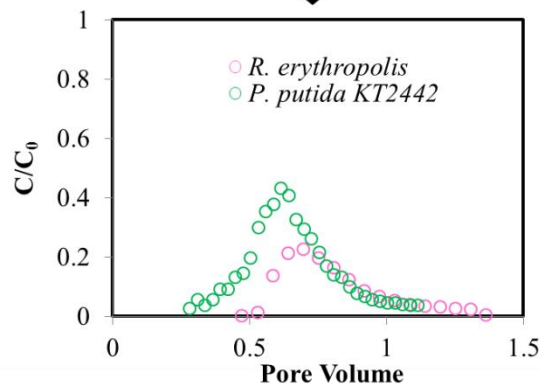
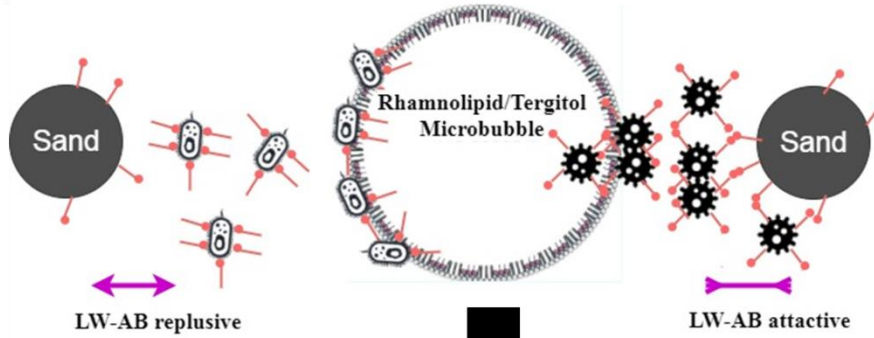
Chapter 4. Upward Transport of *Rhodococcus erythropolis* and *Pseudomonas putida* with Continuously Injected Microbubble in Sand Column

**Keywords:** Bacteria Transport, Continuously injected microbubble, Anionic and nonionic surfactant, Stability, Bacterial hydrophobicity, Porosity

**Graphical abstract**

Hydrophilic *P. Putida* KT2442

Hydrophobic *R. erythropolis*



## 4.1. Introduction

Introducing exogenous microorganism to contaminated soil is a commonly used approach (Romantschuk et al., 2000; Scullion, 2006; Van Hamme, 2004) for *in situ* bioremediation because this activity can expand the population of bacteria that available to degrade pollutants. Previous studies have used surfactant solution to deliver bacteria to soil to overcome the low mobility of bacteria under natural conditions (Gang Chen et al., 2004; Gang Chen and Zhu, 2004; Spasojević et al., 2015; Xiao-Hong et al., 2010; Zhong et al., 2016; Zhu et al., 2013). Although surfactant solution can be effective in promoting bacteria transport, the use of surfactant solution for stimulating *in situ* bioremediation is challenged by factors such as the shortage of oxygen in contaminated soil and the amount of surfactant solution required. Therefore, developing a new strategy to deliver both bacteria and oxygen for bioremediation of contaminated soil in a cost-effective manner is required.

Surfactant microbubbles, suspensions of a large number of minute spherical gas bubbles encapsulated in a soapy liquid film in an aqueous surfactant solution (Sebba, 1987), have emerged as a potential vehicle to carry bacteria and oxygen for *in situ* bioremediation, due to their unique characteristics, e.g. large interfacial areas to adsorb microorganisms (Jauregi and Varley, 1999; Parker, 1989; M. Ripley et al., 2002; Wan et al., 1994), small size (10~100  $\mu\text{m}$ ) (Feng et al., 2009; Jauregi et al., 2000), excellent flow properties (Sebba, 1985) and small buoyant rise velocities. A few laboratory studies have investigated the capacity of pulse injected microbubbles for delivering bacteria/nanoparticles to soil (Andrew Jackson et al., 1998; Park et al., 2009; Shen et al., 2011; Su et al., 2014). Microbubbles were found more cost-efficient compared to surfactant solution alone, because microbubble-aided bacteria transport required smaller amount of surfactant solution to deliver the same number of bacteria to soil (Andrew Jackson et al., 1998). The efficiency of microbubbles as bacteria carriers of can be affected by factors such as the stability of microbubbles, the pore size of soil, and the hydrophobicity of bacteria. The the stability of microbubbles could be affected by surfactant type (Feng et al., 2009; Shen et al., 2011) and method used for microbubble generation (Jauregi et al., 1997; Sebba, 1985). Microbubbles generated from anionic surfactant (e.g. sodium lauryl ether sulphate (SLES) and sodium dodecyl sulfate)

are more stable and has greater ability in retaining nanoparticles than nonionic surfactant (e.g. Tween 20 and Triton X-100) microbubbles to do so (Ding et al., 2013; Shen et al., 2011). In column experiments, anionic surfactant microbubbles generally demonstrated better ability to carry nanoparticles compared to nonionic surfactant microbubbles (Ding et al., 2013; Shen et al., 2011). Microbubble dispersion was also more efficient in sand columns with a coarse pore size of 0.18~0.51 mm than a finer pore size of 0.09~0.18 mm (Ding et al., 2013; Shen et al., 2011). However, in another study microbubbles were better able to penetrate finer sand with a pore size of 0.10~0.20 mm than more coarse sand with a pore size of 0.20~0.57 mm (Su et al., 2014). Bacterial hydrophobicity can affect bacterial adhesion to sand particles and air–water interfaces. For example, hydrophobic bacteria have a stronger affinity to both soil particles and gas-liquid interfaces than hydrophilic bacteria to do so (Gang Chen and Zhu, 2004; Huysman and Verstraete, 1993; Su et al., 2014). However, the effect of these tendencies on bacteria transport for bacterial adhesion to sand particles and air-water interfaces has not yet been investigated. Besides their ability to carry bacteria, microbubbles can also stimulate aerobic biodegradation of organic pollutants in contaminated soil by supplying oxygen (Kristen B Jenkins et al., 1993; D. Michelsen et al., 1984; Catherine N Mulligan and Farzad Eftekhari, 2003; Park et al., 2009; Rothmel et al., 1998). For example, in one of the studies, higher phenanthrene degradation was achieved at the bottom of the column due to the higher gas phase concentration (84%) compared to that at the top of the column where the gas phase concentration was 10% (Park et al., 2009). The relative residual of phenanthrene decreased from 80% to 40% at the bottom of the column, but increased slightly at the top of the column after 21 days (Park et al., 2009). Therefore, *in situ* bioremediation could potentially be enhanced by applying more gas into contaminated soil. Further, continuous injection of microbubbles could provide more air than pulse injected ones. If these continuously supplied microbubbles can deliver bacteria efficiently to contaminated soil, *in situ* bioremediations would be greatly enhanced, and in a cost-effective manner. However, the research on delivering bacteria with continuously supplied microbubbles is very limited and no data have been published to date.

The purpose of this study is to investigate bacteria delivery with continuously supplied microbubbles in sand columns, and explore the effect of microbubble generation method, surfactant type, bacterial hydrophobicity and the porosity of sand column. Two mixers, a propeller and a flat spinning disc, were used to generate microbubble of different stability. Anionic rhamnolipid and nonionic tergitol were used to produce microbubbles and to assess their capability for carrying bacteria. Gram-positive *Rhodococcus erythropolis* and Gram-negative *Pseudomonas putida* were used to represent hydrophobic and hydrophilic bacterial strains in this study. Preliminary batch tests were conducted to examine properties of microbubbles and the capacity of the microbubbles in carrying bacteria. Packed column studies were carried out to explore the microbubble-aided bacteria transport in columns at porosities of 0.23 and 0.38, respectively. Bacteria transport was quantified based on the percentage of bacteria that was eluted out of the column and the dispersion coefficients from the breakthrough curves (BTCs) of bacteria transport. Lifshitz-van der Waals and acid-base (LW-AB) interaction energy between bacteria and sand particles, bacteria and microbubbles were calculated to understand the transport behaviour of bacteria. A fluorescence microscope was employed to visualize the behaviour of bacteria in the presence of microbubbles. The results of this study can serve as a preliminary exploration of bacteria delivery using continuous microbubble supply.

## **4.2. Materials and Method**

### **4.2.1. Surfactants Selection**

Anionic surfactant rhamnolipid (JBR 210, JENEIL ® Biosurfactant Co.) was used as the biosurfactant in this study. It is a rhamnose-containing glycolipid surfactant that is primarily produced by *Pseudomonas aeruginosa* (Desai and Banat, 1997). Nonionic surfactant Tergitol-15-S-12 (Sigma-Aldrich) was applied for the purpose of making comparisons with anionic rhamnolipid. Rhamnolipid and tergitol were chosen because they are readily biodegradable and environmentally friendly (J.-L. Li and Chen, 2009) and show low toxicity to bacteria (J.-L. Li and Chen, 2009; Rothmel et al., 1998; Zhang et al., 1997; Zhu et al., 2013).

#### 4.2.2. Microbubble Generation and Tests

Microbubble generation followed the method that was described by Sebba (1985). Two mixers were employed in this study to generate microbubble at a speed of 8000 rpm. The first mixer uses a propeller to intensify the mixing. The second mixer (VIRTIS® Tempest Virtishear I.Q. with SENTRY® Microprocessor) employed a flat spinning disc to shear the surface of the surfactant solution to generate microbubbles. The concentration of surfactant used was 1000 mg/L, the microbubble generated at this concentration is relatively stable and cost-efficient (Feng et al., 2009).

The half-time of microbubble drainage was recorded to represent the stability of microbubble. The freshly generated microbubble was transferred into a 100 mL cylinder and then the volume of microbubble suspension and drained liquid over a range of time between 0 to 20 minutes was recorded. Halt-time is the time when half of the total volume of liquid ( $V_L$ ) was drained from the microbubble dispersion. The microbubble gas fraction was quantified as the ratio of bubble volume ( $V_M$ ) to total volume ( $V_{M+L}$ ). Likewise, liquid fraction can be expressed as the proportion of  $V_L$  to  $V_{M+L}$ . A microscope was employed to capture the drainage of microbubble suspension with a camera (Nikon ECLIPSE E600, Japan) and the Image J program was used to analyze the image size.

The distribution of bacteria in microbubbles over time was measured to investigate ability of microbubbles in carrying bacteria. Microbubble was produced by shearing 180 mL of surfactant solution with bacterial cells, after which 100 mL of fresh microbubbles were added to a series of 100 mL cylinders ( $M_{total}$ ). The volume of drainage ( $V_L$ ) and microbubble ( $V_M$ ) was recorded over for times ranging from 0 minutes to 20 minutes. 0.5 mL of drained liquid was taken from the cylinder to further examine the number of bacterial cells ( $C_L$ ) in the drained liquid. The fraction of bacteria in microbubble ( $C_M$ ) was calculated:

$$C_M = \frac{M_{total} - C_L \times V_L}{V_M} \quad (4-1)$$

### 4.2.3. Bacterial Strains and Incubation Condition

Bacteria were cultured and harvested in the same manner for each experiment. Pure strains of *Rhodococcus erythropolis* (Gram positive) (New Zealand Reference Culture Collection, ESR, Porirua, New Zealand) (*R. erythropolis*) and *Pseudomonas putida* KT2442 (Gram negative) (New Zealand Reference Culture Collection, Medical Section) (*P. putida* KT2442) were used in this study. These two bacterial strains were selected not only because they are commonly found in the natural soil environment, but also because of their different surface properties and ability in degrading organic pollutants, such as polyaromatic hydrocarbons (Dennis and Zylstra, 2004; Gottfried et al., 2010; Lang et al., 2016; Trzesicka-Mlynarz and Ward, 1995; Yang et al., 2014; Zhao et al., 2009). The seed stocks of bacteria strains were prepared by mixing 0.5 mL of an overnight culture with 0.5 mL of sterile 50 % glycerol in a 1 mL sterile plastic tube and were stored at -80 °C.

***R. erythropolis*:** Water contact angle could indicate the hydrophobicity of bacterial surface: the water contact angle of hydrophilic bacteria is less than 45 °; vice versa (Daffonchio et al., 1995; Grotenhuis et al., 1992). *R. erythropolis* has a hydrophobic surface with a contact angle of 94.7 °. The optimal growth temperature is 25~30 °C. A loopful of seed stock of *R. erythropolis* was taken and placed on a trypticase soy (TS) agar plates and then incubated at 28 °C for 72 hours until visible colonies formed. To obtain enough bacterial cells, we transferred *R. erythropolis* cells to new TS agar plates and again incubated at 28 °C for 72 hours. At least four plates were prepared each time to ensure a sufficient quantity of cells could be harvested for each experiment. Bacteria cells were collected using a moistened swab.

***P. putida* KT2442:** *P. putida* KT2442 has a water contact angle of 36.2 °, indicating a hydrophilic surface. The optimal growth temperature is 25~30 °C. A loopful of the seed stock was taken and plated onto TS agar plates, and then placed in the incubator at 28 °C for 24 hours. After the bacterial cell colonies had formed, the bacterial agar plate was stored in a refrigerator at 4°C and kept for two weeks. To prepare bacteria for experiments, a colony of bacteria was taken from the agar plate and incubated overnight in 20 mL TS broth in a 100 mL sterile centrifuge tubes at 28 °C, under constant shaking at

200 rpm. Then 20 mL of the bacteria solution was transferred to 2000 mL of fresh TS broth and incubated overnight at 28 °C, under constant shaking at 200 rpm. *P. putida* KT2442 cells were harvested by centrifugation at 8000 g for 10 minutes.

Harvested cells were washed three times with saline to remove soluble extracellular polymeric substance and finally resuspended in 0.01M NaCl surfactant solution for the further experiments. The initial concentration for batch and column experiment was  $8.00 \times 10^9$  and  $3.5 \times 10^{10}$  CFU/mL for *R. erythropolis* and *P. putida* KT2442, respectively. The number of bacteria was quantified by measuring the fluorescence signals of the collected samples using a Perkin Elmer EnSpire 2300 multilabel plate reader and the Wallace Envision Manager software program. The experimental details are provided in the appendix. A linear relationship was obtained between fluorescence intensity and CFU/mL, with a  $R^2$  value of 0.9579 (Figure A-1 in the appendix).

#### 4.2.4. Column Set-up

A cylindrical stainless steel column (6.15 cm diameter (d)  $\times$  41 cm length (L)) was designed for column experiments (Figure 4-1). This column had three aqueous sampling ports, termed Port 1, Port 2 and Port 3. The three ports are located at 3.0 cm, 15.5 cm and 30.5 cm from the bottom of the column, respectively. The size of sand particles for the column studies ranged from 0.0625-2 mm with mean size of 0.8050 mm. The purpose of choosing a broad range of grain size was to simulate the real soil environment. Columns were packed with different porosity  $\theta$  (0.23 vs. 0.38) to investigate the effect of the porosity of the column on the microbubble-aided bacteria transport.  $\theta$  describes the fraction of void space in the column, it is defined by the ratio:

$$\theta = \frac{V_w}{\pi \times \left(\frac{d}{2}\right)^2 \times L \times \theta} \quad (4-2)$$

where  $V_w$  is the volume of void-space inside the column which is measured as the difference between the wet weight and dry weight of the packed column.

In this study, for the column with a porosity of 0.23 and 0.38, the volume of the void-space is 280.3 mL and 457.7 mL, respectively. According to Kovscek and Bertin (2003), a column with a porosity 0.24 can be defined as a low-permeable column while a column with a porosity of 0.38 can be defined as a high-permeable column. *Kozeny's* equation (Skorokhod et al., 1988) was used to calculate the mean pore size inside the column:

$$\overline{D}_{po} = \frac{2}{3} \frac{\theta}{1-\theta} \overline{D}_{pa} \quad (4-3)$$

where  $\overline{D}_{po}$  is the mean pore size,  $\overline{D}_{pa}$  is the mean particle size, and  $\theta$  is the porosity of the column.

#### 4.2.5. Bacteria Transport in Columns

In all the column studies for bacteria transport with microbubbles, the column was pre-saturated with 700 mL of surfactant solution to eliminate the effects of surfactant concentration on the quality of microbubbles. The direction of purging was from the bottom to the top of the column, as shown in Figure 4-1. The column was then purged with bacteria-free microbubbles over 3 hours until the same air to water ratio was obtained at the inlet and outlet of the column. Microbubbles with bacteria were pumped into columns at a flow rate of 3 mL/min for 40 minutes, and the eluting agent then switched to bacteria-free microbubbles. Samples were collected from three sampling ports from 0 to 600 minutes and analyzed using the method described in Section 4.2.3. The effluent was collected until the end of the experiment for the determination of the proportion of bacteria that was eluted out of the column.

Bacteria transport with surfactant solution was also conducted to compare its efficiency in bacteria delivery with the efficiency of surfactant microbubble. In the surfactant solution-aided bacteria transport, the column was pre-saturated by purging with 700 mL of surfactant solution (e.g. rhamnolipid and tergitol) before each experiment. After pre-saturation, surfactant solution with bacteria was introduced into the column at a flow rate of 3.0 mL/min for 40 minutes. Samples were collected from three sampling ports from 0 to 300 minutes and analyzed using the method described in Section

4.2.3. The concentration of bacteria (C) in the each sample was normalized to the initial concentration of bacteria (C<sub>0</sub>). A dimensionless time was expressed as actual pore volumes of liquid that passed through the column at time t:

$$\text{Pore volume} = \frac{q \times t \times \mathcal{G}}{\pi \times \left(\frac{d}{2}\right)^2 \times L \times \theta} \quad (4-4)$$

where q is the pumping velocity. t is time (minutes).  $\mathcal{G}$  is the liquid proportion in microbubbles. The value of  $\mathcal{G}$  equalled 1 in the column studies using surfactant solution.

In this study, the normalized bacterial concentration (C/C<sub>0</sub>) was plotted against pore volume, which is known as the breakthrough curve (BTC). All BTCs were averaged from two sets of experiments.

#### 4.2.6. Calculation and Visualization of Microbubble-bacteria Interaction

In this study, the concentration of both rhamnolipid and tergitol used were well above their critical micelle concentration of 40 mg/L and 104 mg/L respectively. It was assumed that surfactant molecules would be closely packed to form a layer outside of the air bubble (Sebba, 1987), as shown in Figure 4-2, and that the bacteria would interact with microbubble through the surfactant layer. Because the high-speed stirring would have moved the bacteria closer to the surfactant layer of the microbubble, the adhesion of bacteria to microbubbles could be calculated using the Lifshitz-van der Waals (LW) and the acid-base (AB) approach. LW-AB interaction energy was also considered between bacteria and sand particles because the addition of surfactant solution did not significantly affect the electrophoretic mobility of bacteria. The LW-AB interaction energy ( $\Delta G_{adh}$ ) between bacteria and microbubble/sand particles can be calculated from the surface tension parameters as follows (Absolom et al., 1983; Busscher et al., 1984; Sharma and Hanumantha Rao, 2002; C. Van Oss, 1995):

$$\Delta G_{bls(m)}^{LW} = -2(\sqrt{\gamma_b^{LW} \gamma_l^{LW}} + \sqrt{\gamma_{s(m)}^{LW} \gamma_l^{LW}} - \sqrt{\gamma_b^{LW} \gamma_{s(m)}^{LW}} - \gamma_l^{LW}) \quad (4-5)$$

$$\Delta G_{bls(m)}^{AB} = 2(\sqrt{\gamma_l^+} (\sqrt{\gamma_b^-} + \sqrt{\gamma_{s(m)}^-} - \sqrt{\gamma_l^-}) + \sqrt{\gamma_l^-} (\sqrt{\gamma_b^+} + \sqrt{\gamma_{s(m)}^+} - \sqrt{\gamma_l^+}))$$

$$-\sqrt{\gamma_b^+ \gamma_{s(m)}^-} - \sqrt{\gamma_b^- \gamma_{s(m)}^+} \quad (4-6)$$

$$\Delta G_{bls(m)} = \Delta G_{bls(m)}^{LW} + \Delta G_{bls(m)}^{AB} \quad (4-7)$$

where subscript *b* denotes bacteria, *l* denotes liquid, *s* denotes solid, *m* denotes microbubble.

The three unknown surface free energy components,  $\gamma^{LW}$  (LW apolar component),  $\gamma^-$  (electron donor),  $\gamma^+$  (electron acceptor), in Equation 4-5 and 4-6 can be determined by using the LW-AB approach and Yong's equation (Knox et al., 1993) and contact angle measurement using three diagnostic liquids with known surface tension components. The contact angle measurement used were based on a previous study (Feng et al., 2013a) where a homogenous bacterial lawn was prepared and measured by a digital goniometer after dropping a diagnostic liquid on the bacteria lawn. Quartz was used as a model surface for the estimation of the surface hydrophobicity of silica sand because it is the major component of silica sand. Details of the contact angle measurements are provided in the appendix. The contact angle results are provided in the appendix (Table A-1).

A fluorescence microscope with a camera (Nikon ECLIPSE E600, Japan) was employed to visualize the adhesion of bacteria to microbubble. Bacteria were cultivated, harvested, prepared and suspended in the surfactants solutions. After microbubble had been generated, a sample of microbubble dispersion with bacteria was transferred to a cavity glass slides and covered with a coverslip. The bacteria in the microbubble sample were then visualized using the fluorescence microscope.

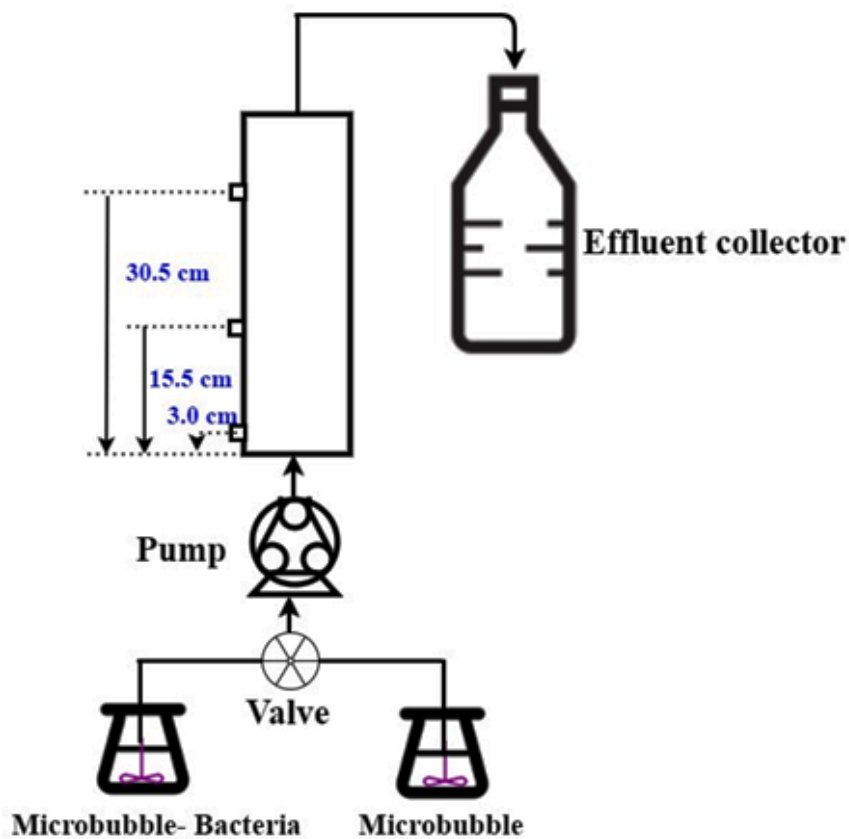


Figure 4-1 Column set up for up flow pumping experiments

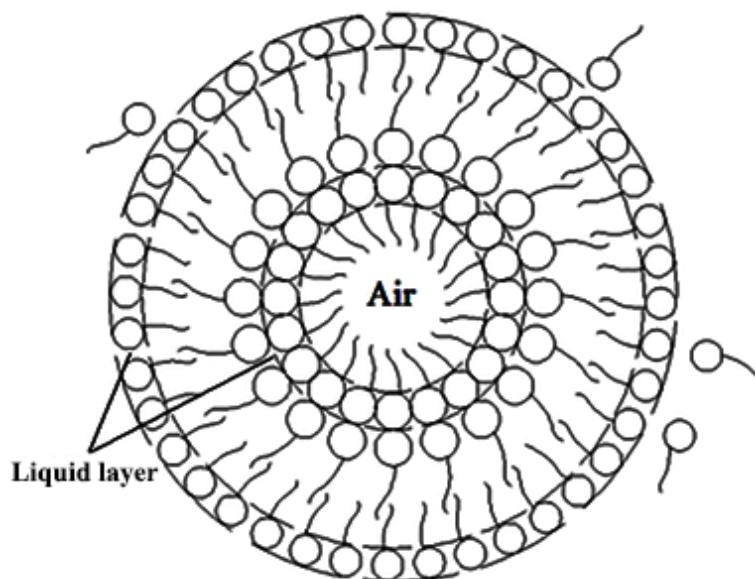


Figure 4-2 Microbubble structure,(Sebba, 1987)

### 4.3. Results and Discussions

#### 4.3.1. Microbubble Stability and Bacterial Drainage from Microbubble

##### 1) Effect of mixer and surfactant type on microbubble stability

#### Chapter 4. Upward Transport of *Rhodococcus erythropolis* and *Pseudomonas putida* with Continuously Injected Microbubble in Sand Column

The microbubble of rhamnolipid and tergitol that were generated by the propeller mixer comprised 62% gas, in line with the 60~70% range reported in the literature (Feng et al., 2009; Sebba, 1987; Subramaniam et al., 1990). The half-time of rhamnolipid microbubbles that were generated by the propeller mixer was 6.60 minutes, compared to tergitol microbubble value of 3.29 minutes, as shown in Figure 4-3. The microbubble of rhamnolipid and tergitol that was generated by the flat spinning disc mixer comprised 80 % gas, which is beyond 60~70% range reported in the literature (Feng et al., 2009; Sebba, 1987; Subramaniam et al., 1990). The half-time of microbubble that was generated by the flat spinning disc mixer was 7.68 minutes for rhamnolipid compared to 6.51 minutes for tergitol (Figure 4-3). Consistent with previous studies, surfactant type did not affect the proportions of gas in microbubbles at all (Feng et al., 2009; Matsushita et al., 1992). No significant change in the stability of microbubble was observed when adding bacteria (Figure 4-3). The mean diameter of rhamnolipid and tergitol microbubble was  $36\pm 11\ \mu\text{m}$  and  $58\pm 20\ \mu\text{m}$ , respectively. These results indicate that the mixing method used to produce microbubbles and surfactant type determines the stability of microbubble.

#### **2) Distribution of bacteria in microbubble**

The distribution of bacteria in gas phase during the drainage of microbubbles was recorded to investigate the capability of microbubble for carrying bacteria. Bacterial cells were drained out of microbubbles along with the liquid, as shown in Figure 4-4. Fifty percent of the total bacteria was drained from microbubbles for both surfactant types at the half-time of microbubble drainage. Compared to hydrophobic *R. erythropolis*, a slightly higher proportion of hydrophilic *P. putida* KT2442 was retained in microbubbles, as shown in Figure 4-4. Our finding is inconsistent with the previous research (Wan and Wilson, 1994) which found that hydrophobic bacteria are strongly attracted to air-water interfaces than hydrophilic bacteria to do so.

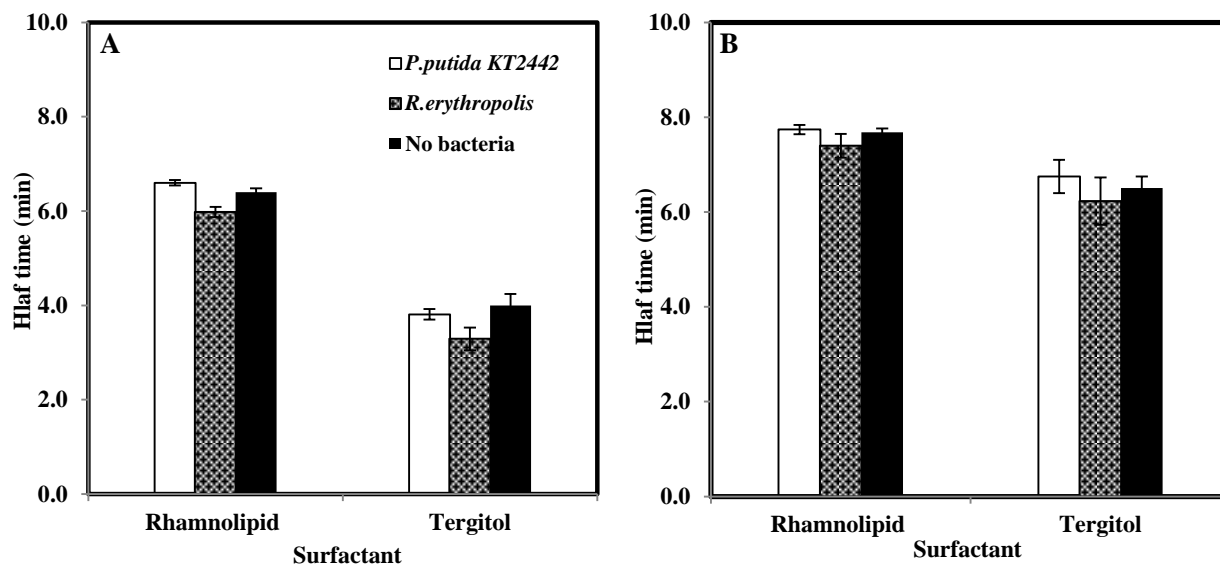


Figure 4-3 Effect of the generation method and bacteria on the half-time of microbubble. (A) the propeller mixer, (B) the flat spinning disc mixer

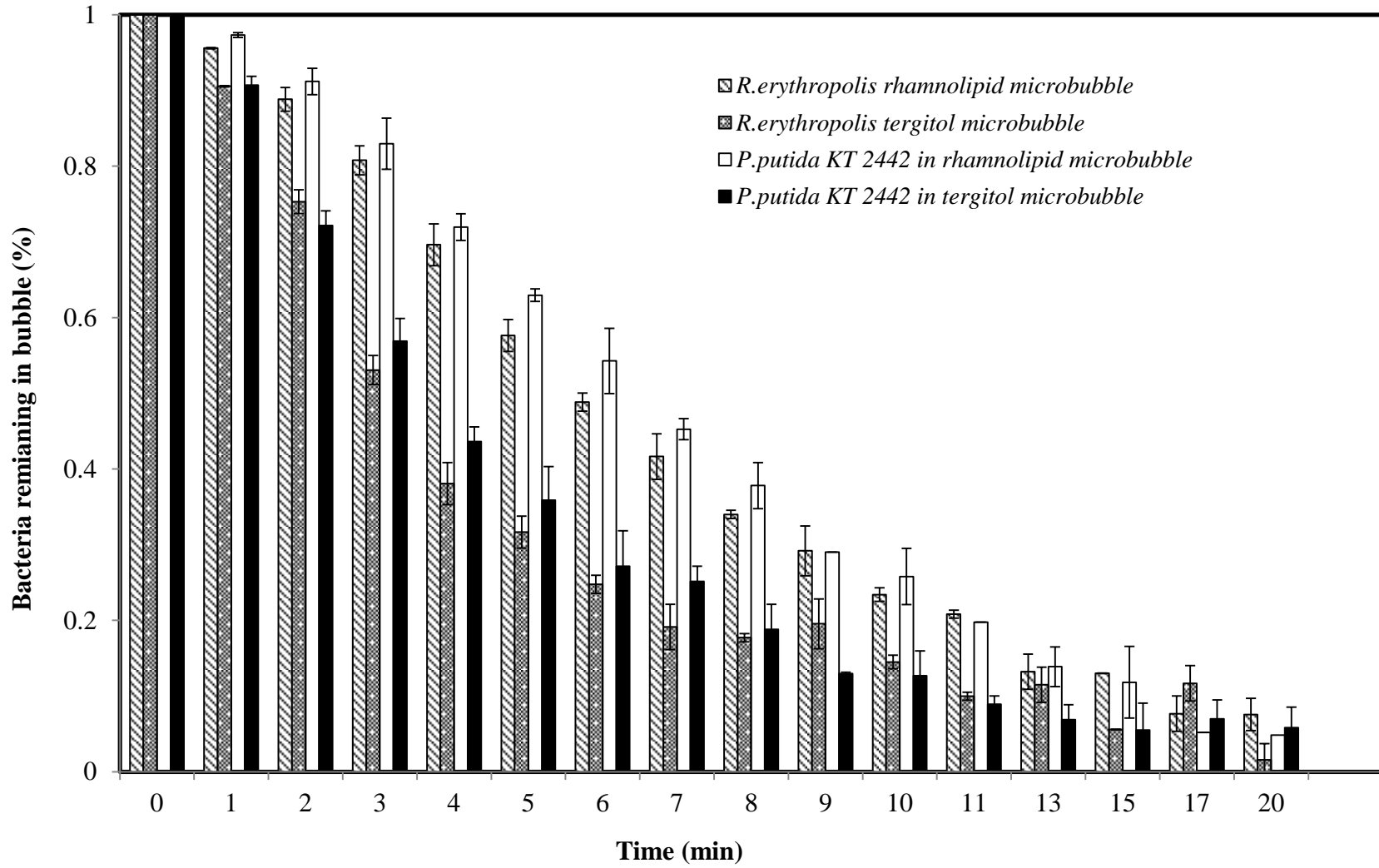


Figure 4-4 The distribution of *R. erythropolis* and *P. putida* KT2442 in rhamnolipid and tergitol microbubble over a range of time between 0 to 20 minutes

### 4.3.2. Comparison of Bacteria Transport in Surfactant Microbubble and Surfactant Solution

Bacteria transport in surfactant microbubbles and solution were compared to investigate the relative efficiency of microbubbles for carrying of bacteria. See Figure 4-5 showing the transport of *P.putida* KT2442 with rhamnolipid microbubbles and solution. Based on liquid volumes that have been injected into the column, bacteria transport with microbubbles moved faster than those were transported with the surfactant solution alone, as shown in the BTCs (Figure 4-5). For example, surfactant solutions required 2.6 pore volumes of surfactant solution to elute bacteria out of the column, while surfactant microbubbles reduced the usage of surfactant solution to approximately 1.3 pore volumes. Microbubbles eluted a higher percentage of bacteria out of the column than surfactant solution to do so, when the same volumes surfactant solution has been injected into the column. For example, 99.0% *P. putida* KT2442 has been eluted out of the column by rhamnolipid microbubble after eluting with 1.3 pore volumes of surfactant solution, while bacteria had only started to be eluted out of the column in the surfactant solution-aided bacteria transport. Our observation is in line with previous studies (Andrew Jackson et al., 1998; Su et al., 2014) where the use of pulse injected microbubble reduced the mass of surfactant solution that is needed to deliver the same amount of bacteria/nanoparticles through porous media. These results indicate that use of microbubble could be a cost-effective method for delivering bacteria into columns. The shapes of BTCs obtained in microbubble-aided bacteria transport were narrower than these were produced by surfactant solution (Figure 4-5), due to microbubbles comprising 80% gas. According to Equation 4-4, the volume of bacteria suspension that has been injected into the column was 0.086 and 0.430 pore volumes for surfactant microbubbles and solution, respectively.

The earlier comparisons were made on a liquid volume basis. As the microbubbles contain 80% gas, the time that was needed for *P. putida* KT2442 to pass through the column was 10 hours and 4 hours in the presence of surfactant microbubbles and surfactant solution, respectively. This observation is consistent with previous studies (Andrew Jackson et al., 1998; Wan and Wilson, 1994) showing that air-water interfaces retarded the transport of colloids in the columns compared to those transported with

Chapter 4. Upward Transport of *Rhodococcus erythropolis* and *Pseudomonas putida* with Continuously Injected Microbubble in Sand Column  
 surfactant solution. This indicates that microbubble-aided bacteria transport could extend the retention time of bacteria in the soil.

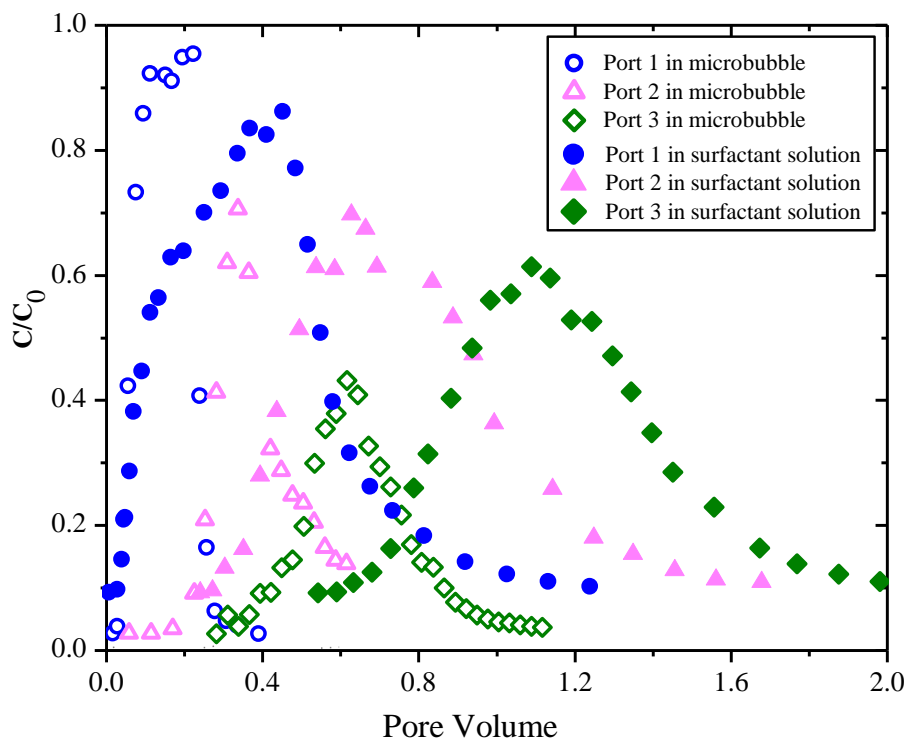


Figure 4-5 Comparison of BTCs of *P. putida* KT 2442 transport with surfactant microbubble (empty symbols) and surfactant solution (solid symbols). O,  $\Delta$  and  $\diamond$  shows the data obtained in the presence of rhamnolipid microbubble at Port 1, Port 2 and Port 3, respectively; Symbols are averages of experiments that were run in duplicate.

### 4.3.3. The Effect of Microbubble Generating Method, Surfactant Type, Bacterial Hydrophobicity and Sand Media Porosity on Bacteria Transport with Continuously Injected Microbubble

#### 1) The effect of microbubble generation method

Figure 4-6 and 4-7 compared bacteria transport with microbubbles that were produced by a propeller mixer and a flat spinning disc mixer. The efficiency of microbubbles in delivering bacteria was investigated based on the proportion of bacteria that was eluted out of the columns. As shown in Table 4-1, the percentage of *R. erythropolis* that was eluted out of the column with tergitol microbubbles that were generated by the flat spinning disc mixer was 21.7 %, almost twice as much as that produced by the propeller mixer (13.2%). For the case of *P. putida* KT2442, the tergitol microbubbles that were generated by the flat spinning disc mixer enhanced the proportion of eluted bacteria by almost 3.3 times (81%) compared to the amount was generated by the propeller mixer (24.5%). Comparing the dispersion coefficient for the BTCs of bacteria transport, a greater value in the bacterial dispersion was

obtained when using microbubble that was produced by the propeller mixer than these was generated by the flat spinning disc mixer (Table 4-2). This is because the fact that microbubbles that were generated by the propeller mixer and the flat spinning disc mixer had gas proportions of 62% and 80%, respectively. Therefore, according to Equation 4-4, the liquid volumes of bacteria suspension that have been injected into the column were 0.163 and 0.086, respectively. These results indicate that the mixing method used to produce microbubbles affect the transport of bacteria.

## 2) The effect of surfactant type

When bacteria were transported with anionic rhamnolipid microbubble, higher proportions of bacteria were eluted out of the columns than under same conditions when bacteria were transported with nonionic tergitol microbubble (Table 4-1). For example, 58.0% and 98% of total injected *R. erythropolis* and *P. putida* KT2442 were eluted out of the column, respectively, in the presence of rhamnolipid microbubble that was generated by the propeller mixer, as shown in Table 4-1. However, for the nonionic surfactant microbubbles, much lower proportions of total injected *R. erythropolis* and *P. putida* KT2442 were eluted out of the column, at 13.2% and 21.7%, respectively (Table 4-1). The dispersion coefficient in BTCs was calculated to investigate the dispersion of bacteria with different types of surfactant microbubbles. The transport of bacteria had the similar dispersion coefficient values in the presence of rhamnolipid and tergitol microbubble, as shown in Table 4-2. For example, the values of dispersion coefficient for *P. putida* KT 2442 were 0.168, 0.168 and 0.166 cm<sup>2</sup>/min for Port 1, Port 2 and Port 3, respectively, in the presence of rhamnolipid microbubble. The transport of *P. putida* KT 2442 with microbubble of tergitol had dispersion coefficients with values of 0.143, 0.147 and 0.091 cm<sup>2</sup>/min for Port 1, Port 2 and Port 3, respectively (Table 4-2). Surfactant type had a similar effect on the percentage of bacteria that was eluted out of columns and dispersion coefficient when using microbubble generated from the flat spinning disc mixer (Table 4-1 and Table 4-2). Our observations are consistent with a previous finding (Ding et al., 2013; Shen et al., 2011) that anionic surfactant SLES was more effective than nonionic surfactant Tween-20 in carrying nanoparticles. These results reveal

that anionic rhamnolipid microbubble is more favourable than nonionic tergitol microbubble in delivering both hydrophobic and hydrophilic bacteria through sand media.

### 3) The effect of bacterial hydrophobicity

Comparing the transport of hydrophilic and hydrophobic bacteria in the presence of microbubbles, higher percentages of hydrophilic *P. putida* KT2442 were eluted out of column than for hydrophobic *R. erythropolis* in all cases (Table 4-1). For example, a much higher proportion, approximately 98.0%, of hydrophilic *P. putida* KT2442 was eluted out of the column in the presence of rhamnolipid microbubble that was generated by the propeller mixer, compared to the ~58.0% of hydrophobic *R. erythropolis* under the same conditions (Table 4-1). The peak positions of the BTCs for hydrophilic *P. putida* KT2442 were always higher than those for hydrophobic *R. erythropolis* (e.g. Figure 4-6A vs. 4-6C). However, no difference was found in the dispersion coefficient between these two bacterial strains. These results indicate that the hydrophobicity of bacteria also plays an important role in determining their transport behaviour with microbubbles, with hydrophilic bacteria cells transporting more easily than hydrophobic bacteria.

### 4) The effect of the media porosity of the column

The permeability of soil is another parameter that determines bacteria transport. In previous Sections, experiments were conducted in low permeable columns with a porosity of 0.23. For the sake of comparison, an experiment was conducted to study the transport of *P. putida* KT2442 in a column with a porosity of 0.38 (high-permeable column) in the presence of rhamnolipid microbubble that was generated by the flat spinning disc mixer. Figure 4-8A shows that a small amount of *P. putida* KT2442 was observed at Port 2 and Port 3 soon after the injection of bacteria and the peak in the BTCs of *P. putida* KT2442 were achieved after 0.1, 0.2 and 0.3 pore volume of total liquid has been injected into the column with a porosity of 0.38. In the column with a lower porosity of 0.23 (Figure 4-8B), it took approximately 0.2, 0.3 and 0.5 pore volumes of liquid for the BTCs of *P. putida* KT2442 to reach the peak positions. This indicates that microbubbles moved faster in porous media with a coarse pore size

Chapter 4. Upward Transport of *Rhodococcus erythropolis* and *Pseudomonas putida* with Continuously Injected Microbubble in Sand Column  
 than in porous media with a fine pore size, which is in agreement with observations from previous studies (Ding et al., 2013; Wan et al., 2001).

**Table 4-1 The percentage of bacteria that was eluted out of the column, %**

Bacterial strain	The propeller mixer		The flat spinning disc mixer	
	Rhamnolipid	Tergitol	Rhamnolipid	Tergitol
<i>R. erythropolis</i>	58.1	13.2	68.8	24.5
<i>P. putida</i> KT2442	98.0	21.7	99.0	81.0

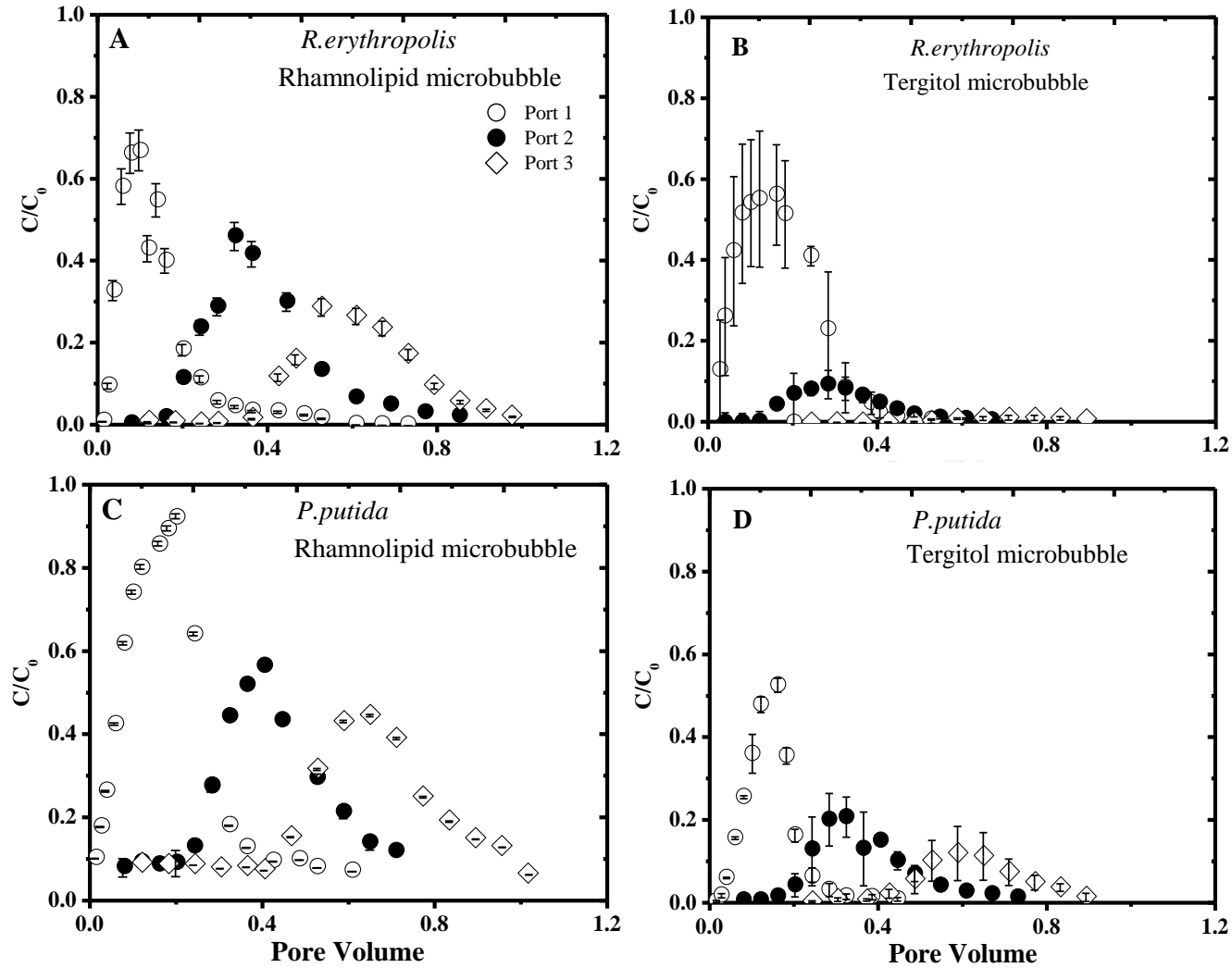


Figure 4-6 Comparison of the observed breakthrough curves of *R. erythropolis* and *P. putida* KT2442 that were transport with rhamnolipid and tergitol microbubbles that were generated by the propeller mixer. A, B: *R. erythropolis* with rhamnolipid microbubble and tergitol microbubble; C,D: *P. putida* KT2442 with rhamnolipid microbubble and tergitol microbubble; O, ● and ◇ shows the data obtained at Port 1, Port 2 and Port 3, respectively; Symbols are averages of individual values (-) for experiments run in duplicate. The missing data points are due a problem with the technique. The pore volume of pulse injected of bacteria suspension is 0.163 PV.

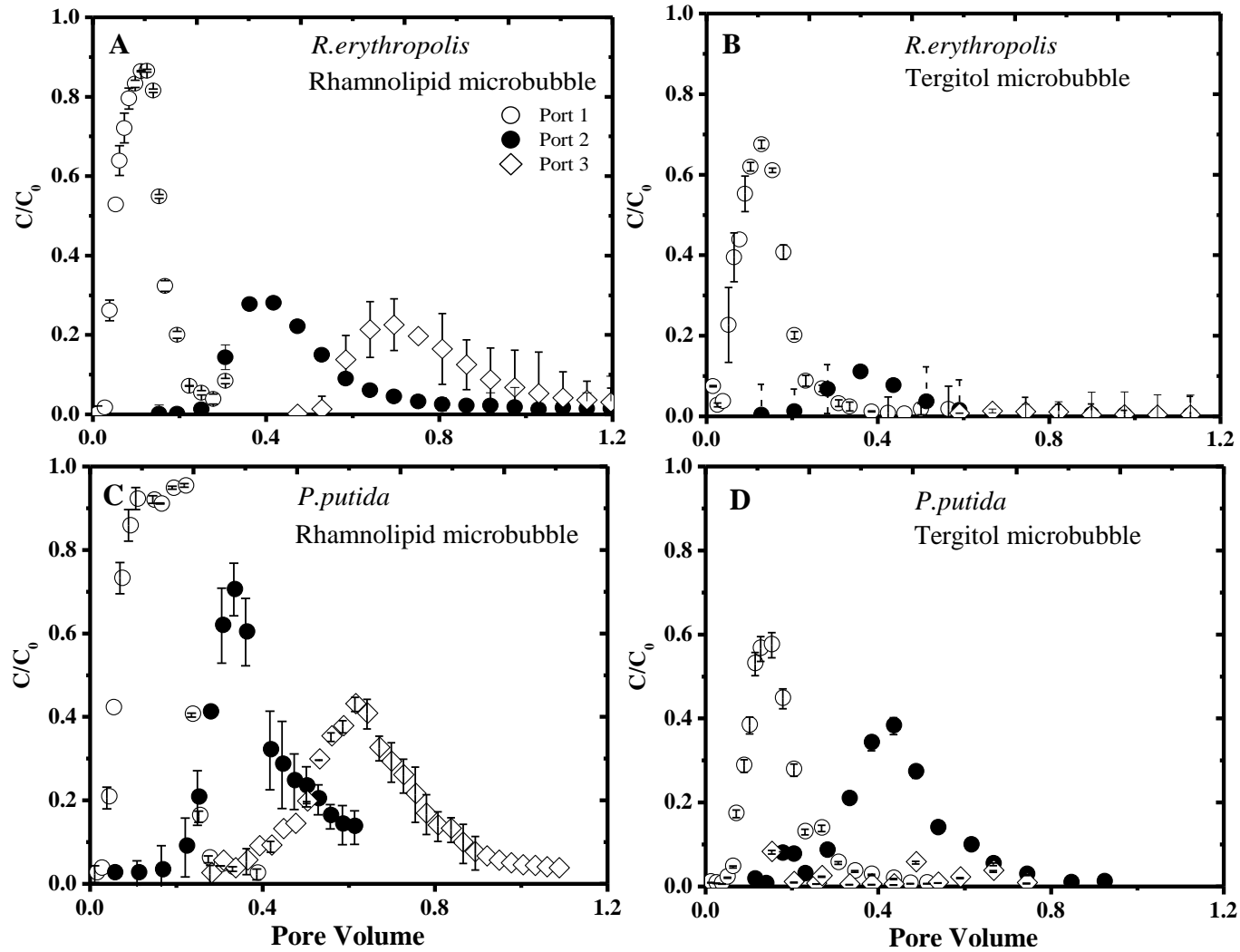


Figure 4-7 Comparison of the observed breakthrough curves of *R. erythropolis* and *P. putida* KT2442 that were transported with rhamnolipid and tergitol microbubbles that were generated by the flat spinning disc mixer. A, B: *R. erythropolis* with rhamnolipid microbubble and tergitol microbubble; C, D: *P. putida* KT2442 with rhamnolipid microbubble and tergitol microbubble; O, ● and ◇ shows the data obtained at Port 1, Port 2 and Port 3, respectively; “PV” represents the volumes of injected liquid solutions in terms of the pore volume of the columns. Symbols are averages of individual values (-) for experiments run in duplicate. The missing data points are due a problem with the technique. The pore volume of pulse injected of bacteria suspension is 0.086 PV

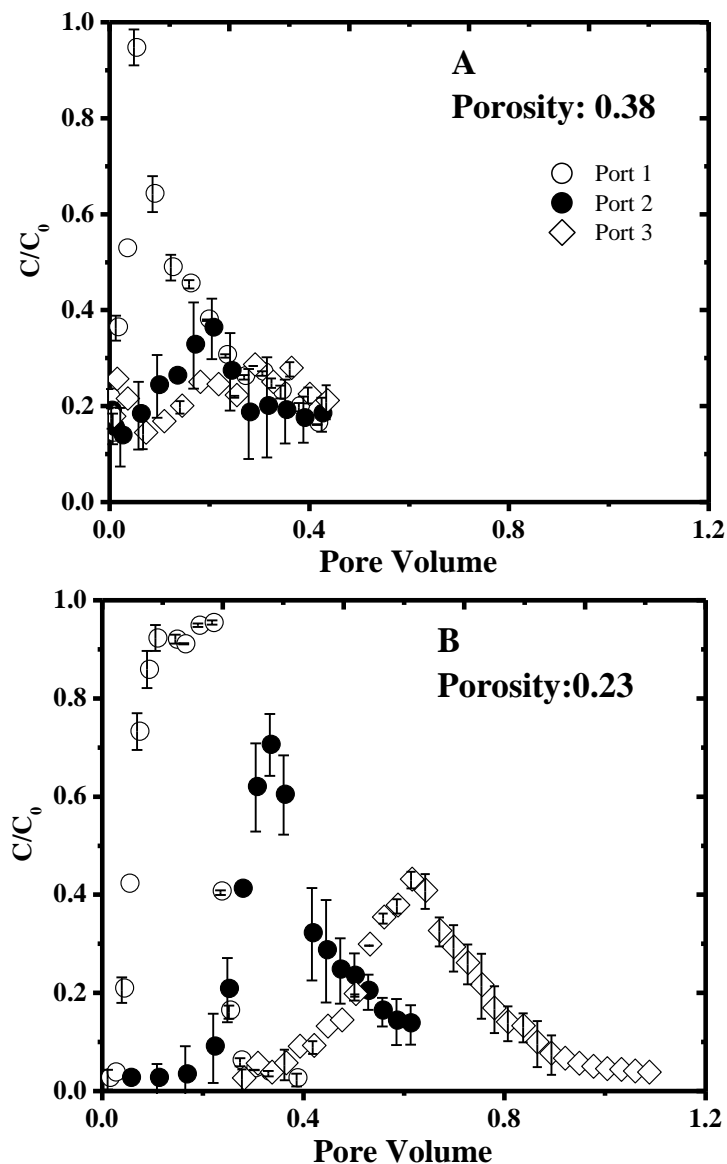


Figure 4-8 Comparison of high and low permeable columns on the transport of *P. putida* with rhamnolipid microbubble. A: porosity of 0.38; B: porosity of 0.23. Symbols are averaged from experiments run in duplicate.

Table 4-2 The dispersion coefficient in BTCs of bacteria transport with microbubble, cm<sup>2</sup>/min

	Port	<i>R. erythropolis</i>		<i>P. putida</i> KT2442	
		Rhamnolipid	Tergitol	Rhamnolipid	Tergitol
Propeller mixer	1	0.156±0.018	0.154±0.038	0.168±0.068	0.143±0.009
	2	0.171±0.020	0.105±0.046	0.168±0.027	0.147±0.052
	3	0.147±0.013	/	0.166±0.032	0.091±0.014
Flat spinning disc mixer	1	0.047±0.005	0.041±0.006	0.080±0.011	0.025±0.006
	2	0.064±0.007	0.050±0.008	0.049±0.003	0.039±0.007
	3	0.068±0.010	/	0.065±0.008	/

#### 4.3.4. Discussions

##### 1) Ability of microbubble for carrying bacteria

Microbubble drainage experiments were conducted with the aim of assessing the ability of microbubble for carrying bacteria. Both hydrophobic and hydrophilic bacteria strains adsorbed on microbubble, with a slightly greater affinity of hydrophilic bacteria to microbubbles. This was not consistent with previous research (Wan and Wilson, 1994) reporting that hydrophobic bacteria were more strongly attracted to air-water interfaces than hydrophilic bacteria to do so. To obtain an accurate evaluation of the adhesion tendency of bacteria to microbubble, the LW-AB interaction energy between bacteria and microbubble was calculated. As shown in Table 4-3, the values of LW-AB interaction energy ( $\Delta G_{adh}$ ) between *P. putida* KT2442 and microbubble were positive (15.05 and 28.03 mJ/m<sup>2</sup> for rhamnolipid and tergitol microbubbles, respectively). Negative values of  $\Delta G_{adh}$  were obtained between *R. erythropolis* and microbubble (-12.80 mJ/m<sup>2</sup> and -12.05 mJ/m<sup>2</sup> for rhamnolipid and tergitol microbubble, respectively). By definition, the adhesion of *P. putida* KT2442 to microbubble is not energetically favourable, but the adhesion of *R. erythropolis* to microbubble is energetically favourable, which can be accounted for the adhesion of both hydrophobic and hydrophilic bacteria to microbubbles. Therefore, in this study, the intensive mixing processes during microbubble generation possibly cause the adhesion of both hydrophobic and hydrophilic bacteria to air-water interfaces. Microbubble was generated by stirring and mixing at a speed of 8000 rpm, which allowed bacterial cells and microbubble to interact with each other. The slightly greater adhesion of hydrophilic bacteria to microbubble could be because hydrophobic bacteria aggregate in air-water interfaces (Figure 4-9A), while the adhesion of hydrophobic bacteria to air-water interfaces was more homogeneously distributed (Figure 4-9B). Consequently, the aggregated hydrophobic *R. erythropolis* would drag bacterial cells from the air-water interfaces into the liquid due to gravity. The effect of surfactant type on their ability to carry bacteria is possibly due to two reasons. First, the adhesion of bacteria to rhamnolipid microbubble is slightly stronger than to tergitol microbubble (Table 4-3). For example, the adhesion energy of *R. erythropolis* to rhamnolipid microbubbles is -12.80 mJ/m<sup>2</sup> while its value for tergitol microbubbles is -12.05 mJ/m<sup>2</sup>.

Second, rhamnolipid microbubble was generally more stable and lasted longer than tergitol microbubble, consequently, rhamnolipid microbubble would provide more air-water interfaces which could form reservoirs for bacteria (Parker, 1989). The drainage experiment indicated that the adhesion of bacteria to microbubble is a reversible process.

## **2) Possible mechanism for the transport of bacteria with microbubble**

To date, no data have been published regarding bacteria transport with continuously injected microbubble in porous media. Consistent with findings from studies conducted with pulse injected microbubble (Andrew Jackson et al., 1998; Shen et al., 2011; Su et al., 2014) this study demonstrated that continuously injected surfactant microbubbles can facilitate bacteria transport and reduce the usage of surfactant solutions. This study found that the bubble density decreased with the increased traveling distance, by taking samples from the different locations along the column. Therefore, we can assume that microbubble separated into liquid and gas phase directly after injection (Choi et al., 2008b), and released bacteria into the liquid phase during microbubble collapse. The drained liquid then moved as a free phase while the gas flowed as a discontinuous phase by reforming and breaking bubbles as it escaped upwards (Kovscek and Radke, 1994). As a consequence, some of the drained bacteria would have been trapped by microbubble (reformed or freshly injected, or both) and moved upward, some of the drained bacteria moved with the liquid or settled on the sand particles. Therefore, the interaction between bacteria, microbubble and sand particles is possibly responsible for the transport of bacteria with microbubble. The interaction between bacteria and the microbubble, and bacteria and sand particles was compared to explore this point of view. Both bacteria strains tend to have stronger adhesion to microbubble than to sand particles, as shown in Table 4-3. The preferred adhesion of bacteria to microbubble and the buoyancy of microbubble (Choi et al., 2008b) might help bacteria move forward thereby promoting bacteria transport in the presence of surfactant microbubbles compared to the surfactant solution.

Microbubbles generated by the different mixer showed different capacities to deliver bacteria. This may be because the microbubbles that were produced by the flat spinning disc mixer showed greater gas content and was more stable than the propeller mixer generated microbubble. The higher the proportion of gas in the microbubble and the more stable it was, possibly offering a greater number of air-water interfaces (Jauregi and Varley, 1999; Parker, 1989). Since bacteria have preferential sorption to air-water interfaces compared to sand particles (Table 4-2), the adsorbed bacteria moved upward with the mobile gas-water interfaces and then eluted out of the column. Therefore, higher percentages of bacteria were eluted out of the column with microbubble generated by the flat spinning disc mixer.

At least two reasons could be account for the effect of surfactant type on bacteria transport with microbubbles. First, in the presence of anionic rhamnolipid microbubble, a greater difference between the value of  $\Delta G_{adh}$  (bacteria-microbubble) and  $\Delta G_{adh}$  (bacteria-sand particles) consistently found compared to the corresponding values for nonionic tergitol microbubble (Table 4-3). Second, as shown in the batch experiment, rhamnolipid microbubble is more stable and has greater capability for retaining bacteria. As a result, fewer bacteria would drain out from rhamnolipid microbubble and the drained bacteria would be more likely to be trapped in the (reformed or freshly injected) microbubble of rhamnolipid and moved upward.

The lower percentages of hydrophobic bacteria that were eluted out of column could be due to the stronger adhesion of hydrophobic bacteria to sand particles compared to hydrophilic bacteria. Comparing the value of  $\Delta G_{adh}$  for both *P. putida* KT2442 and *R. erythropolis* between microbubble and sand particles, the adhesion of *P. putida* KT2442 is not energetically favourable ( $\Delta G_{adh} > 0$ ). In contrast, the adhesion of *R. erythropolis* is energetically favourable ( $\Delta G_{adh} < 0$ ). Both hydrophobic and hydrophilic bacteria, that were retained in microbubble would transport upward with the microbubble. However, the drained hydrophobic *R. erythropolis* could adsorb on the sand particles apart from being transported upward with the liquid and microbubble. As a consequence, more *P. putida* KT2442 was been eluted out of the columns.

The excellent transport of *P. putida* KT2442 in the column with greater porosity is possibly attributable to the pore size inside the column. To examine this point of view, the mean pore size was calculated using Equation 4-3. It was found that the mean pore size in the high-permeable column (329.0  $\mu\text{m}$ ) was nearly twice the mean pore size in the low-permeable column (164.0  $\mu\text{m}$ ). As a result, it was easier for bacterial carrier microbubbles with smaller bubble size to penetrate in sand columns with larger pore size.

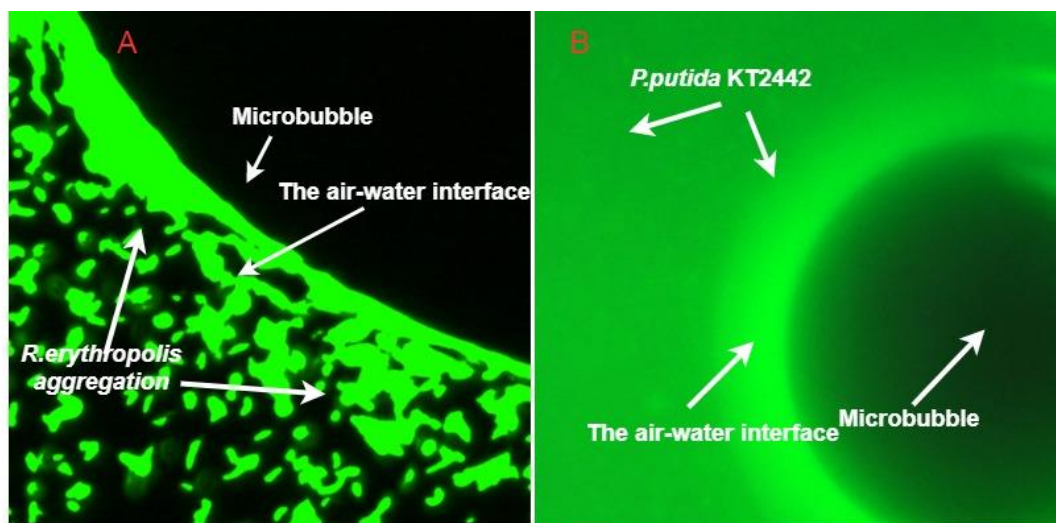


Figure 4-9 Fluorescence image of bacteria in the presence of rhamnolipid microbubble. A: *R. erythropolis*; B: *P. putida* KT2442

Table 4-3 The adhesion energy of bacteria to microbubble film and sand particles

Interaction energy	To microbubble			To sand particles			
	$G_{adh}$ (mJ/m <sup>2</sup> )	$\Delta G_{adh}^{LW}$ (mJ/m <sup>2</sup> )	$\Delta G_{adh}^{AB}$ (mJ/m <sup>2</sup> )	$G_{adh}$ (mJ/m <sup>2</sup> )	$\Delta G_{adh}^{LW}$ (mJ/m <sup>2</sup> )	$\Delta G_{adh}^{AB}$ (mJ/m <sup>2</sup> )	
<i>R. erythropolis</i>	Rhamnolipid	-12.80	-3.30	-9.50	-5.90	-3.70	-2.20
	Tergitol	-12.05	-5.02	-7.03	-10.00	-3.90	-6.20
<i>P. putida</i> KT2442	Rhamnolipid	15.06	-1.90	16.90	32.6	-2.10	34.70
	Tergitol	30.60	-5.80	37.10	23.7	-5.00	28.70

#### 4.4. Conclusion

This study investigated the efficiency of continuously injected microbubble to deliver bacteria in sand columns. The method used to generate microbubble and surfactant type affected the stability of microbubble. The stability of microbubble is found to be positively related to their ability in carrying bacteria. Surfactant microbubble-aided bacteria transport required less surfactant solution than the

amount needed in the surfactant solution-aided bacteria transport to elute bacteria out of columns.

Anionic rhamnolipid microbubble served as a more promising vehicle for carrying bacteria than nonionic tergitol microbubble, which is due to rhamnolipid microbubble is more stable and it has a greater affinity for bacteria. Hydrophilic bacteria were found more likely to transport with microbubble than hydrophobic bacteria due to the greater affinity of hydrophobic bacteria to sand particles. Increased the porosity of the column can promote the transport of bacteria, which is due to the increase of pore size inside the column.

Parameters including microbubble generation methods, surfactant type, bacterial hydrophobicity and the porosity of the column were investigated to assess their effect on the efficiency of continuously injected microbubble as the bacterial carrier. This study demonstrated that rhamnolipid microbubble is potentially an effective vehicle for carrying hydrophilic bacteria to contaminated sites for *in situ* bioremediation, particularly in the high-permeable column. This paper has also presented a preliminary study of the potential application of continuously injected microbubble for delivering both bacteria and oxygen for *in situ* soil bioremediation.

## **Acknowledgments**

This work was supported by research funding from the University of Auckland (New Zealand) and China Scholarship Council (China).

## **Chapter 5. Employing a Novel Optical Biosensor for *in situ* Monitoring of Bacteria Transport in Saturated Column in Varying Physicochemical Conditions**

Papre in preparation for Journal Environmental Science & Technology

W. Tao<sup>a</sup>, Yantao Song<sup>a</sup>, C. McGoverin<sup>b</sup>, F. Vanholsbeeck<sup>b</sup>, S. Swift<sup>c</sup>, and Naresh Singhal<sup>a,\*</sup>

<sup>a</sup> Department of Civil and Environmental Engineering, <sup>b</sup> The Dodds-Walls Centre for Photonic and Quantum Technologies, Department of Physics, <sup>c</sup> School of Medical Sciences, The University of Auckland, Private Bag 92019, Auckland 1010, New Zealand.

\*Corresponding author:

FAX: +64 9 373 7462

Phone: +64 9 923 4512

Email: n.singhal@auckland.ac.nz

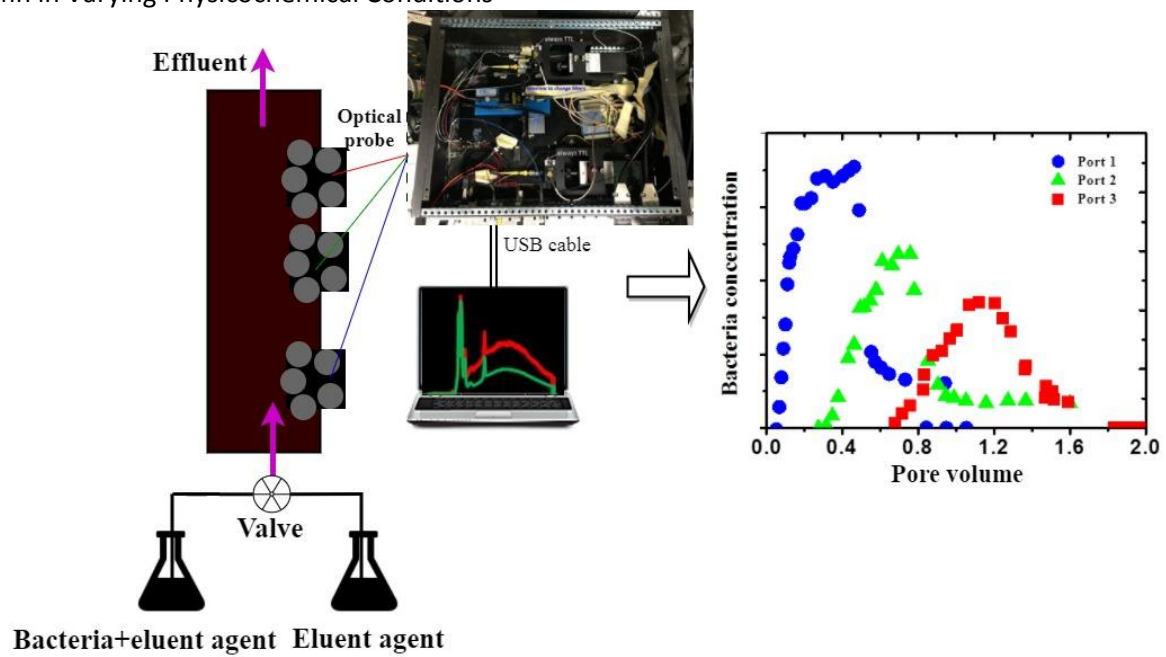
## Abstract

*In situ* monitoring of bacteria transport offers a rapid, real-time and cost-effective protocol for detecting the distribution of bacteria in soil when introducing exogenous bacteria to contaminated soil. This study investigated bacteria transport in saturated sand columns using a real-time spectrometer, the optrode, as an *in situ* monitoring method. The optrode measurements were conducted with and without taking samples for *ex situ* measurements with a microplate photometer. The results were compared for both *in situ* and *ex situ* measurements, and for the effect of sampling on the monitoring results. Two bacterial strains, hydrophilic *Pseudomonas putida* and hydrophobic *Rhodococcus erythropolis* were examined. The breakthrough curves (BTCs) of the three sampling regimes were compared. Similar BTCs were obtained when examining *ex situ* measurements and the optrode measurements where *ex situ* samples were not taken. When samples were removed for *ex situ* measurements, the BTCs produced by the optrode were significantly different from the BTCs collected by *ex situ* measurements. The sampling for *ex situ* measurements slightly modified the cell concentration and velocity inside the column but these modifications were not able to explain the distinct transport behaviour obtained by the optrode when sampling for *ex situ* measurements. BTCs observed by the optrode without sampling for *ex situ* measurements showed that hydrophilic *P. putida* tended to transport more easily in the column than hydrophobic *R. erythropolis*, and surfactant rhamnolipid promoted the transport of both hydrophilic and hydrophobic bacteria. These transport behaviours were due to the different Lifshitz–van der Waals forces and acid-base interactions between bacteria and sand. In conclusion, the optrode may serve as a very useful tool for monitoring *in situ* microbial transport in the soil without collecting samples.

**Keywords:** Optrode; Bacterial monitoring; Transport; Rhamnolipid, Fluorescence

Graphical abstract

Chapter 5. Employing a Novel Optical Biosensor for *in situ* Monitoring of Bacteria Transport in Saturated Column in Varying Physicochemical Conditions



## 5.1. Introduction

*In situ* bioremediation has emerged as a cost-effective and environmentally friendly treatment method compared to *ex situ* bioremediation (Mohan et al., 2006). *In situ* bioremediation treatment time can be relatively long due to the limited number of indigenous bacteria available for degrading pollutants. Introducing exogenous bacteria to contaminated soil is a commonly used approach to stimulate *in situ* bioremediation by expanding the population of bacteria. However, the distribution of exogenous bacteria can be affected by hydrophobicity of bacteria and soil. For example, hydrophobic bacteria have a stronger affinity to soil than hydrophilic bacteria (Gang Chen and Zhu, 2004; Huysman and Verstraete, 1993). Bacteria are easier to attach to a hydrophobic surface than to a hydrophilic surface (Gang Chen and Strevett, 2001; Zhong et al., 2016). The addition of surfactant could alter the surface hydrophobicity of bacteria and soil thereby promoting bacteria transport (G. Bai et al., 1997; Gang Chen and Strevett, 2001; Zhong et al., 2016).

When monitoring bacteria transport in the soil, the most frequently used is to collect liquid samples from the effluent or by removing liquid samples from a particular sampling port (Lang et al., 2016; Unc and Goss, 2003; Zhong et al., 2016). These liquid samples are then analyzed by methods such as total viable counts on agar plates, epifluorescence microscopy and microscopic fluorescence counts and flow cytometry (Banning et al., 2002; Maraha et al., 2004). However, this traditional monitoring method is constrained by factors such as difficulties in monitoring the attached bacteria, how the time-consuming the process is from sampling, through to transportation, and analysis (Barbee and Brown, 1986), and the limited sample sizes. Monitoring microbial transport in the soil in a rapid, real-time and cost-effective method has therefore received increasing research focus when introducing bacteria to contaminated soil.

*In situ* methods for the measuring of bacterial concentration have become increasingly accepted for the characterisation of bacterial transport, particularly with the development of advanced measurement technologies such as biosensors. Electrochemical, microbial fuel cell and optical biosensors, are able to

quantify or semi-quantify the analyte by using a biological recognition element retained in direct spatial contact with an electrochemical transduction element (Thévenot et al., 2001). Optical biosensors have been proven to outperform other types of sensors in multi-target sensing and continuous real-time on-site monitoring (Long et al., 2013). Advances in molecular biology have allowed molecular biologists to develop genetically modified microorganisms as biosensor microorganisms, thereby paving the way for *in situ* monitoring of bacterial activity (Belkin, 2003; Hewitt et al., 2012; Paul et al., 2005; Urgan-Demirtas et al., 2006). A few fluorescence optical systems based on biosensors have been introduced for environmental monitoring (Dorn et al., 2005; Heitzer et al., 1994; Ivask et al., 2007; Yolcubal et al., 2000), including identifying and quantifying particular pollutants and the growth of microorganisms. For example, an optical whole-cell biosensor has been used to monitor the concentration of naphthalene and the bioavailability of salicylate in waste streams (Heitzer et al., 1994), and to characterize the gene regulation or toxicity response (Yagi, 2007). The degradation of naphthalene and microbial growth activities in porous media have been measured by using the lux reporter bacterium, *Pseudomonas putida* RB1353 (Dorn et al., 2005). Fluorescent systems have been used to measure the concentration and degradation of pollutants or the growth activity of bacteria. However, there are few publications which reported the using of fluorescence as an *in situ* monitoring method to study bacteria transport.

Since 2008, the Physics Department at the University of Auckland has been developing a time-resolved fibre-optic spectroscopic probe system called the optrode. The optrode has been used to rapidly identify and quantify green/red fluorescent protein labelled microorganisms in batch experiments (Hewitt et al., 2012) and rapidly enumerate acridine orange-stained *Escherichia coli* in liquid media (Guo et al., 2017). The optrode is uniquely suited to take measurements from columns in the laboratory because it offers a non-destructive method for gauging bacteria transport in columns in a rapid and real-time manner.

The aim of this paper is to investigate the transport of bacteria using the optrode in a saturated sand column to simulate bacteria transport in the soil environment. This paper begins by comparing breakthrough curves (BTCs) obtained by the optrode with and without sampling for *ex situ*

Chapter 5. Employing a Novel Optical Biosensor for *in situ* Monitoring of Bacteria Transport in Saturated Column in Varying Physicochemical Conditions  
measurements and *ex situ* measurements. The effects of bacterial hydrophobicity and surfactant rhamnolipid on bacteria transport behaviour were monitored by the optrode without sampling for *ex situ* measurements. Two representative bacteria species, hydrophilic *Pseudomonas. putida* and hydrophobic *Rhodococcus erythropolis* were used in the study. Bacteria transport parameters were obtained by fitting BTCs through the convection-dispersion equation in CXTFIT in Stanmod. The interaction between bacteria and sand particles was calculated to understand bacteria transport behaviour. These results could validate the use of such an approach to optimize *in situ* bioremediation because due to its capability for providing real-time information on bacterial distribution without disturbing the system.

## 5.2. Materials and Methods

### 5.2.1. Material

Biosurfactant rhamnolipid (JBR 210, JENEIL ® Biosurfactant Co.) was used as the eluting agent to create a more complex environment inside the column. Rhamnolipid is a rhamnose-containing glycolipid surfactant that is primarily produced by *Pseudomonas aeruginosa*. Rhamnolipid was chosen because of its low toxicity to bacteria (Zhang et al., 1997; Zhu et al., 2013).

### 5.2.2. Bacterial Preparation

The bacteria were cultured and harvested in the same manner for each experiment. Pure strains of hydrophilic *Pseudomonas putida* KT2442 (Gram negative) (New Zealand Reference Culture Collection, Medical Section) chromosomally labelled with a gene expressing GFP (*P. putida* KT2442-GFP), and hydrophobic *Rhodococcus erythropolis* (Gram positive) (New Zealand Reference Culture Collection, ESR, Porirua, New Zealand) labeled with plasmid DNA expressing the red fluorescent protein Tomato (pTEC23 td Tomato) *R. erythropolis*-pTEC23 td Tomato) were used as biosensor microorganism. The properties of these two bacteria strains are displayed in Table 5-1. These two strains were selected because (1) bacterial hydrophobicity can affect the transport of bacteria (Abu-Lail and Camesano, 2003; Dong et al., 2002; Gannon et al., 1991; Q. Li and Logan, 1999; Tsuneda et al., 2003), and (2) they are

commonly found in the natural soil environment. The seed stocks of the bacteria strains were prepared by mixing 0.5 mL of an overnight culture with 0.5 mL of sterile 50 % glycerol in a 1 mL sterile plastic tube and then stored at -80 °C.

***P. putida* KT2442-GFP:** The water contact angle could indicate the hydrophobicity of bacterial surface: it is regarded that the water contact angle of hydrophilic bacteria is less than 45 °, vice versa (Daffonchio et al., 1995; Grotenhuis et al., 1992). *P. putida* KT2442-GFP has a hydrophilic surface with a water contact angle of 36.2 °. The optimal growth temperature for *P. putida* KT2442-GFP is 25~30 °C. A loopful of the seed stock was taken from the vial and plated onto a TS agar plates, and then placed in the incubator at 28 °C for 24 hours. After the bacterial cell colonies had formed, the bacterial agar plate was stored in a refrigerator at 4°C with less than 2 weeks. To prepare bacteria for experiments, a colony of bacteria was taken from the agar plate and incubated overnight in 20 mL TS broth in a 100 mL sterile flask at 28 °C, under constant shaking at 200 rpm. Then 2 mL of the bacteria solution was transferred to 200 mL of fresh TS broth in 2000 mL flasks and incubated overnight at 28 °C, under constant shaking at 200 rpm. *P. putida* KT2442-GFP was harvested by centrifugation at 8000 g for 10 minutes.

***R. erythropolis* pTEC23 td Tomato:** *R. erythropolis*-pTEC23 td Tomato has a water contact angle of 94.7 °, indicating a hydrophobic surface. Its optimal growth temperature is 25~30 °C. A loopful of seed stock of *R. erythropolis*-pTEC23 td Tomato was taken and placed on TS agar plates and then incubated at 28 °C for 72 hours until visible colonies formed. To obtain enough bacteria, we then transferred *R. erythropolis*-pTEC23 td Tomato to new TS agar plates and incubated them at 28 °C for 72 hours. At least four plates were prepared each time to ensure a sufficient quantity of bacteria could be harvested for each experiment. Bacteria were collected using a moistened swab. The harvested cells were then washed three times with saline to remove soluble extracellular polymeric substance and finally resuspended in the eluting agent solution for further experiments. The number of bacteria was quantified by measuring the fluorescence signals of collected samples using a Perkin Elmer EnSpire 2300 multilabel plate reader and the Wallace Envision Manager software program. The experimental

Chapter 5. Employing a Novel Optical Biosensor for *in situ* Monitoring of Bacteria Transport in Saturated Column in Varying Physicochemical Conditions  
details are provided in the appendix. A linear relationship was obtained between fluorescence intensity and CFU/mL, with a  $R^2$  value of 0.9579 (Figure A-1 in the appendix)

### 5.2.3. The Optrode Detection System

**The optrode system:** The optrode setup has been described previously by A. Y. H. Chen et al. (2010) and Hewitt et al. (2012) (Figure 5-1). In this study, the optrode used 100 mW diodes pumped solid state at 473 nm (the blue laser) and 532 nm (the green laser) to excite the GFP gene and pTEC23 td Tomato protein, respectively. Following a setup stabilization period of 60 minutes, the power of the laser was measured from the free end of the fibre using a photodiode and then adjusted to 7 mW. The numerical aperture of the fibre core is 0.22, and the cladding and coating diameters are 200  $\mu\text{m}$ , 220  $\mu\text{m}$ , and 250  $\mu\text{m}$ , respectively. The fluorescence intensity in liquid media is collected from a cone with a core diameter of 200  $\mu\text{m}$  and a depth of 900  $\mu\text{m}$  Hewitt et al. (2012). The effect of external factors, like soil particles and rhamnolipid surfactant, can be minimized by using the signal from portions of the spectrum where the background is minimal (Hewitt et al., 2012; Tai et al., 2007). The optrode probe was prepared by fitting the fibre through a 22 g flat-point needle (OD 0.72 mm) with epoxy fill to avoid the damaging of the fibre when submerging the probe inside the column, as shown in Figure 5-2.

**Data collection and analysis:** A custom LabVIEW (National Instruments Co) routine was developed to collect and analyze the optrode fluorescence intensity. The software recorded the laser power and spectra at different integration times. The integration times used 8, 16, 32, 64, 128, 256, 512, 1024 and 2048 ms. The minimum integration time to achieve a signal-to-noise ratio (SNR) of 10. The background spectrum for each sampling port was recorded before injecting the bacterial suspension into the column. For each sample spectrum the dark noise and background (after removal of darknoise) spectra of the same integration time was subtracted. The resulting spectrum was normalized to 1 mW. Finally, the sample spectra were normalized to 1 ms.

### 5.2.4. Calibration of the Optrode Intensity to Bacterial Concentration

A good linear relationship was observed between the fluorescence intensity collected by the optrode and bacterial concentration in the liquid media found previously (Hewitt et al., 2012). Two sets of batch experiment were carried out to calibrate the optrode intensity with bacterial concentration. The first set of batch experiment was conducted in a 1:2 dilution liquid media and in the second batch experiment sand particles were added to the 1:2 dilution liquid media to simulate the column condition. Details are provided in the appendix for Chapter 5. All samples were prepared in triplicate, and in the absence and presence of rhamnolipid. Background spectra were collected from bacteria-free samples. The bacteria concentration was obtained using the method described in section 5.2.2. By regrouping the data in the two sets of batch experiments above, a linear relationship between optrode signal intensity and the number of bacteria in the sand batch experiment was obtained; all with an  $R^2$  value of 0.9495 or greater (Figure A-4, A-5 and A-6 in the appendix for Chapter 5). The bacteria concentration in this study can be determined by using these calibration curves. To ensure a fluorescence signal was observed in the *in situ* measurements,  $3.5 \times 10^{10}$  CFU/mL and  $8.00 \times 10^9$  CFU/ mL of *P. putida* KT2442-GPF and *R. erythropolis*-pTEC23 td Tomato were used as the initial input, respectively.

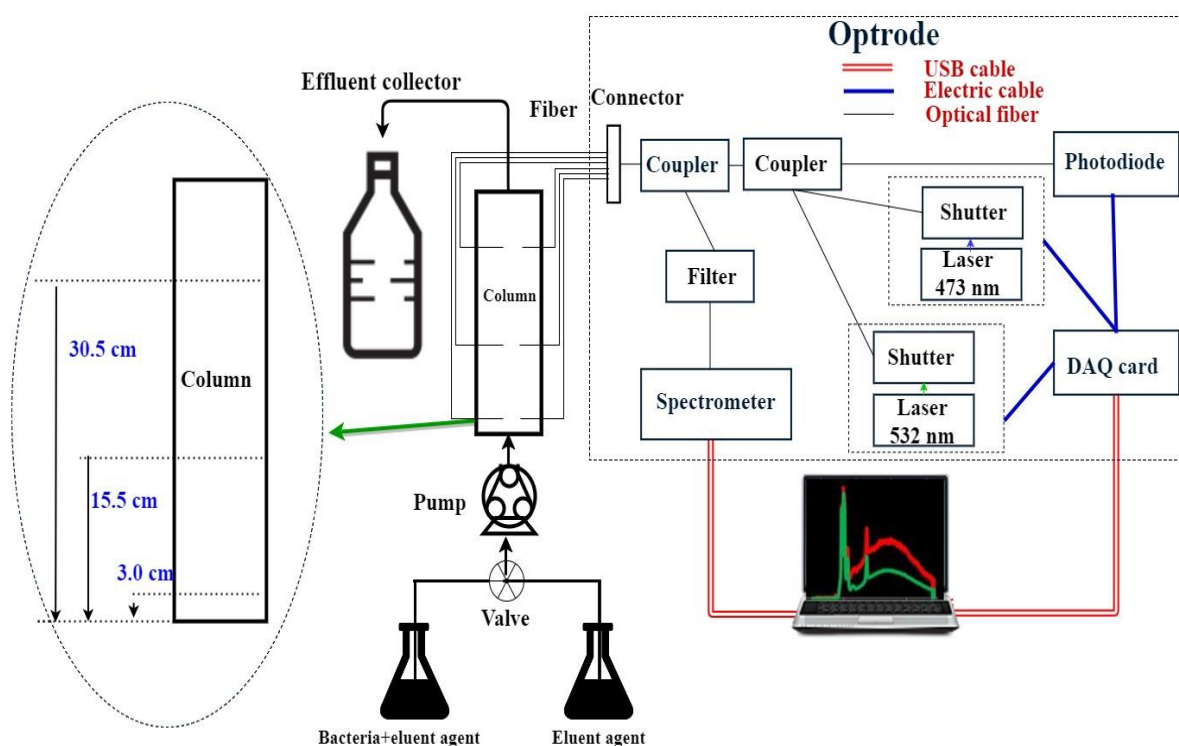


Figure 5-1 Schematic diagram of optical fibre detection system for column study

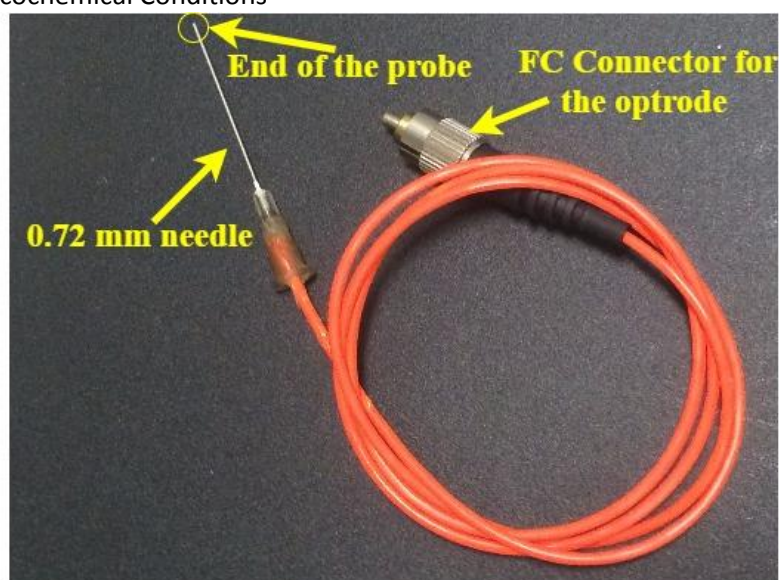


Figure 5-2 Optical fibre probe

### 5.2.5. Column Preparation and Column Experiments

A cylindrical stainless steel column (6.15 cm diameter ( $d$ )  $\times$  41 cm length ( $L$ )) was designed with three aqueous sampling ports, termed Port 1, Port 2 and Port 3. Ports 1, 2 and 3 are located at 3.0 cm, 15.5 cm and 30.5 cm from the inlet of the column (Figure 5-1), respectively. The sampling port for the optrode probe is positioned opposite to the position of the liquid sampling ports, and with at the same distance from the inlet of the column as shown in Figure 5-1. For each experiment, the column was uniformly packed with 1852.4 g of sterilized sand of particle sizes ranging from 0.0625 mm to 2 mm, and with a mean size 0.8050 mm. The porosity ( $\theta$ ) of the packed column was 0.23 using gravimetric analysis.

The background intensity inside the column was collected by the optrode after the column had been pre-equilibrated with bacteria-free solutions. Bacteria suspension was then pumped into the column for 40 minutes at a flow rate of 0.43 cm/min, followed by eluting with 700 mL of bacteria-free solution. Two sets of column experiments were conducted to compare the performance of the optrode and *ex situ* measurements in monitoring bacteria transport in column studies. Both the optrode and *ex situ* measurements were carried out in the first set of column experiments. In the second set of column experiments, the optrode measurements were conducted without sampling *ex situ* measurements. The reservoir bacteria suspension was stirred using a magnetic stirrer during each experiment prevent the

bacterial cells from settling down. Bacteria transport was expressed as bacteria cell concentration (CFU/mL) measured against the actual pore volumes of eluent liquid agent that was passed through the column. The subsequent plots are known as breakthrough curves (BTCs). In this study, the optrode data at Port 1, Port 2 and Port 3 are not from the same run due to shielding of the probe by sand particles during the experiment. The actual pore volumes of eluent liquid agent that passed through the column at time  $t$  were calculated:

$$\text{Pore volume} = \frac{q \times t}{\pi \times \left(\frac{d}{2}\right)^2 \times L \times \theta} \quad (5-1)$$

where  $q$  is velocity in mL/min,  $t$  is time (minutes),  $d$  is the diameter of the column in cm, and  $\theta$  is the porosity of column.

**Table 5-1 Summary the properties of *P. putida* KT2442 and *R. erythropolis***

Bacteria	<i>P. putida</i> KT2442	<i>R. erythropolis</i>
Gram-staining	Gram-negative	Gram-positive
Cell shape	Rods	Cocci
Cell size	1 × 2 μm	0.5 μm
Fluorescent	Green fluorescent protein	plasmid DNA expressing the red fluorescent protein Tomato
Excitation wavelength	473 nm	554nm
Emission wavelength	535 nm	581 nm

### 5.2.6. Interaction Energy Calculation and Surface Tension Parameters Measurement

Because the addition of surfactant solution did not significantly affect the electrophoretic mobility of bacteria, this study only considered the Lifshitz-van der Waals and acid-base (LW-AB) interactions between bacteria and sand particles. The Lifshitz-van der Waals (LW) component and the acid-base (AB) energy ( $\Delta G_{adh}$ ) can be calculated from the surface tension parameters as follows (Absolom et al., 1983; Busscher et al., 1984; Sharma and Hanumantha Rao, 2002; C. Van Oss, 1995):

$$\Delta G_{bls}^{LW} = -2 \left( \sqrt{\gamma_b^{LW} \gamma_l^{LW}} + \sqrt{\gamma_s^{LW} \gamma_l^{LW}} - \sqrt{\gamma_b^{LW} \gamma_s^{LW}} - \gamma_l^{LW} \right) \quad (5-2)$$

$$\Delta G_{bls}^{AB} = 2 \left( \sqrt{\gamma_l^+} (\sqrt{\gamma_b^-} + \sqrt{\gamma_s^-} - \sqrt{\gamma_l^-}) + \sqrt{\gamma_l^-} (\sqrt{\gamma_b^+} + \sqrt{\gamma_s^+} - \sqrt{\gamma_l^+}) - \sqrt{\gamma_b^+ \gamma_s^-} - \sqrt{\gamma_b^- \gamma_s^+} \right) \quad (5-3)$$

where subscript *b* denotos bacteria, *l* denotes liquid, *s* denotes solid.

The three unknown surface free energy components,  $\gamma^{LW}$  (LW apolar component),  $\gamma^-$  (electron donor),  $\gamma^+$  (electron acceptor), in Equation 5-2 and 5-3 can be determined using the LW-AB approach and Yong's equation (Absolom et al., 1983; Busscher et al., 1984; Sharma and Hanumantha Rao, 2002; C. Van Oss, 1995) based on the contact angle measurement of three diagnostic liquids with known surface tension components. The contact angle measurement for bacteria followed the method used in a previous study (Knox et al., 1993). Briefly, a homogenous bacterial lawn was prepared and then contact angle was measured by a digital goniometer after dropping a diagnostic liquid onto the bacteria lawn. Since quartz is the major component of silica sand, it also offers a homogeneous surface for estimating the surface hydrophobicity of silica sand. Details of contact angle measurements and results are provided in the appendix (Table A-2).

### 5.2.7. Data Analysis

This study calculated the proportion of bacteria and liquid which had been collected for *ex situ* measurements to investigate the effect of the sample removal on the bacterial concentration and velocity of each sampling port. The percentages of bacteria and liquid withdrawn from the column were calculated based on the frequency and size of sampling, the amount of cells in the liquid sample and the total amount of liquid and bacteria that had been pumped into the column. Due to the gravity, it was assumed that the liquid sample came from the top of the sampling port; therefore, *ex situ* sampling would slightly reduce the velocity at the following port. Thus, the flow rate ( $q_s$ ) was calculated:

$$q_s = \frac{Q_s}{\pi\left(\frac{d}{2}\right)^2\theta} \quad (5-4)$$

where  $Q_s$  is the sampling rate, which is 1.2 mL/min,  $d$  is the diameter of the column in cm, and  $\theta$  is the porosity of column.

The averaged velocity of each sampling port could then be calculated:

$$q = \frac{[q_0 t \times 60 + (n - n1) q_s \times 10]}{t \times 60} \quad (5-5)$$

where  $q_0$  is the pumping rate,  $n$  is the sum of sampling times at the sampling port at time  $t$ , and  $n1$  is the total number of sampling times at the previous sampling port.

The mathematical model used in this study considered the transport of bacteria in the column to be the result of convection and diffusion of liquid through the silica sand due to the concentration gradient (Feng et al., 2013a). The bacteria were considered to be transporting through a uniform, one-dimensional, saturated porous media, otherwise known as bacteria transport in a steady-state flow. The one-dimensional convection-dispersion equation (CDE) (Gang Chen and Zhu, 2004) was used, and reduced (Van Genuchten and Alves, 1982) as follows:

$$R \frac{\partial C}{\partial t} = D \frac{\partial^2 C}{\partial x^2} - v \frac{\partial C}{\partial x} - \mu C + \gamma \quad (5-6)$$

where  $C$  is the bacteria concentration,  $D$  is the dispersion coefficient (includes both diffusion and hydrodynamic dispersion),  $t$  is the time, and  $v$  ( $v=q/\epsilon$  ( $LT^{-1}$ )) is the average velocity inside the column. In this study, the equilibrium equation and nonequilibrium equation were solved by CXTFIT model in STANMOD (a Windows-based software package) (Van Genuchten and ALVES, 1982), which has been used previously to successfully predict the adsorption and transport of *E. coli* and *P. fluorescens* (Parker and Van Genuchten, 1984). Parameters including dispersion coefficient ( $D$ ), retardation coefficient ( $R_d$ ), first order deposition coefficient ( $\mu$ ) and the coefficient of determination ( $R^2$ ) were estimated. All modeling was performed at zero initial concentration and zero production.

### 5.3. Results and Discussions

#### 5.3.1. *In situ* versus *ex situ* Measurements

The transport of bacteria that were obtained by the optrode, with and without sampling for *ex situ* measurements, were compared to those observed from *ex situ* measurements in Figure 5-3, Figure 5-4, Figure 5-5 and Figure 5-6. Significantly different BTCs were produced by the optrode with sampling for *ex situ* measurements and *ex situ* measurements ( $P < 0.05$ ). A lower cell concentration was observed in the BTCs of *P. putida* KT2442 GFP collected by the optrode with sampling for *ex situ* measurements (Figure 5-3A and B, and Figure 5-4A and B). At Port 2 and Port 3, BTCs of *P. putida* KT2442 GFP that were collected by the optrode, with sampling for *ex situ* measurements, broke through each port later than these were detected by *ex situ* measurements (Figure 5-3 A vs. B and Figure 5-4A vs. B). A maximum delay of 0.5 PV in the BTCs of *P. putida* KT2442-GFP in the presence of rhamnolipid (Figure 5-4 B) was observed using the optrode when sampling for *ex situ* measurements. The fitted transport parameters for the optrode and *ex situ* measurements at different sampling ports are presented in Table 5-2. No trend was found in the value of dispersion coefficients between the optrode with sampling for *ex situ* measurements and the *ex situ* measurements. However, the values for retardation coefficient and first order decay obtained by the optrode with sampling for *ex situ* measurement were greater than the value of *ex situ* measurements in all cases (Table 5-2).

Without the disturbance from *ex situ* sampling, BTCs obtained with the optrode showed no significant difference ( $P > 0.05$ ) from those produced by *ex situ* measurements, as shown in Figure 5-3 (A vs. C), Figure 5-4 (A vs. C), Figure 5-5 (A vs. C) and Figure 5-6 (A vs. C). The optrode occasionally obtained variable concentrations in the BTCs (e.g. Figure 5-3 C and Figure 5-6C), which is possibly due to shielding of the probe by sand particles. The values of first order decay obtained by the optrode were larger than those obtained by *ex situ* measurements. The measures of bacterial dispersal ability obtained by the optrode were equivalent to these produced by *ex situ* measurements, except for the transport of *R. erythropolis*-pTEC23 td Tomato in the presence of rhamnolipid (Table 5-2). In BTCs that were produced by the optrode without sampling for *ex situ* measurements, the dispersion coefficients values

of the different sampling ports were close (Table 5-2). No consistent trends were found in the values of retardation coefficients between the optrode without sampling for *ex situ* measurements and the *ex situ* measurements, but the data collected by the optrode demonstrated lower error and were more consistent (Table 5-2). These results indicate that the optrode is able to detect bacterial mobility efficiently when the column system was not disturbed by the removal of sample. Accordingly, the next section focused on the transport behaviour of bacteria by applying the *in situ* optrode approach without taking samples for *ex situ* measurements.

### 5.3.2. Optrode Monitored Hydrophilic and Hydrophobic Bacteria Transport under Varying Physicochemical Conditions

Similar patterns were observed for all BTCs collected by the optrode without sampling for *ex situ* measurements. Specifically, the maximum concentration of bacteria in BTCs decreased with an increase in the travelling distance (Figure 5-3C, Figure 5-4C, Figure 5-5C and Figure 5-6C). The CDE model performed reasonably well in describing the BTCs as the  $R^2$  values were in the range 0.7570 to 0.9820 (Table 5-2). The fitted parameters for all column experiments showed similar patterns: the highest value of first order decay was always observed at Port 1, and values decreased with increasing travelling distance. No significant difference was found in the dispersion and retardation values between the different ports.

#### 1) The optrode monitored bacteria transport in water

In the absence of rhamnolipid, the value of the first order decay ( $\mu$ ) for hydrophilic *P. putida* KT2442-GFP was  $0.0472 \text{ min}^{-1}$ ,  $0.0338 \text{ min}^{-1}$  and  $0.0134 \text{ min}^{-1}$  for Port 1, Port 2 and Port 3, respectively (Table 5-2). The transport of hydrophobic *R. erythropolis*-pTEC23 td Tomato obtained larger respective values of  $\mu$  of  $0.0700$ ,  $0.0332$  and  $0.0200 \text{ min}^{-1}$  for Port 1, Port 2 and Port 3. This indicates that hydrophilic *P. putida* KT2442-GFP tended to transport more easily through columns than hydrophobic *R. erythropolis*-pTEC23 td Tomato (Figure 5-3C and Figure 5-5C). This phenomenon is similar to the findings demonstrated in the by *ex situ* measurements. However, no significant differences were found for retardation coefficient ( $R_d$ ) and dispersion coefficient (D) between these two bacteria.

## 2) The optrode monitored bacteria transport in the presence of rhamnolipid

Rhamnolipid can create a complex environment in columns because it can alter the surface properties of sand particles and bacteria and it can also emit fluorescence signal when it is excited by the optrode lights. In the presence of rhamnolipid surfactant, the BTCs of bacteria transport were similar to those in water runs, as shown in Figure 5-4C and Figure 5-6C. However, a higher peak position in the BTCs for both bacterial strains was observed with rhamnolipid present. For both bacterial species, the value of the first order decays ( $\mu$ ) decreased when adding rhamnolipid (Table 5-2). Taking hydrophilic *P. putida* KT2442-GFP as an example, the value of  $\mu$  decreased from 0.0472 to 0.0411  $\text{min}^{-1}$ , from 0.0338 to 0.0046  $\text{min}^{-1}$  and from 0.0134 to 0.0076  $\text{min}^{-1}$  for Port 1, Port 2 and Port 3, respectively (Table 5-2). A slight increase in the value of  $D$  was obtained when adding rhamnolipid. There was no evidence to show that rhamnolipid influenced the retardation coefficient values (Table 5-2). Rhamnolipid had a similar effect on the transport behaviour of hydrophobic *R. erythropolis*-pTEC23 td Tomato compared to hydrophilic *P. putida* KT2442-GFP, as shown in Table 5-2. When comparing the transport behaviour of hydrophobic and hydrophilic bacteria, BTCs of hydrophilic *P. putida* KT2442-GFP showed a greater value for  $D$  and  $R_d$  than the BTCs of hydrophobic *R. erythropolis*-pTEC23 td Tomato. However, a smaller value of  $\mu$  was observed for hydrophilic *P. putida* KT2442-GFP compared to hydrophobic *R. erythropolis*-pTEC23 td Tomato.

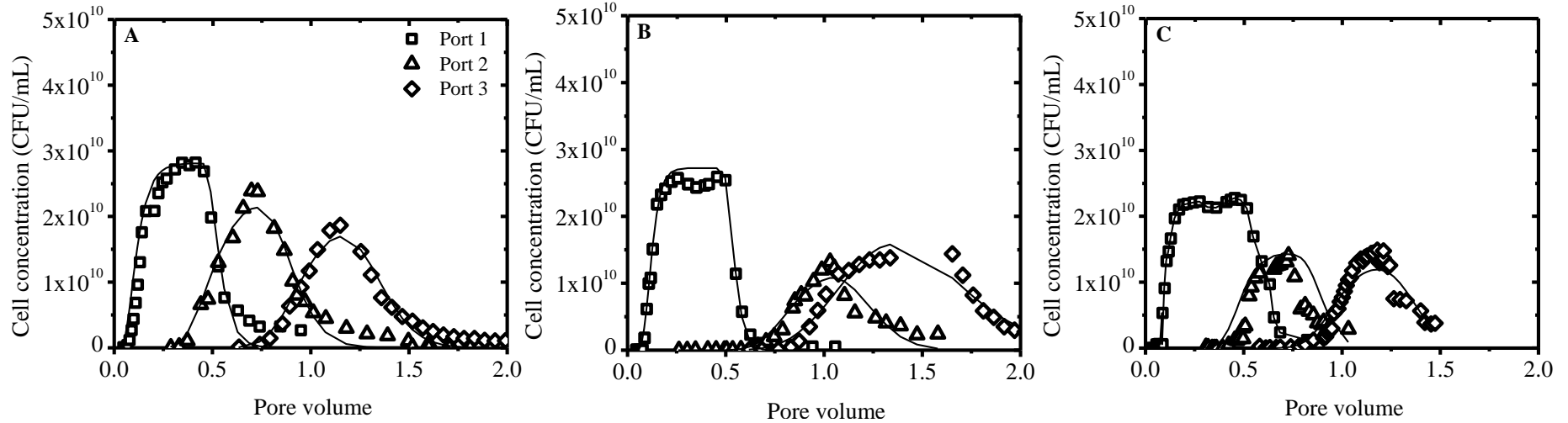


Figure 5-3 Comparison of the observed and fitted breakthrough curves of *P. putida* KT2442 in water that were obtained by *ex situ* measurements (A), the optrode with sampling for *ex situ* measurements (B) and the optrode without sampling for *ex situ* measurements (C).  $\square$ ,  $\Delta$  and  $\diamond$  shows the data obtained at Port 1, Port 2 and Port 3; Symbols are the observed data; lines are the fitted data. *Ex situ* measurement data is the average of duplicate data. The optrode data at Port 1, Port 2 and Port 3 are not from the same run.

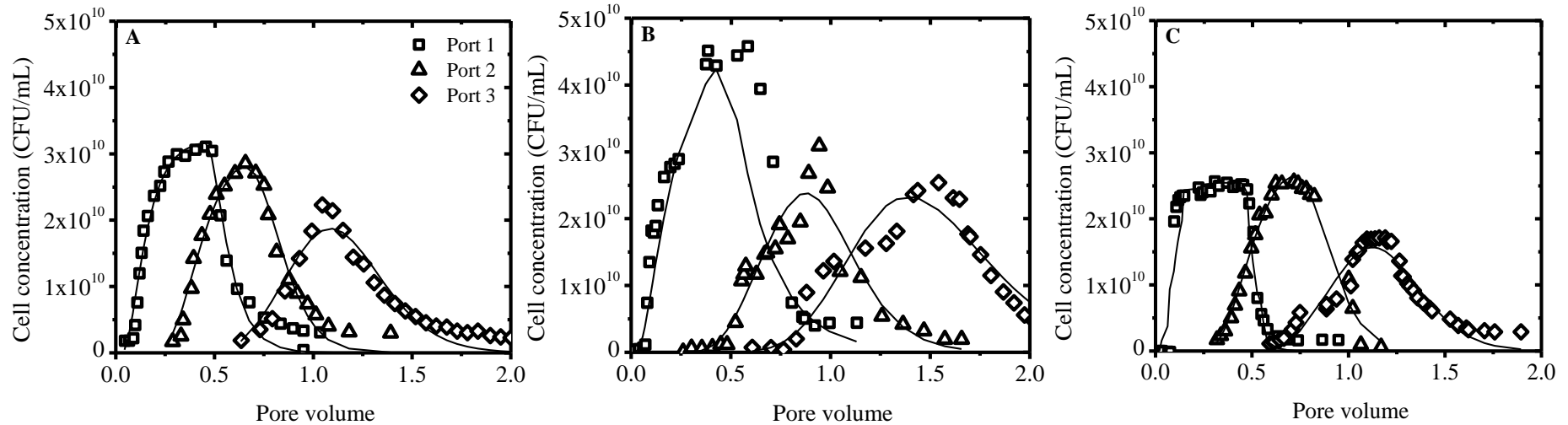
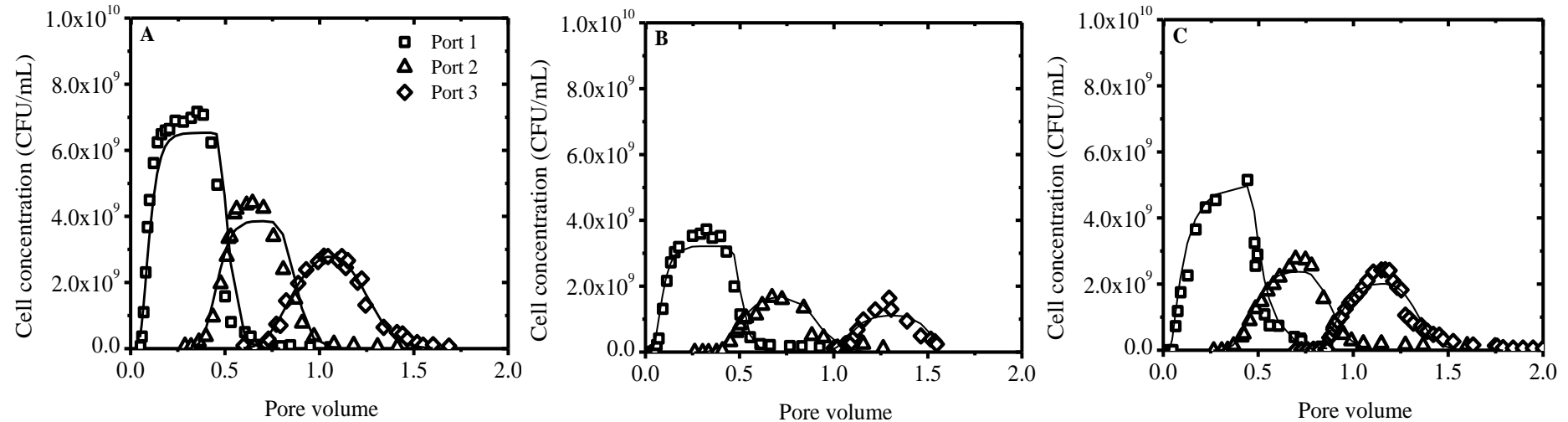
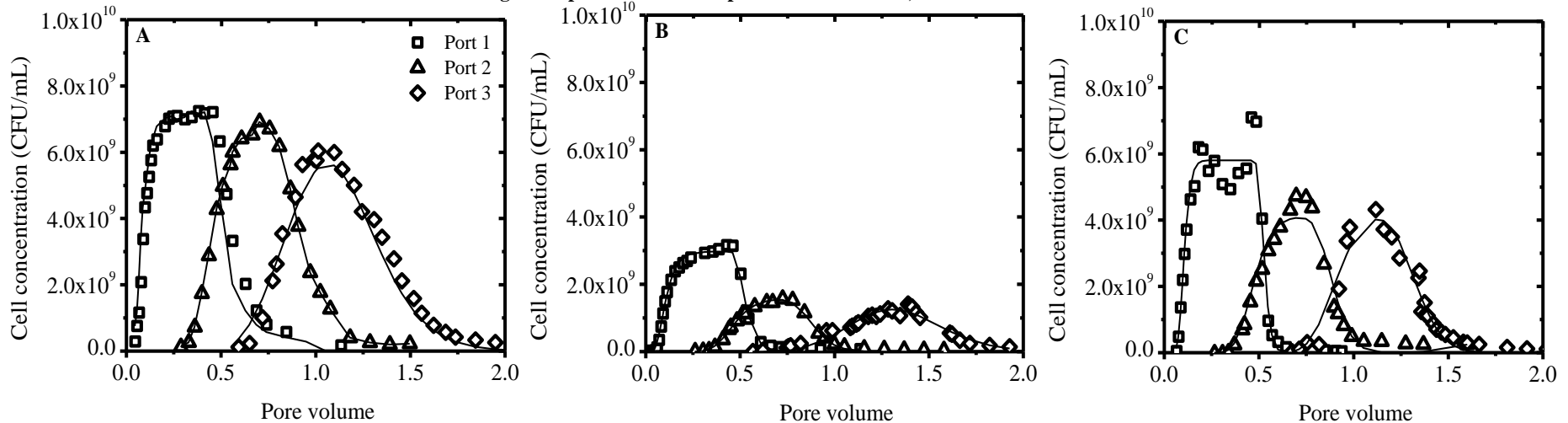


Figure 5-4 Comparison of the observed and fitted breakthrough curves of *P. putida* KT2442 in rhamnolipid that were obtained by *ex situ* measurements (A), the optrode with sampling for *ex situ* measurements (B) and the optrode without sampling for *ex situ* measurements (C).  $\square$ ,  $\Delta$  and  $\diamond$  shows the data obtained at Port 1, Port 2 and Port 3; Symbols are the observed data; lines are the fitted data. *Ex situ* measurement data is the average of duplicate data. The optrode data at Port 1, Port 2 and Port 3 are not from the same run.



**Figure 5-5** Comparison of the observed and fitted breakthrough curves of *R. erythropolis*-pTEC23 td Tomato in water that were obtained by *ex situ* measurements (A), the optrode with sampling for *ex situ* measurements (B) and the optrode without sampling for *ex situ* measurements (C).  $\square$ ,  $\Delta$  and  $\diamond$  shows the data obtained at Port 1, Port 2 and Port 3; Symbols are the observed data; lines are the fitted data. *Ex situ* measurement data is the average of duplicate data. The optrode data at Port 1, Port 2 and Port 3 are not from the same run



**Figure 5-6** Comparison of the observed and fitted breakthrough curves of *R. erythropolis*-pTEC23 td Tomato in rhamnolipid that were obtained by *ex situ* measurements (A), the optrode with sampling for *ex situ* measurements (B) and the optrode without sampling for *ex situ* measurements (C).  $\square$ ,  $\Delta$  and  $\diamond$  shows the data obtained at Port 1, Port 2 and Port 3; Symbols are the observed data; lines are the fitted data. *Ex situ* measurement data is the average of duplicate data. The optrode data at Port 1, Port 2 and Port 3 are not from the same run.

Chapter 5. Employing a Novel Optical Biosensor for *in situ* Monitoring of Bacteria Transport in Saturated Column in Varying Physicochemical Conditions

**Table 5-2 Transport parameters in BTCs of *P. putida* KT2442-GFP and *R. erythropolis*-pTEC23 td Tomato that were monitored by *ex situ* measurements and the optrode**

	Bacteria stains	Experiment condition	Sampling port	D (cm <sup>2</sup> /min)	R <sub>d</sub>	μ (/min)	R <sup>2</sup>
<i>Ex situ</i> measurements	<i>P. putida</i> KT2442-GFP	Water	Port 1	0.12±0.04	1.73±0.06	0.030±0.005	0.952
			Port 2	0.20±0.04	1.30±0.02	0.012±0.001	0.964
			Port 3	0.14±0.02	1.24±0.01	0.008±0.001	0.957
		Rhamnolipid	Port 1	0.23±0.05	1.90±0.06	0.007±0.004	0.960
			Port 2	0.29±0.05	1.09±0.02	0.003±0.001	0.965
			Port 3	0.35±0.06	1.19±0.02	0.004±0.001	0.911
	<i>R. erythropolis</i> -pTEC23 td Tomato	Water	Port 1	0.05±0.02	1.08±0.03	0.031±0.004	0.961
			Port 2	0.20±0.04	1.12±0.02	0.019±0.001	0.927
			Port 3	0.11±0.01	1.11±0.01	0.013±0.001	0.984
		Rhamnolipid	Port 1	0.25±0.08	1.34±0.06	0.010±0.003	0.932
			Port 2	0.24±0.02	1.18±0.08	0.0001±0.001	0.990
			Port 3	0.25±0.03	1.14±0.01	0.0001±0.0003	0.940
Optrode with sampling for <i>ex situ</i> measurements	<i>P. putida</i> KT2442-GFP	Water	Port 1	0.07±0.01	1.76±0.03	0.1000±0.0030	0.986
			Port 2	0.10±0.04	2.27±0.04	0.0424±0.0020	0.917
			Port 3	0.42±0.06	1.68±0.02	0.0088±0.0006	0.928
		Rhamnolipid	Port 1	0.48±0.2	2.55±0.23	0.0010±0.0100	0.795
			Port 2	0.28±0.05	1.87±0.05	0.0122±0.0019	0.886
			Port 3	0.50±0.08	1.69±0.03	0.0004±0.0007	0.881
	<i>R. erythropolis</i> -pTEC23 td Tomato	Water	Port 1	0.17±0.08	1.47±0.13	0.1652±0.0062	0.946
			Port 2	0.11±0.05	1.38±0.04	0.0500±0.0015	0.903
			Port 3	0.03±0.02	1.48±0.02	0.0313±0.0012	0.791
		Rhamnolipid	Port 1	0.17±0.02	1.79±0.05	0.1781±0.0019	0.993
			Port 2	0.13±0.03	1.31±0.01	0.0525±0.0004	0.993
			Port 3	0.25±0.04	1.59±0.02	0.0247±0.0006	0.936
Optrode without sampling for <i>ex situ</i> measurements	<i>P. putida</i> KT2442-GFP	Water	Port 1	0.20±0.06	1.30±0.06	0.0472±0.0056	0.896
			Port 2	0.15±0.04	1.26±0.02	0.0338±0.0011	0.757
			Port 3	0.12±0.03	1.28±0.01	0.0134±0.0005	0.892
		Rhamnolipid	Port 1	0.22±0.04	1.20±0.07	0.0411±0.0057	0.915
			Port 2	0.26±0.06	1.24±0.06	0.0046±0.0008	0.982
			Port 3	0.30±0.07	1.22±0.02	0.0076±0.0007	0.911
	<i>R. erythropolis</i> -pTEC23 td Tomato	Water	Port 1	0.14±0.05	1.35±0.04	0.0700±0.0044	0.836
			Port 2	0.16±0.03	1.30±0.02	0.0332±0.0012	0.941
			Port 3	0.10±0.02	1.25±0.01	0.0200±0.0003	0.896
		Rhamnolipid	Port 1	0.15±0.07	1.30±0.03	0.0380±0.0028	0.894
			Port 2	0.15±0.04	1.24±0.01	0.0184±0.0008	0.946
			Port 3	0.15±0.02	1.20±0.01	0.0089±0.0003	0.921

Estimated value ± standard deviation

### 5.3.3. Discussions

#### 1) The influence of the sampling protocol

In this study, retardation and lower bacteria concentration were monitored by the optrode when the optrode and *ex situ* measurements were conducted together. The heterogeneity of the column may have contributed to the differences obtained by two sampling techniques. The optrode was used to collect data inside the column at horizontal distances of 17 mm and 10 mm from the outer edge to test this possibility. However, no significant difference was observed between these two sets of data ( $P > 0.05$ ), which showed a mean correlation of 0.8631 (Figure A-7 in the appendix for Chapter 5). This finding indicates that the column was homogeneously packed. A previous study (Gang Chen and Zhu, 2004) showed that differences in transport behaviour must be considered when comparing results produced by different monitoring methods. It was hypothesized in this study that that scale issue caused by the sampling volume could lead to different transport behaviour observed by the optrode and *ex situ* measurements. The optrode collects the emission spectra in a tiny volume around the optical fibre (Campbell et al., 1999), which can be regarded as a sampling point. Each *ex situ* measurement collects 0.2 mL of liquid sample from the sampling port, which could represent the average concentration in a relatively large area above the sampling port. *Ex situ* measurements removed 2.7% the total injected cell mass, and 6.0% of the total injected liquid from the column, respectively. No impact was found in the velocity at Port 1 (0.43 cm/min) when withdrawing *ex situ* samples from the (Figure A-8 in the appendix for Chapter 5). *Ex situ* measurements slightly decreased the velocity at Port 2 and Port 3 (from 0.43 cm/min to 0.42 cm/min and 0.42 cm/min, respectively), although the ANOVA test suggests *ex situ* measurements had a significant effect on the velocity at Port 2 and Port 3 ( $P < 0.05$ ). These analyses partially supported the finding of lower bacterial concentration and retardation in the BTCs produced by the optrode when samples were withdrawn for *ex situ* measurements. A possible reason could be that the optrode captured the disturbance created by the *ex situ* measurements on the pore scale when they were carried out together, although *ex situ* measurements did not appear to have a significant influence on the velocity inside of the column. As a consequence, the optrode possibly

monitored distinct bacteria transport behaviour when *ex situ* measurements created disturbance on the pore scale.

When these two measurements were carried out independently, BTCs produced by the optrode had a similar pattern and but slightly lower concentration compared to those collected by *ex situ* measurements. This difference could be due to the scale issue as a result of sampling volumes, or lower mass balance during the calibration procedure, or both. This phenomenon is acceptable and must be considered when comparing results obtained with different monitoring techniques. These results indicate that the optrode is sensitive to changes in the column and can provide more data on the pore scale. This *in situ* technique can be applied to monitor bacteria transport in *in situ* bioremediation in the future. It also offers the possibility of monitoring bacteria transport in a larger field, like 2D and 3D column, where the averaged *ex situ* samples are not able to represent the flow. The next section discusses the bacteria transport behaviour obtained by the optrode under different conditions without *ex situ* sampling.

## **2) The optrode monitored bacteria transport behaviour**

Without the disturbance from *ex situ* measurements, the optrode monitored a greater transport of hydrophilic bacteria compared to hydrophobic bacteria in this study (Figure 5-3 C vs Figure 5-5C). The optrode also observed how the addition of rhamnolipid promoted the transport of both bacterial strains. Those findings match observations from earlier studies (Hewitt et al., 2012; Tai et al., 2007). Since the optrode measures the bacteria transport from the pore scale, the interaction energy between bacteria and sand particles could possibly explain bacteria transport that was collected by the optrode. As shown in Figure 5-6, the hydrophobic bacteria had attractive LW-AB interaction ( $-34.6$  and  $-5.9$   $\text{mJ/m}^2$  in the presence of water and rhamnolipid, respectively) with sand particles. Repulsive LW-AB interaction ( $10.2$  and  $32.6$   $\text{mJ/m}^2$  in the presence of water and rhamnolipid, respectively) was obtained between hydrophilic bacteria and sand particles. The results for the LW-AB interaction energy support the observation that hydrophilic is easier to transport inside the column than hydrophobic bacteria.

Rhamnolipid increased the value of the LW-AB interaction energy between both strains and sand particles thereby weakening the attraction between hydrophobic bacteria and sand particles but enhancing the repulsive interaction between bacteria and sand particles. As a consequence, an enhanced bacteria transport was obtained with the addition of rhamnolipid for both bacterial strains. These results therefore suggest that the optrode can monitor bacteria transport and quantify the changes in physicochemical conditions.

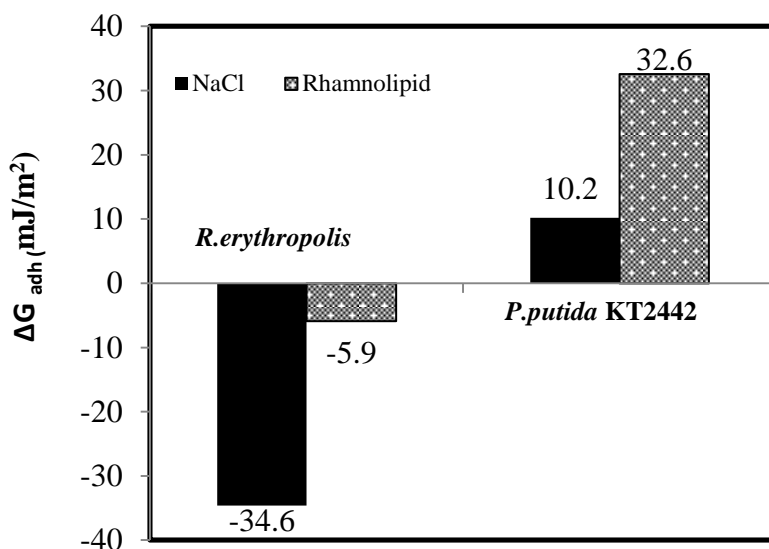


Figure 5-7 The value of  $\Delta G_{adh}$  between bacteria and sand particles with the addition of rhamnolipid

## 5.4. Conclusion

This study compared the transport behaviour of bacteria using the *in situ* optrode and *ex situ* measurements, and highlighted bacteria transport behaviour collected by the optrode without sampling for *ex situ* in the absence and presence of biosurfactant rhamnolipid. The *in situ* optrode and *ex situ* measurements monitored the transport of bacteria from different scales: a point and averaged liquid sample, respectively. The optrode was found to be sensitive to the modification of bacterial concentration and velocity on pore scale which is caused by *ex situ* measurements. When not sampling for *ex situ* measurements, the optrode is able to provide *in situ* bacteria transport data from pore scale and the effect of bacterial hydrophobicity and rhamnolipid on the bacteria transport in sand columns. More consistent values were obtained in fitted transport parameters of BTCs collected by the optrode without sampling for *ex situ* measurement. The optrode monitored bacteria transport under different

conditions could be understood through the LW-AB interaction energy between bacteria and sand particles.

As such, this study successfully demonstrated the use of the optrode *in situ* monitoring of bacterial mobility from the pore scale in the column despite the fact that the optrode occasionally collected variable values. This technique is particularly useful when collecting samplings that would be difficult or not possible in simulated soil environment. This study is possibly the first to document the monitoring of bacteria transport using a fluorescence optical biosensor. One limitation for the application of the optrode is that the optrode, like all other spectrometry method, can capture all signals that are excited at a specific wavelength without differentiating the source of each signal.

## **Acknowledgments**

This work was funded by the University of Auckland (New Zealand) and China Scholarship Council (China).

## **Chapter 6. Conclusions, Implications, and Recommendations for Future Research**

Over the last several decades, the research evidence for the incubation of contaminated soil with exogenous bacteria using surfactant solution has grown. More recent studies have considered the use of surfactant microbubbles to provide oxygen to oxygen-deficient soil. However, no detailed experimental investigation has been reported on the effect of surfactant type (anionic vs. nonionic) and bacterial hydrophobicity (hydrophobic vs. hydrophilic) on microbial transport after treatment with surfactant solution and surfactant microbubbles. Further, no study has considered monitoring bacterial transport *in situ*. This chapter summarizes the study's findings, discusses implications for *in situ* bioremediation, and makes recommendations for further study on the use of bacteria for bioremediation.

### **6.1. Conclusions and Implications for Bioremediation**

This thesis had five hypotheses and three primary objectives. The conclusion for each objective, the validity of each hypothesis, and the implications for *in situ* bioremediation were discussed as follows:

1) The different surfactant types altered bacterial hydrophobicity to different extents, but had an equivalent modification effect on the hydrophobicity of sand particles. In the absence of surfactant solution, hydrophilic bacteria were more likely to transport through the column than hydrophobic bacteria. The addition of surfactant solution modified the interaction energy between the bacteria and sand particles, resulting in enhanced transport for both hydrophobic and hydrophilic bacteria. Rhamnolipid showed a slight advantage over nonionic tergitol in enhancing bacteria transport, which is due to the weaker LW-AB interaction energy between bacteria and sand in the presence of rhamnolipid. This study is the first to consider and compare the effect of anionic and nonionic surfactant on the transport behaviour of both hydrophobic and hydrophilic bacteria. The results from this study could be used to help match bacteria and surfactant type when introducing microorganisms to contaminated soil.

2) Continuously injected microbubble reduced the usage of surfactant solution compared to the amount of surfactant solution that was required by surfactant solution aided bacteria transport. Anionic rhamnolipid microbubbles were shown to be a more promising vehicle for carrying bacteria in the column than nonionic tergitol microbubbles, which was due to the bacteria's preference for adhering to microbubbles rather than sand particles in the presence of rhamnolipid microbubbles. Hydrophilic bacteria were more likely to transport with microbubbles than hydrophobic bacteria, which was due to the greater adhesion tendency of hydrophobic bacteria to sand particles. Bacteria transport was promoted with the increased porosity of the column because of the increase in pore size. Rhamnolipid microbubble showed potential as an efficient vehicle for carrying hydrophilic bacteria to contaminated sites for *in situ* bioremediation, especially in the high permeable column. This study presented a preliminary investigation on the potential application of continuously injected microbubble for delivering both bacteria and oxygen for *in situ* bioremediation was also carried. The findings of this study could be utilized to gain insight into parameters that affect the distribution of bacteria with continuously injected microbubble. The findings of the study could also provide information to maximize the efficiency of the continuously injected microbubbles in the delivery of both bacteria and oxygen to oxygen-deficient soil environments.

3) The *in situ* optrode monitored bacteria on pore scale inside the column and was sensitive to the disturbance on bacterial concentration and velocity on pore scale. The optrode used without sampling for *ex situ* measurement could provide information on the effect of bacterial hydrophobicity and rhamnolipid on bacteria transport. Fitted transport parameters in BTCs that were collected by the optrode were more consistent among different sampling ports. The optrode monitored bacteria transport under various conditions could be understood through the calculation of LW-AB interaction energy between bacteria and sand particles. As such, the optrode provided *in situ* monitoring of bacteria mobility from pore scale in the column. It is possibly the first documented to monitor bacteria transport using a fluorescence optical biosensor. This technique offers a simpler and relatively cost-effective approach to monitor bacteria transport in soil environments where it is difficult or not possible to

collect samples. Like all another spectrometry method, the application of the optrode will be affected because the optrode captures all signals that are excited at a specific wavelength without differentiating the source of each signal.

## 6.2. Recommendations for Future Research

Work still remains to be done to enhance our knowledge of potential approaches for *in situ* bioremediation of contaminated soil. The following work is recommended for future research:

- 1) Only two strains of bacteria and two types of surfactant solutions were investigated in this study. Since bacterial hydrophobicity and surfactant type would affect the efficiency of bacteria transport, more data on bacteria transport in the presence of surfactant solution would be required to generalize these findings to gain a more accurate and realistic prediction of penetration of bacteria in the soil. Therefore, what is needed in the future is transport study involving a greater number of bacterial strains with different surface hydrophobicity, various surfactant types and various environmental factors. Another possible area of future research is to study the interaction between bacteria and pollutants and the distribution of pollutants in the contaminated soil when introducing bacteria.
- 2) The permeability of the porous media is an important parameter yet to be further explored in the future because the permeability of porous media is one of the key factors determining the penetration of microbubble. Another possible area of future research would be adjusting stirring speed, surfactant type, surfactant concentration and ionic strength of solution to generate smaller microbubble, or increase the stability of microbubble, thereby promoting the penetration of microbubble thus enhancing bacteria transport. Finally, if the microbubble is employed for *in situ* bioremediation in the future, a study similar to this study should be carried out on pollutants in contaminated soil. Knowledge of all of these factors has the potential to advance and stimulate *in situ* bioremediation.
- 3). In future studies, the optrode should be used in more complex soil environments in the laboratory, which is used to more closely simulate the real soil environment and gain more information on the

## Chapter 6. Conclusions, Implications and Recommendations for Future Research

distribution of bacteria when introducing exogenous bacteria. For example, it would be interesting to extend this work to two even three-dimensional columns to access bacterial distribution by using probes with different length. Moreover, no spectra data are available in the presence of microbubble because the microbubble is likely reflecting the excitation and emission light. Challenge remains to be for the application of *in situ* monitoring technique to systems with microbubbles and gain a clearer picture of the bacteria transport in the presence of microbubbles.

## Appendix

This appendix information provides calibration of the fluorescence intensity and concentration of bacteria, and contact angle measurement procedure and results.

### 1) The relationship between fluoresces intensity and CFU/mL

The number of bacteria was quantified by measuring the fluorescence signals of collected samples using a Perkin Elmer EnSpire 2300 multilabel plate reader and the Wallace Envision Manager software program. The fluorescence of *P. putida* KT2442-GFP was detected using excitation and emission wavelengths of 473 nm and 535 nm, respectively. The fluorescence of *R. erythropolis*-pTEC23 td Tomato was detected using excitation and emission wavelengths of 554 nm and 581 nm, respectively. To determine the relationship between the bacterial fluorescence intensity and cell concentration, a double dilution series of culture in saline was counted using fluorescence multiwell plate reader immediately and then be spread on nutrient agar plates and cultivated overnight. The colony-forming units (CFU) were counted the next day since it is assumed that a single bacterium grows into a single colony on the agar plate. A linear relationship was obtained between fluorescence intensity and CFU/mL, with a  $R^2$  value of 0.9597.

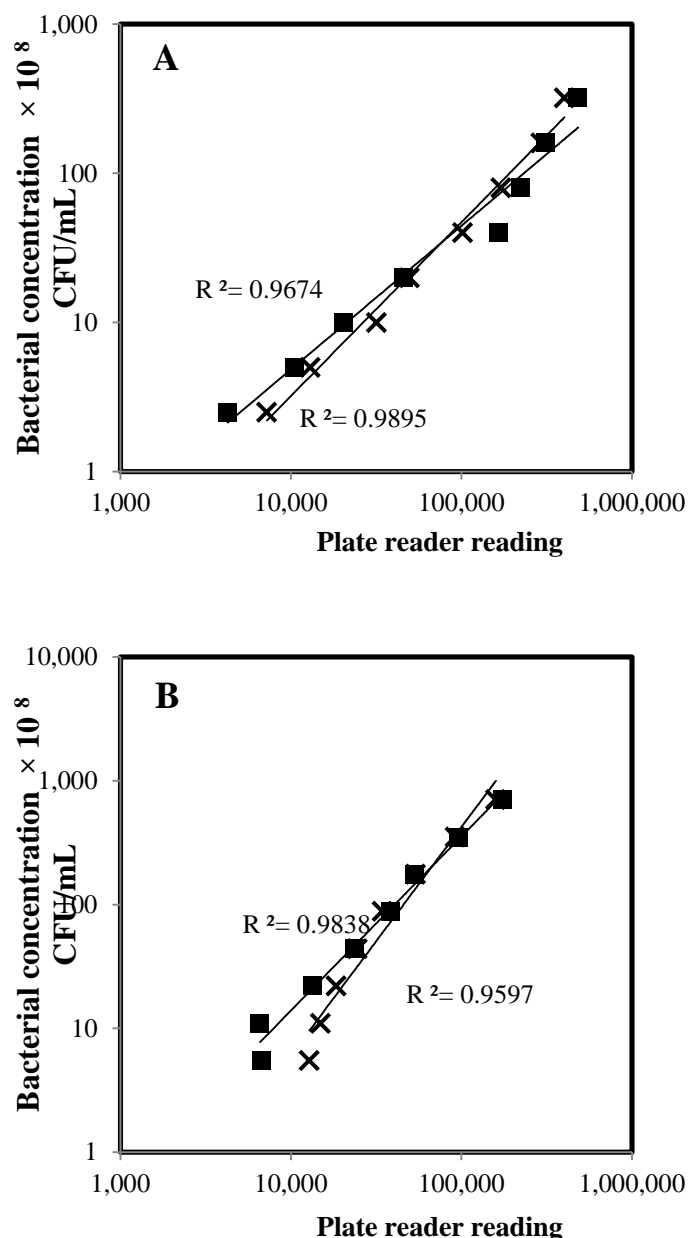


Figure A-1 Intensities of plate reader reading over doubling dilutions relative to cell concentration (CFU/mL). A: *R.e. rythropolis*-pTEC23 td Tomato; B: *P. putida* KT2442-GFP; ■ (dash line): water; × (solid line): rhamnolipid solution; A log-log scale is used.

## 2) Contact Angle Measurement

The contact angle measurement procedure was the same as used in a previous study (Feng et al., 2013b). Bacterial solution was prepared with optical density ( $OD_{600}$ ) = 0.3 to prepare the bacteria lawn. The consistency and accuracy of contact angle results mainly depend on a homogeneous bacterial lawn. To determine the minimum volume of bacterial suspension required for a homogeneous lawn, scanning electron microscopy (SEM) was used to check the bacterial lawn on 0.45  $\mu\text{m}$  (pore size) nitrocellulose membranes. In this study, 40 mL of bacterial solution was used with  $OD_{600}$  of 0.3 for *P. putida*

## Appendix

KT2442-GFP and *R. erythropolis*-pTEC23 td Tomato. Quartz is the major component of sand and quartz slides were used to represent sand when calculating the free energy interactions. The quartz slides were equilibrated with 0.01M NaCl and rhamnolipid solution for 48 hours and dried at room temperature for 12 hours before contact angle measurement was taken. Table S-1 is the list of probe liquids can be used as diagnostic liquid.

A digital goniometer was applied to measure the contact angle of the homogenous bacteria lawn and the contact angle was obtained using the CAM software. Three diagnostic liquids, Milli-Q water, formamide, and 1-bromonaphthalene were used (Bos, Mei, et al., 1999). Each result is the mean of five measurements. The contact angle of diagnostic liquid behaves differently between polar and nonpolar liquids. For nonpolar liquids, the contact angle keeps the same drop volume, drop height and base diameter during the recording period, i.e. 20 s (Figure S-3). However, the contact angle of the polar liquid changes with time (Figure S-4), which is consistent with previous findings (Sharma and Hanumantha Rao, 2002). Once the liquid drops on the bacterial lawn, it takes around 0.1 seconds for the probe liquid to spread on the surface and the volume of diagnostic liquid stays constant during this stage. After this stage, the contact angle of liquid drop remains constant with the same drop volume, height and base diameter. This equilibrium stage would last about 1-3 second. Then the contact angle decreases due to the absorbance of the polar liquid into the bacterial lawn. The decreasing stage is accompanied by a steady decrease of liquid volume and height as well as a constant increase in drop diameter. In this study, the digital goniometer was set up to capture the contact angle at time zero and beyond. Contact angle data at 2 seconds was selected as the finally contact angle for all the diagnostic liquid in this study.

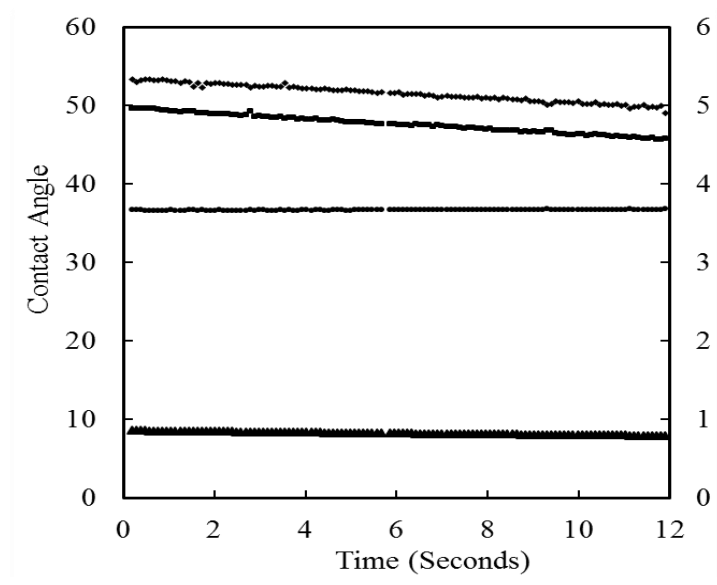


Figure A-2 The contact angle parameters of nonpolar liquid (1-bromonaphalene) as a function of time. ♦ is contact angle, ■ is drop volume, ▲ is height and ● is the base diameter

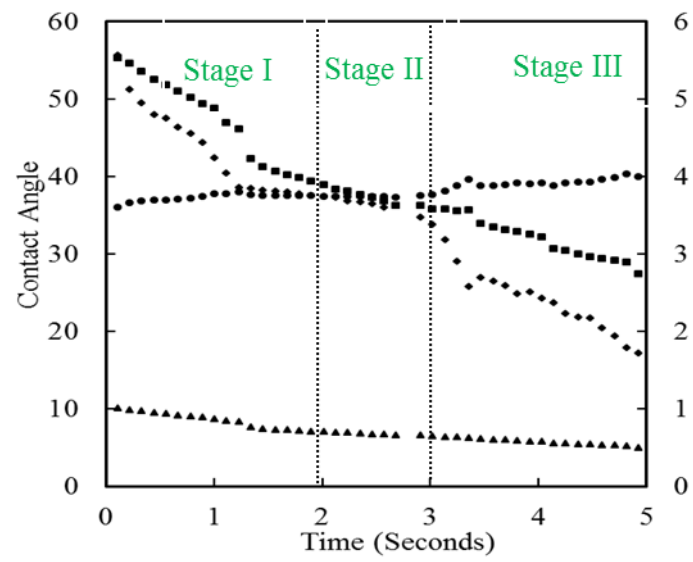


Figure A-3 The contact angle parameters of polar liquid (water) as a function of time. ♦ is contact angle, ■ is drop volume, ▲ is height and ● is base diameter

### 3) Contact angle results

**Table A-1 Contact angle ( $\theta$ ) for lawns of *R. erythropolis*-pTEC23 td Tomato and *P. putida* KT2442-GFP treated with surfactant**

Bacteria	Experimental conditions	$\hat{\theta}_{\text{Water}}$	$\hat{\theta}_{\text{Formamide}}$	$\hat{\theta}_{\text{1-Bromonaphthalene}}$
<i>R. erythropolis</i> - pTEC23 td Tomato	Water	94.7±0.3	67.9±0.4	41.2±0.6
	Rhamnolipid	84.0±0.4	62.6±0.8	41.2±0.4
	Tergitol	90.0±0.3	66.7±0.2	40.6±0.4
<i>P. putida</i> KT2442- GFP	Water	36.2±0.4	46.4±0.2	49.2±0.9
	Rhamnolipid	39.2±0.2	46.2±0.4	53.1±0.7
	Tergitol	39.7±0.5	33.8±0.7	30.4±0.8
Quartz	Water	46.7±1.3	17.7±3.2	30.1±1.5
	Rhamnolipid	14.8±1.2	14.7±0.8	28.7±3.4
	Tergitol	14.1±1.6	14.4±1.1	27.2±0.5

Obtained value ± standard deviation

## Appendix Information for Chapter 3

### 1) Free energy of bacteria aggregation

Based on surface tension parameters, the free energy of aggregation of bacterial cell immersed in water (Van der Mei et al., 1998; C. Van Oss, 1995) which indicates bacterial hydrophobicity can be calculated as:

$$\Delta G_{bwb} = -2(\sqrt{\gamma_b^{LW}} - \sqrt{\gamma_w^{LW}})^2 - 4(\sqrt{\gamma_b^+ \gamma_b^-} + \sqrt{\gamma_w^+ \gamma_w^-} - \sqrt{\gamma_b^+ \gamma_w^-} - \sqrt{\gamma_b^- \gamma_w^+}) \quad (\text{A-1})$$

where subscript  $b$  denotes bacteria,  $w$  denotes water.

If the interaction between two bacterial cells is stronger than the interaction between the cell with water, by definition, the cell are considered to be hydrophobic since  $\Delta G_{bwb} < 0$ , vice versa.

### 2) Nonequilibrium model for CDE

Solute transport in the subsurface is affected by a variety of chemical and physical nonequilibrium process. Chemical nonequilibrium may occur as a result of kinetic adsorption while physical

## Appendix

nonequilibrium is caused by a heterogeneous flow regime. Chemical nonequilibrium models consider adsorption on some of the adsorption sites to be instantaneous, while adsorption on the remaining sites is governed by the first-order kinetics. In contrast, physical nonequilibrium is often modelled by using a two-region type of formulation. The medium contains two distinct mobile and immobile liquid regions; mass transfer between the two is modelled as a first-order process.

This study considered the bacteria to be transporting through a uniform, one-dimensional, saturated porous media, therefore the chemical nonequilibrium CDE is described by the two-site models:

$$\left(1 + \frac{f\rho_b K_d}{\theta}\right) \frac{\partial C}{\partial t} = D \frac{\partial^2 C}{\partial x^2} - v \frac{\partial C}{\partial x} - \frac{\alpha\rho_b}{\theta} [(1-f)K_d C - s_k] \quad (\text{A-2})$$

$$-\mu_l C - \frac{f\rho_b K_d \mu_{s,e} C}{\theta} + \gamma_l(x) + \frac{f\rho_b \gamma_{s,e}(x)}{\theta} \quad (\text{A-3})$$

$$\frac{\partial s_k}{\partial t} = \alpha [(1-f)K_d C - s_k] - \mu_{s,k} s_k + (1-f)\gamma_{s,k}(x) \quad (\text{A-4})$$

where  $C$  is the bacteria concentration ( $\text{ML}^{-3}$ ),  $D$  is the dispersion coefficient ( $\text{L}^2\text{T}^{-1}$ ),  $\theta$  is the volumetric water content ( $\text{M}^3\text{L}^{-3}$ ),  $x$  is the distance ( $\text{L}$ ),  $t$  is the time ( $\text{T}$ ),  $\alpha$  is a first-order kinetic rate coefficient ( $\text{T}^{-1}$ ),  $f$  is the fraction of exchange sites that are always at equilibrium,  $\mu_l$  and  $\mu_s$  are the first order decay coefficient for degradation of solute in the liquid and adsorbed phase,  $\rho_b$  is the soil bulk density ( $\text{ML}^{-3}$ ), and the subscripts  $e$  and  $k$  refer to equilibrium and kinetic adsorption sites, respectively.

Table A-1 Dimensionless parameters for the nonequilibrium CDE

Parameters	Model	Parameters	Model
$T$	$\frac{vt}{L}$	$C_1$	$\frac{C}{C_0}$
$Z$	$\frac{x}{L}$	$C_2$	$\frac{s_k}{(1-f)K_d C_0}$
$P$	$\frac{vL}{L}$	$\mu_1$	$\frac{L(\theta\mu_l + f\rho_b K_d \mu_{s,e})}{\theta v}$
$R$	$1 + \frac{\rho_b K_d}{\theta}$	$\mu_2$	$\frac{L(1-f)\rho_b K_d \mu_{s,k}}{\theta v}$
$\beta$	$\frac{\theta + f\rho_b K_d}{\theta + \rho_b K_d}$	$\gamma_1$	$\frac{L(\theta\gamma_l + f\rho_b \gamma_{s,e})}{\theta v C_0}$
$\omega$	$\frac{\alpha(1-\beta)RL}{v}$	$\gamma_2$	$\frac{L(1-f)\rho_b \gamma_{s,k}}{\theta v C_0}$

According to the dimensionless parameters listed in Table A-1, the two-site model reduces to the same dimensionless form:

$$\beta R \frac{\partial C_1}{\partial T} = \frac{1}{P} \frac{\partial^2 C_1}{\partial Z^2} - \frac{\partial C_1}{\partial Z} - \omega(C_1 - C_2) - \mu_1 C_1 + r_1(Z) \quad (\text{A-5})$$

$$(1-\beta)R \frac{\partial C_2}{\partial T} = \omega(C_1 - C_2) - \mu_2 C_2 + r_2(Z) \quad (\text{A-6})$$

where the subscripts 1 and 2 refer to equilibrium and nonequilibrium sites, respectively.  $B$  is a partitioning coefficient, and  $\omega$  is a dimensionless mass transfer coefficient.

**3) Fitted parameters using nonequilibrium model****Table A-2 Fitted parameters using nonequilibrium model**

Bacteria	Experiment condition	Depth cm	D (cm <sup>2</sup> /min)	R <sub>d</sub>	$\beta$	$\mu$ (/min)	R <sup>2</sup>	
<i>R. erythropolis</i>	Water	3.0	0.05	1.065	0.9949	0.07332	0.960	
		15.5	0.1441	1.297	0.9999	0.027	0.964	
		30.5	0.11	1.117	0.9999	0.03276	0.982	
	Rhamnolipid	3.0	0.2128	1.256	0.9999	0.0001	0.931	
			15.5	0.22	1.217	0.999	0.0001	0.961
			30.5	0.265	1.13	0.6564	0.0001	0.967
		Tergitol	3.0	0.3476	2.159	0.9204	0.02415	0.934
			15.5	0.264	1.202	0.9999	0.01364	0.995
			30.5	0.1915	1.113	0.9999	0.1250	0.992
	<i>P. putida</i> KT2442	Water	3.0	0.1316	1.737	0.9999	0.09229	0.952
			15.5	0.1	1.35	0.773	0.02628	0.966
			30.5	0.1508	1.243	0.9999	0.01928	0.954
Rhamnolipid		3.0	0.2899	1.888	0.9999	0.1968	0.959	
			15.5	0.05	1.165	0.7326	0.00732	0.920
			30.5	0.3537	1.186	0.9999	0.008563	0.910
		Tergitol	3.0	0.4096	2.148	0.9999	0.02047	0.977
			15.5	0.1109	1.527	0.6934	0.005065	0.979
			30.5	0.2996	1.246	0.1487	0.007653	0.990

**Appendix Information for Chapter 5**

This Supplementary Information provides results of the calibration of the optrode in batch and the *ex situ* measurement results, the correlation of the optrode intensity collected from different depth inside the column, and the effect of *ex situ* measurement on the velocity at each sampling port.

**1) Calibration of the optrode**

A good linear relationship was observed between the fluorescence intensity collected by Optrode and bacterial concentration in liquid solution in our previous study (Hewitt et al., 2012; Hewitt et al., 2012). Since while the relationship is hard to obtain directly inside the column due to the complex environment, two sets of batch experiment were carried out to gain an indirect calibration between the optrode intensity and bacterial concentration in the sand column. In the first set of experiment, the

## Appendix

batch experiment was carried out in the double diluted liquid solution in the absence of sand particles. The 1000 uL bacterial cell solution with double dilution were prepared in 1.5 mL microtubes. The fluorescence intensity was collected by submerging the probe in bacterial cell solutions, and the concentration of bacterial cell was determined by plate count protocol. The second batch experiment was carried out in the presence of sand particles to simulate the column condition. The sand particle was wet mixed in a microtube with the same water ratio inside the column (1:0.23) and the fluorescence intensity was collected by submerging the probe in the sand system. The relationship between fluorescence intensity and bacterial concentration can be determined by regrouping the two sets of experiment above. The entire sample was prepared in triplicate in absence and presence of rhamnolipid. Background eliminations were achieved by taking the reading of bacterial-free blank samples. Six blank samples were prepared and checked for the consistency of emission spectra intensity.

A linear relationship between optrode fluorescence intensity and the concentration of bacteria cells was observed in all cases (Figure A-4), with an  $R^2$  value of 0.9833. Our result was consistent with that obtained by the previous study Hewitt et al. (2012) that the bacterial culture with doubling dilutions demonstrated a good linear relationship with the optrode fluorescence intensity collected from *E. coli* labeled with GFP and DsRed genes. The optrode fluorescence intensity collected in the presence of rhamnolipid was close to that collected in the absence of rhamnolipid, which indicates that the optrode was able to overcome the influence of rhamnolipid in the liquid solution although rhamnolipid can contribute to the optrode fluorescence intensity. Compared with the optrode fluorescence intensity collected from *P. putida* KT2442- GFP, a stronger intensity was collected from *R. erythropolis*-pTEC23 cells, which indicates that the fluorescence intensity from *R. erythropolis*-pTEC23 was more sensitive than that from *P. putida* KT2442-GFP cells.

The second experiment collected the spectrum intensities of bacteria after adding sand particles to the centrifuge tubes (Figure A-5). The optrode fluorescence intensity obtained in the sand system was generally lower than what was obtained in liquid solutions for both bacterial strains, with an  $R^2$  value of

Appendix

0.9593. To investigate the relationship between the optrode signal intensity and the number of bacterial cells in the absence and presence of rhamnolipid in the sand column, data in Figure A-4 and Figure A-5 were regrouped in Figure A-6. A linear relationship was obtained between the optrode signal intensity and the number of bacteria cells, with an  $R^2$  value of 0.9459. After this calibration procedure, the bacterial concentration in the column experiment can be determined through the normalized calibration curves.

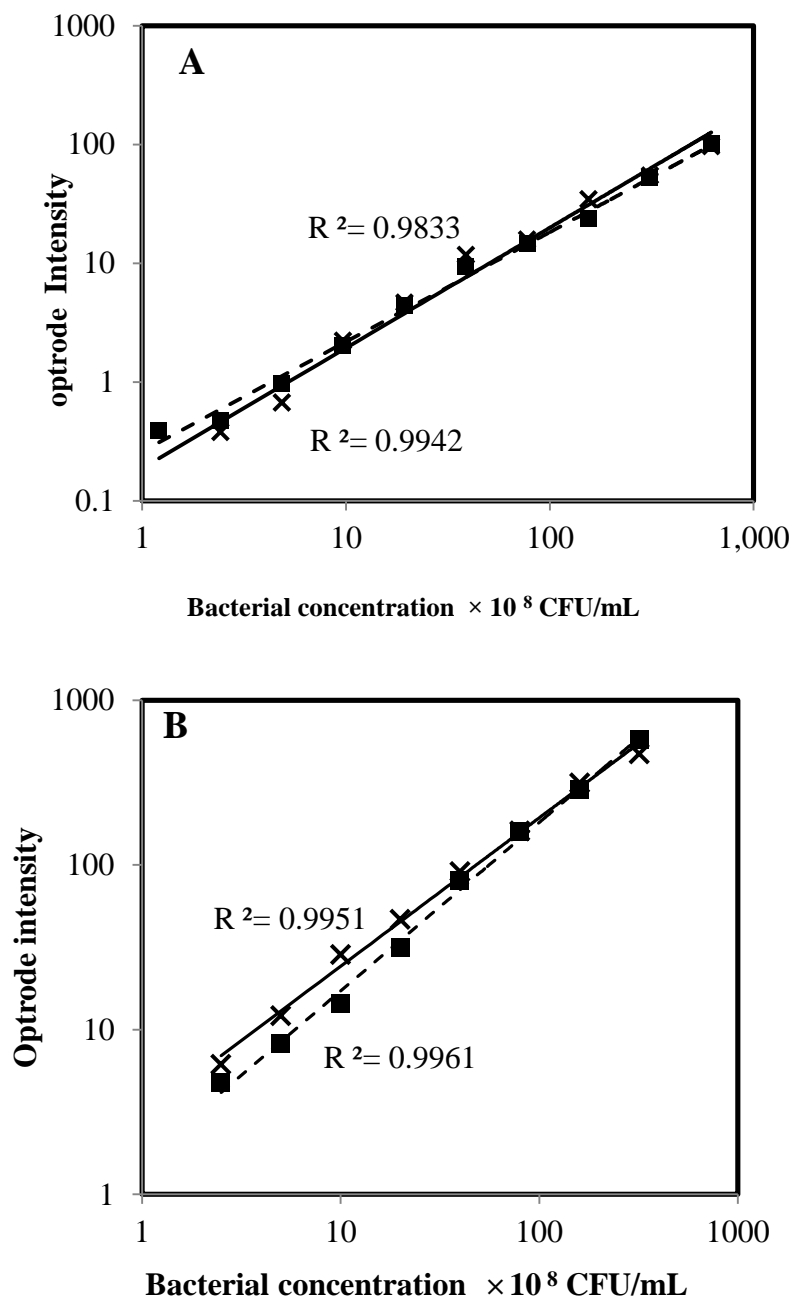


Figure A-4 Normalized Spectrum intensities over doubling dilutions relative to cell concentration in liquid media. A: *P. putida* KT2442-GFP; B: *R. e rythropolis*-pTEC23 td Tomato; ■ (dash line): water; × (solid line): rhamnolipid solution; A log-log scale is used.

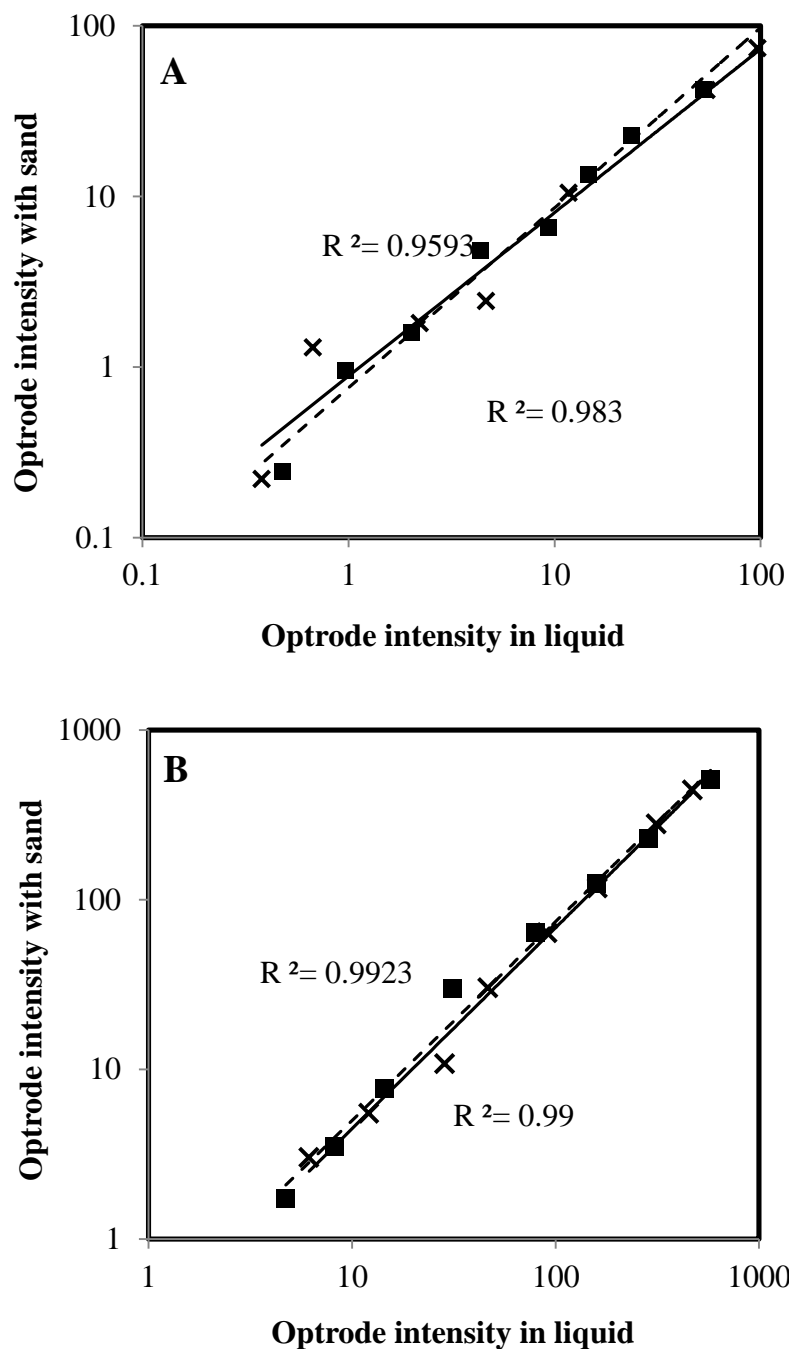


Figure A-5 Normalized Spectrum intensities over doubling dilutions in liquid and sand system. A: *P. putida* KT2442-GFP; B: *R. erythropolis*-pTEC23 tdTomato; ■ (dash line): in liquid; × (solid line): sand system; A log-log scale is used.

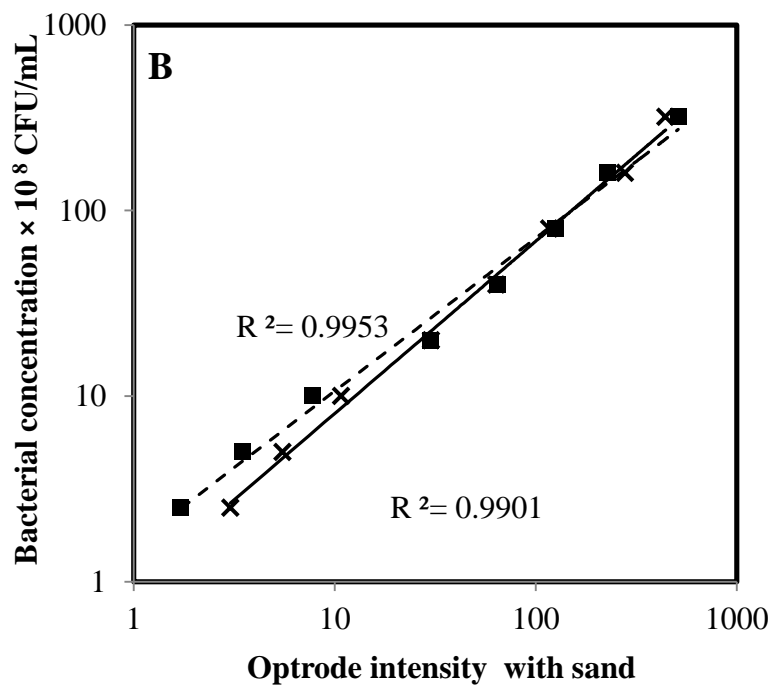
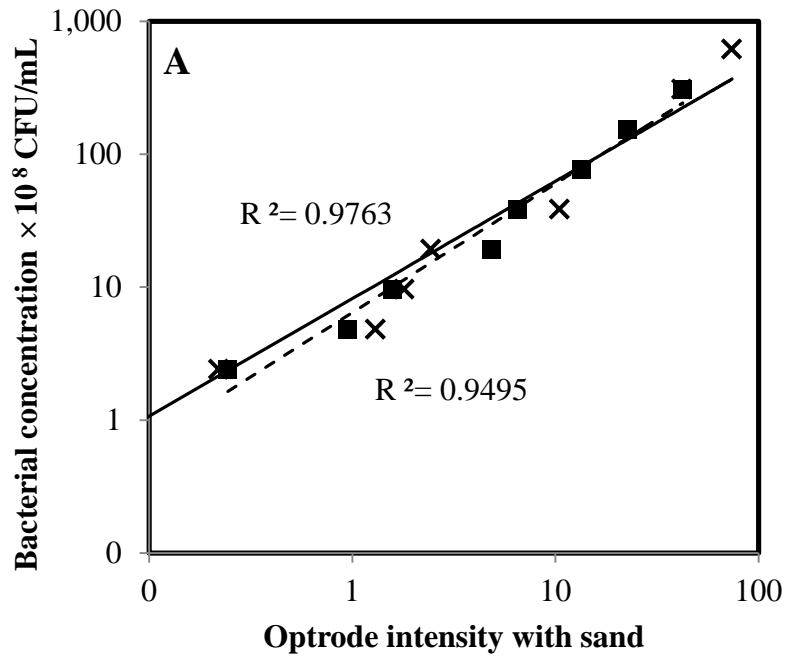


Figure A-6 Normalized Spectrum intensities over doubling dilutions relative to cell concentration with sand. A: *P. putida* KT2442-GFP; B: *R. erythropolis*-pTEC23 td Tomato; ■ (dash line): in liquid; × (solid line): with sand; A log-log scale is used.

2) The correlation of the optrode intensity collected from 10 mm and 17 mm inside the column

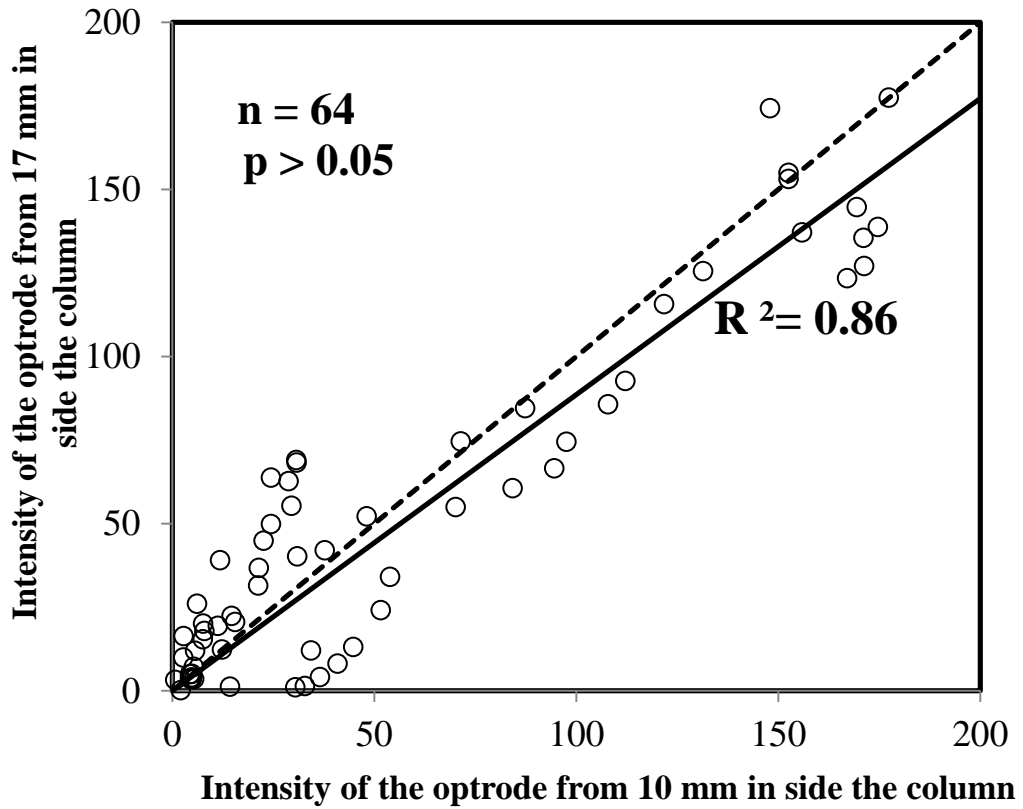
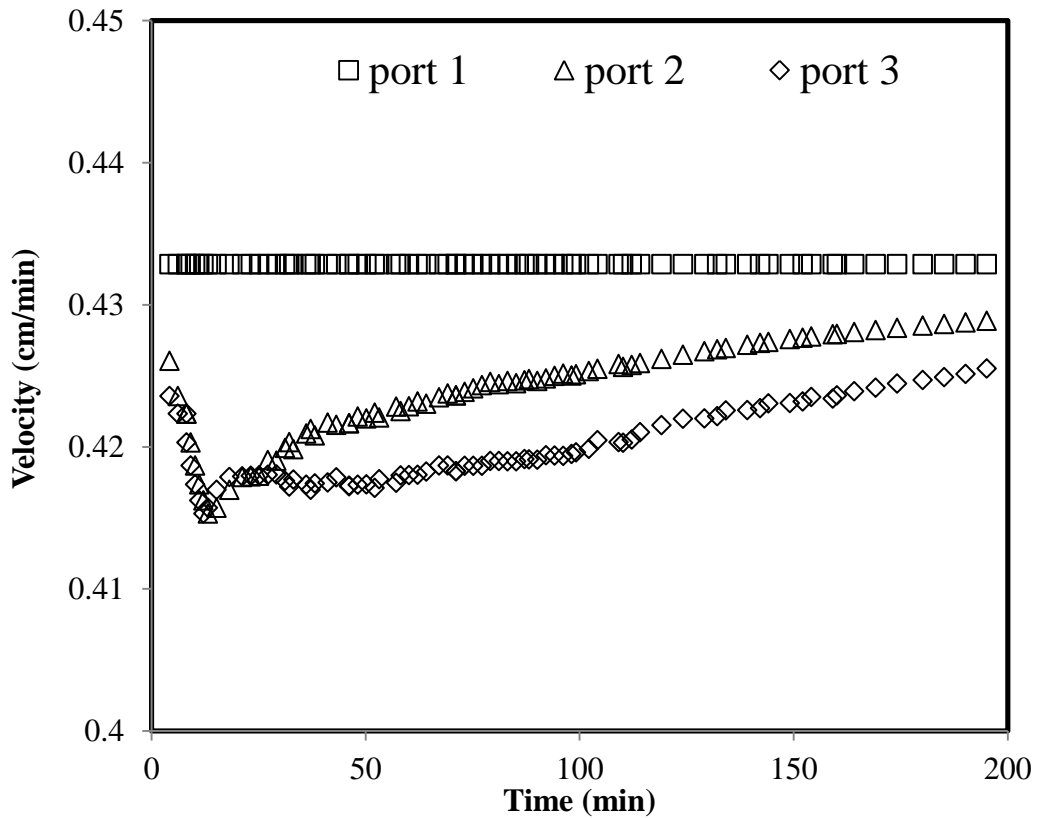


Figure A-7 Correlation of the optrode intensity collected from 10 mm and 17 mm inside the column

3) The velocity inside the column at different sampling port due to the effect of *ex situ* sampling



FigureA-8 The velocity inside the column at different stamping port due to effect of *ex situ* sampling

## Bibliography

- Abalos, A., Vinas, M., Sabate, J., Manresa, M., Solanas, A. (2004). Enhanced biodegradation of Casablanca crude oil by a microbial consortium in presence of a rhamnolipid produced by *Pseudomonas aeruginosa* AT10. *Biodegradation*, 15(4), 249-260.
- Abbott, A., Rutter, P., Berkeley, R. (1983). The influence of ionic strength, pH and a protein layer on the interaction between *Streptococcus mutans* and glass surfaces. *Microbiology*, 129(2), 439-445.
- Absolom, D. R., Lamberti, F. V., Policova, Z., Zingg, W., van Oss, C. J., Neumann, A. (1983). Surface thermodynamics of bacterial adhesion. *Applied and environmental microbiology*, 46(1), 90-97.
- Abu-Lail, N. I., Camesano, T. A. (2003). Role of lipopolysaccharides in the adhesion, retention, and transport of *Escherichia coli* JM109. *Environmental science & technology*, 37(10), 2173-2183.
- Abu-Zreig, M., Rudra, R., Dickinson, W. (2003). Effect of application of surfactants on hydraulic properties of soils. *Biosystems Engineering*, 84(3), 363-372.
- Aitken, M. D., Stringfellow, W. T., Nagel, R. D., Kazunga, C., Chen, S.-H. (1998). Characteristics of phenanthrene-degrading bacteria isolated from soils contaminated with polycyclic aromatic hydrocarbons. *Canadian journal of microbiology*, 44(8), 743-752.
- Al-Tahhan, R. A., Sandrin, T. R., Bodour, A. A., Maier, R. M. (2000). Rhamnolipid-induced removal of lipopolysaccharide from *Pseudomonas aeruginosa*: effect on cell surface properties and interaction with hydrophobic substrates. *Applied and environmental microbiology*, 66(8), 3262-3268.
- Atlas, R. M., Bartha, R. (1981). *Microbial ecology: fundamentals and applications*: Addison-Wesley Publishing Company.
- Avramova, T., Sotirova, A., Galabova, D., Karpenko, E. (2008). Effect of Triton X-100 and rhamnolipid PS-17 on the mineralization of phenanthrene by *Pseudomonas* sp. cells. *International Biodeterioration & Biodegradation*, 62(4), 415-420.
- Bai, G., Brusseau, M. L., Miller, R. M. (1997). Influence of a Rhamnolipid Biosurfactant on the Transport of Bacteria through a Sandy Soil. *Applied and environmental microbiology*, 63(5), 1866-1873.
- Bai, H., Cochet, N., Pauss, A., Lamy, E. (2016). Bacteria cell properties and grain size impact on bacteria transport and deposition in porous media. *Colloids and Surfaces B: Biointerfaces*, 139, 148-155. doi: <http://dx.doi.org/10.1016/j.colsurfb.2015.12.016>
- Banning, N., Toze, S., Mee, B. (2002). *Escherichia coli* survival in groundwater and effluent measured using a combination of propidium iodide and the green fluorescent protein. *Journal of applied microbiology*, 93(1), 69-76.
- Barbee, G., Brown, K. (1986). Comparison between Suction and Free-Drainage Soil Solution Samplers. *Soil Science*, 141(2), 149-154.
- Belkin, S. (2003). Microbial whole-cell sensing systems of environmental pollutants. *Current Opinion in Microbiology*, 6(3), 206-212.
- Beveridge, T. (1981). *Ultrastructure, chemistry, and function of the bacterial wall*: Academic Press.
- Bos, R., Mei, H. C., Busscher, H. J. (1999). Physico-chemistry of initial microbial adhesive interactions—its mechanisms and methods for study. *FEMS microbiology reviews*, 23(2), 179-230.
- Bos, R., Van der Mei, H. C., Busscher, H. J. (1999). Physico-chemistry of initial microbial adhesive interactions—its mechanisms and methods for study. *FEMS microbiology reviews*, 23(2), 179-230.
- Bouwer, E. J., Zehnder, A. J. (1993). Bioremediation of organic compounds—putting microbial metabolism to work. *TRENDS in Biotechnology*, 11(8), 360-367.

## Bibliography

- Bradford, S. A., Bettahar, M., Simunek, J., Van Genuchten, M. T. (2004). Straining and attachment of colloids in physically heterogeneous porous media. *Vadose Zone Journal*, 3(2), 384-394.
- Bradford, S. A., Simunek, J., Bettahar, M., van Genuchten, M. T., Yates, S. R. (2003). Modeling colloid attachment, straining, and exclusion in saturated porous media. *Environmental science & technology*, 37(10), 2242-2250.
- Bradford, S. A., Yates, S. R., Bettahar, M., Simunek, J. (2002). Physical factors affecting the transport and fate of colloids in saturated porous media. *Water Resources Research*, 38(12), 63-61-63-12.
- Brown, D. G., Jaffé P. R. (2006). Effects of nonionic surfactants on the cell surface hydrophobicity and apparent Hamaker constant of a *Sphingomonas* sp. *Environmental science & technology*, 40(1), 195-201.
- Busscher, H., Weerkamp, A., Van der Mei, H., Van Pelt, A., De Jong, H., Arends, J. (1984). Measurement of the surface free energy of bacterial cell surfaces and its relevance for adhesion. *Applied and environmental microbiology*, 48(5), 980-983.
- Campbell, C. G., Ghodrati, M., Garrido, F. (1999). Comparison of time domain reflectometry, fiber optic mini-probes, and solution samplers for real time measurement of solute transport in soil. *Soil Science*, 164(3), 156-170.
- Champion, J. T., Gilkey, J. C., Lamparski, H., Retterer, J., Miller, R. M. (1995). Electron microscopy of rhamnolipid (biosurfactant) morphology: effects of pH, cadmium, and octadecane. *Journal of Colloid and Interface Science*, 170(2), 569-574.
- Chen, A. Y. H., Vanholsbeeck, F., Tai, D. C. S., Svrcek, M., Smail, B. H. (2010). *Time-resolved all fiber fluorescence spectroscopy system*.
- Chen, G., Qiao, M., Zhang, H., Zhu, H. (2004). Bacterial desorption in water-saturated porous media in the presence of rhamnolipid biosurfactant. *Research in microbiology*, 155(8), 655-661.
- Chen, G., Strevett, K. A. (2001). Impact of surface thermodynamics on bacterial transport. *Environmental microbiology*, 3(4), 237-245.
- Chen, G., Walker, S. L. (2007). Role of solution chemistry and ion valence on the adhesion kinetics of groundwater and marine bacteria. *Langmuir*, 23(13), 7162-7169.
- Chen, G., Zhu, H. (2004). Bacterial deposition in porous medium as impacted by solution chemistry. *Research in microbiology*, 155(6), 467-474.
- Chen, G., Zhu, H. (2005). Bacterial adhesion to silica sand as related to Gibbs energy variations. *Colloids and Surfaces B: Biointerfaces*, 44(1), 41-48.
- Choi, Y. J., Kim, Y.-J., Nam, K. (2009). Enhancement of aerobic biodegradation in an oxygen-limiting environment using a saponin-based microbubble suspension *Environmental pollution* (Vol. 157, pp. 2197-2202).
- Choi, Y. J., Park, J. Y., Kim, Y.-J., Nam, K. (2008a). Flow Characteristics of Microbubble Suspensions in Porous Media as an Oxygen Carrier. *Clean*, 36(1), 59-65.
- Choi, Y. J., Park, J. Y., Kim, Y. J., Nam, K. (2008b). Flow characteristics of microbubble suspensions in porous media as an oxygen carrier. *Clean–Soil, Air, Water*, 36(1), 59-65.
- D'souza, S. (2001). Microbial biosensors. *Biosensors and Bioelectronics*, 16(6), 337-353.
- Daffonchio, D., Thaveesri, J., Verstraete, W. (1995). Contact angle measurement and cell hydrophobicity of granular sludge from upflow anaerobic sludge bed reactors. *Applied and Environmental Microbiology*, 61(10), 3676-3680.
- Davis, J., Vaughan, D. H., Cardosi, M. F. (1995). Elements of biosensor construction. *Enzyme and Microbial Technology*, 17(12), 1030-1035.
- Dean, S. M., Jin, Y., Cha, D. K., Wilson, S. V., Radosevich, M. (2001). Phenanthrene degradation in soils co-inoculated with phenanthrene-degrading and biosurfactant-producing bacteria. *Journal of Environmental Quality*, 30(4), 1126-1133.
- Dennis, J. J., Zylstra, G. J. (2004). Complete Sequence and Genetic Organization of pDTG1, the 83 Kilobase Naphthalene Degradation Plasmid from *Pseudomonas putida* strain NCIB 9816-4. *Journal of Molecular Biology*, 341(3), 753-768. doi: <http://dx.doi.org/10.1016/j.jmb.2004.06.034>

## Bibliography

- Derjaguin, B. (1993). A theory of interaction of particles in presence of electric double layers and the stability of lyophobic colloids and disperse systems. *Progress in Surface Science*, 43(1), 1-14.
- Derjaguin, B., Landau, L. (1941). Theory of the stability of strongly charged lyophobic sols and of the adhesion of strongly charged particles in solutions of electrolytes. *Acta physicochim. URSS*, 14(6), 633-662.
- Desai, J. D., Banat, I. M. (1997). Microbial production of surfactants and their commercial potential. *Microbiology and molecular Biology reviews*, 61(1), 47-64.
- Dickinson, R. B. (2006). Bacteria: Surface Behavior *Encyclopedia of Surface and Colloid Science, Second Edition* (pp. 884-893).
- Ding, Y., Liu, B., Shen, X., Zhong, L., Li, X. (2013). Foam-assisted delivery of nanoscale zero valent iron in porous media. *Journal of Environmental Engineering*, 139(9), 1206-1212.
- Dong, H., Rothmel, R., Onstott, T. C., Fuller, M. E., DeFlaun, M. F., Streger, S. H., Dunlap, R., Fletcher, M. (2002). Simultaneous transport of two bacterial strains in intact cores from Oyster, Virginia: biological effects and numerical modeling. *Applied and environmental microbiology*, 68(5), 2120-2132.
- Dorn, J. G., Brusseau, M. L., Maier, R. M. (2005). Real-time, in situ monitoring of bioactive zone dynamics in heterogeneous systems. *Environmental science & technology*, 39(22), 8898-8905.
- Feng, W., Singhal, N., Swift, S. (2009). Drainage mechanism of microbubble dispersion and factors influencing its stability. *Journal of Colloid and Interface Science*, 337(2), 548-554.
- Feng, W., Swift, S., Singhal, N. (2013a). Effects of surfactants on cell surface tension parameters and hydrophobicity of *Pseudomonas putida* 852 and *Rhodococcus erythropolis* 3586. *Colloids and Surfaces B: Biointerfaces*, 105, 43-50.
- Feng, W., Swift, S., Singhal, N. (2013b). Effects of surfactants on cell surface tension parameters and hydrophobicity of *Pseudomonas putida* 852 and *Rhodococcus erythropolis* 3586. *Colloids and Surfaces B: Biointerfaces*, 105, 43-50.
- Fontes, D. E., Mills, A., Hornberger, G., Herman, J. (1991). Physical and chemical factors influencing transport of microorganisms through porous media. *Applied and Environmental Microbiology*, 57(9), 2473-2481.
- Gannon, J., Manilal, V., Alexander, M. (1991). Relationship between cell surface properties and transport of bacteria through soil. *Applied and environmental microbiology*, 57(1), 190-193.
- Gargiulo, G., Bradford, S., Simunek, J., Ustohal, P., Vereecken, H., Klumpp, E. (2008). Bacteria transport and deposition under unsaturated flow conditions: The role of water content and bacteria surface hydrophobicity. *Vadose Zone Journal*, 7(2), 406-419.
- Gilbert, P., Evans, D., Evans, E., Duguid, I., Brown, M. (1991). Surface characteristics and adhesion of *Escherichia coli* and *Staphylococcus epidermidis*. *Journal of Applied Bacteriology*, 71(1), 72-77.
- Gottfried, A., Singhal, N., Elliot, R., Swift, S. (2010). The role of salicylate and biosurfactant in inducing phenanthrene degradation in batch soil slurries. *Applied microbiology and biotechnology*, 86(5), 1563-1571.
- Gross, M. J., Logan, B. E. (1995). Influence of different chemical treatments on transport of *Alcaligenes paradoxus* in porous media. *Applied and environmental microbiology*, 61(5), 1750-1756.
- Grotenhuis, J., Plugge, C., Stams, A., Zehnder, A. (1992). Hydrophobicities and electrophoretic mobilities of anaerobic bacterial isolates from methanogenic granular sludge. *Applied and environmental microbiology*, 58(3), 1054-1056.
- Guo, R., McGoverin, C., Swift, S., Vanholsbeeck, F. (2017). A rapid and low-cost estimation of bacteria counts in solution using fluorescence spectroscopy. *Analytical and bioanalytical chemistry*, 409(16), 3959-3967.
- Hartmann, L. (1966). Effect of surfactants on soil bacteria *Bulletin of environmental contamination and toxicology* (pp. 219-224): Springer.
- Heitzer, A., Malachowsky, K., Thonnard, J. E., Bienkowski, P. R., White, D. C., Sayler, G. S. (1994). Optical biosensor for environmental on-line monitoring of naphthalene and salicylate

## Bibliography

- bioavailability with an immobilized bioluminescent catabolic reporter bacterium. *Applied and environmental microbiology*, 60(5), 1487-1494.
- Hendry, M., Lawrence, J., Maloszewski, P. (1999). Effects of velocity on the transport of two bacteria through saturated sand. *Groundwater*, 37(1), 103-112.
- Herzig, J., Leclerc, D., Goff, P. L. (1970). Flow of suspensions through porous media—application to deep filtration. *Industrial & Engineering Chemistry*, 62(5), 8-35.
- Hewitt, B. M., Singhal, N., Elliot, R. G., Chen, A. Y., Kuo, J. Y., Vanholsbeeck, F. d. r., Swift, S. (2012). Novel fiber optic detection method for in situ analysis of fluorescently labeled biosensor organisms. *Environmental science & technology*, 46(10), 5414-5421.
- Hogt, A. H., DANKERT, J., Feijen, J. (1985). Adhesion of *Staphylococcus epidermidis* and *Staphylococcus saprophyticus* to a hydrophobic biomaterial. *Microbiology*, 131(9), 2485-2491.
- Hogt, A. H., Dankert, J., Hulstaert, C., Feijen, J. (1986). Cell surface characteristics of coagulase-negative staphylococci and their adherence to fluorinated poly (ethylenepropylene). *Infection and immunity*, 51(1), 294-301.
- Huang, C.-W., Chang, C.-H. (2000). A laboratory study on foam-enhanced surfactant solution flooding in removing n-pentadecane from contaminated columns. *Colloids and Surfaces A: Physicochemical and Engineering Aspects*, 173(1), 171-179.
- Huang, G., Huang, Q., Zhan, H. (2006). Evidence of one-dimensional scale-dependent fractional advection–dispersion. *Journal of Contaminant Hydrology*, 85(1), 53-71.
- Huysman, F., Verstraete, W. (1993). Water-facilitated transport of bacteria in unsaturated soil columns: influence of cell surface hydrophobicity and soil properties. *Soil Biology and Biochemistry*, 25(1), 83-90.
- Ishigami, Y., Gama, Y., Nagahora, H., Yamaguchi, M., Nakahara, H., Kamata, T. (1987). The pH-sensitive conversion of molecular aggregates of rhamnolipid biosurfactant. *Chemistry Letters*, 16(5), 763-766.
- Ivask, A., Green, T., Polyak, B., Mor, A., Kahru, A., Virta, M., Marks, R. (2007). Fibre-optic bacterial biosensors and their application for the analysis of bioavailable Hg and As in soils and sediments from Aznalcollar mining area in Spain. *Biosensors and Bioelectronics*, 22(7), 1396-1402.
- Jackson, A., Kommalapati, R., Roy, D., Pardue, J. (1998). Enhanced transport of bacteria through a soil matrix using colloidal gas aphyron suspensions. *J. Environ. Sci. Health*, 33, 369-384.
- Jackson, A., Kommalapati, R., Roy, D., Pardue, J. (1998). Enhanced transport of bacteria through a soil matrix using colloidal gas aphyron suspensions. *Journal of Environmental Science & Health Part A*, 33(3), 369-384.
- Jansson, J. K. (2003). Marker and reporter genes: illuminating tools for environmental microbiologists. *Current Opinion in Microbiology*, 6(3), 310-316.
- Jauregi, P., Gilmour, S., Varley, J. (1997). Characterisation of colloidal gas aphyrons for subsequent use for protein recovery. *The Chemical Engineering Journal and The Biochemical Engineering Journal*, 65(1), 1-11.
- Jauregi, P., Mitchell, G. R., Varley, J. (2000). Colloidal gas aphyrons (CGA): dispersion and structural features. *AIChE journal*, 46(1), 24-36.
- Jauregi, P., Varley, J. (1999). Colloidal gas aphyrons: potential applications in biotechnology. *TRENDS in Biotechnology*, 17(10), 389-395.
- Jenkins, K. B., Michelsen, D. L., Novak, J. T. (1993). Application of oxygen microbubbles for in situ biodegradation of p-xylene-contaminated groundwater in a soil column. *Biotechnol. Prog.*, 9, 394-400.
- Jenkins, K. B., Michelsen, D. L., Novak, J. T. (1993). Application of Oxygen Microbubbles for in Situ Biodegradation of p - Xylene - Contaminated Groundwater in a Soil Column. *Biotechnology Progress*, 9(4), 394-400.
- Jeong, S.-W., Corapcioglu, M. Y., Roosevelt, S. E. (2000). Micromodel study of surfactant foam remediation of residual trichloroethylene. *Environmental science & technology*, 34(16), 3456-3461.

## Bibliography

- Johnsen, A. R., Wick, L. Y., Harms, H. (2005). Principles of microbial PAH-degradation in soil. *Environmental pollution*, 133(1), 71-84.
- Kilbane, J., Liu, B., Conrad, J., Srivastava, V. (1997). Novel application of foam for in-situ soil remediation. Topical report, April 1992-September 1993: Institute of Gas Technology, Des Plaines, IL (United States).
- Klute, A. (2003). Solute dispersion coefficients and retardation factors. *Transport*, 44, 2.1.
- Knox, R. C., Sabatini, D. A., Canter, L. W. (1993). *Subsurface transport and fate processes*: Lewis publishers.
- Ko, S.-O., Schlautman, M. A., Carraway, E. R. (1998). Effects of solution chemistry on the partitioning of phenanthrene to sorbed surfactants. *Environmental science & technology*, 32(22), 3542-3548.
- Kovscek, A., Bertin, H. (2003). Foam mobility in heterogeneous porous media. *Transport in Porous Media*, 52(1), 17-35.
- Kovscek, A., Radke, C. (1994). *Fundamentals of foam transport in porous media*: ACS Publications.
- Kuhnt, G. (1993). Behavior and fate of surfactants in soil. *Environmental Toxicology and Chemistry*, 12(10), 1813-1820.
- Kwok, C.-K., Loh, K.-C. (2003). Effects of Singapore soil type on bioavailability of nutrients in soil bioremediation. *Advances in Environmental Research*, 7(4), 889-900.
- Lang, F. S., Destain, J., Delvigne, F., Druart, P., Ongena, M., Thonart, P. (2016). Biodegradation of Polycyclic Aromatic Hydrocarbons in Mangrove Sediments Under Different Strategies: Natural Attenuation, Biostimulation, and Bioaugmentation with *Rhodococcus erythropolis* T902. 1. *Water, Air, & Soil Pollution*, 227(9), 297.
- Leahy, J. G., Colwell, R. R. (1990). Microbial degradation of hydrocarbons in the environment. *Microbiological Reviews*, 54(3), 305-315.
- Leeson, A., Hinchee, R. E. (1996). Principles and practices of bioventing. Volume I: Bioventing principles: DTIC Document.
- Leneva, N., Kolomytseva, M., Baskunov, B., Golovleva, L. (2009). Phenanthrene and anthracene degradation by microorganisms of the genus *Rhodococcus*. *Applied biochemistry and microbiology*, 45(2), 169-175.
- Li, J.-L., Chen, B.-H. (2009). Effect of nonionic surfactants on biodegradation of phenanthrene by a marine bacteria of *Neptunomonas naphthovorans*. *Journal of hazardous materials*, 162(1), 66-73.
- Li, Q., Logan, B. E. (1999). Enhancing bacterial transport for bioaugmentation of aquifers using low ionic strength solutions and surfactants. *Water Research*, 33(4), 1090-1100.
- Long, F., Zhu, A., Gu, C., Shi, H. (2013). *Recent Progress in Optical Biosensors for Environmental Applications*.
- Maier, R. M. (2003). Biosurfactants: evolution and diversity in bacteria. *Advances in applied microbiology*, 52, 101-121.
- Mamun, C., Rong, J., Kam, S., Liljestrand, H., Rossen, W. (2002). *Extending foam technology from improved oil recovery to environmental remediation*. Paper presented at the SPE Annual Technical Conference and Exhibition.
- Maraha, N., Backman, A., Jansson, J. K. (2004). Monitoring physiological status of GFP-tagged *Pseudomonas fluorescens* SBW25 under different nutrient conditions and in soil by flow cytometry. *FEMS microbiology ecology*, 51(1), 123-132.
- Martin, M. J., Logan, B. E., Johnson, W. P., Jewett, D. G., Arnold, R. G. (1996). Scaling bacterial filtration rates in different sized porous media. *Journal of Environmental Engineering*, 122(5), 407-415.
- Matsushita, K., Mollah, A., Stuckey, D., Del Cerro, C., Bailey, A. (1992). Predispersed solvent extraction of dilute products using colloidal gas aphrons and colloidal liquid aphrons: aphron preparation, stability and size. *Colloids and Surfaces*, 69(1), 65-72.
- McCaulou, D. R., Bales, R. C., McCarthy, J. F. (1994). Use of short-pulse experiments to study bacteria transport through porous media. *Journal of Contaminant Hydrology*, 15(1), 1-14.

## Bibliography

- McNaught, A. D., McNaught, A. D. (1997). *Compendium of chemical terminology* (Vol. 1669): Blackwell Science Oxford.
- Melnyk, A., Dettlaff, A., Kuklińska, K., Namieśnik, J., Wolska, L. (2015). Concentration and sources of polycyclic aromatic hydrocarbons (PAHs) and polychlorinated biphenyls (PCBs) in surface soil near a municipal solid waste (MSW) landfill. *Science of the Total Environment*, 530, 18-27.
- Michelsen, D., Wallis, D., Sebba, F. (1984). In - situ biological oxidation of hazardous organics. *Environmental progress*, 3(2), 103-107.
- Michelsen, D. L., Wallis, D. A., Sebba, F. (1984). In-situ biological oxidation of hazardous organics. *Environ. Prog.*, 3, 103-107.
- Mohan, S. V., Kisa, T., Ohkuma, T., Kanaly, R. A., Shimizu, Y. (2006). Bioremediation technologies for treatment of PAH-contaminated soil and strategies to enhance process efficiency. *Reviews in Environmental Science and Bio/Technology*, 5(4), 347-374.
- Mueller, J. G., Cerniglia, C. E., Pritchard, P. H. (1996). Bioremediation of environments contaminated by polycyclic aromatic hydrocarbons. *Biotechnology Research Series*, 6, 125-194.
- Mulligan, C. N., Eftekhari, F. (2003). Remediation with surfactant foam of PCP-contaminated soil. *Engineering Geology*, 70, 269-279.
- Mulligan, C. N., Eftekhari, F. (2003). Remediation with surfactant foam of PCP-contaminated soil. *Engineering Geology*, 70(3), 269-279.
- Nitschke, M., Costa, S. G., Contiero, J. (2005). Rhamnolipid surfactants: an update on the general aspects of these remarkable biomolecules. *Biotechnology Progress*, 21(6), 1593-1600.
- Noordman, W. H., Janssen, D. B. (2002). Rhamnolipid stimulates uptake of hydrophobic compounds by *Pseudomonas aeruginosa*. *Applied and environmental microbiology*, 68(9), 4502-4508.
- Pantsyrnaya, T., Blanchard, F., Delaunay, S., Goergen, J., Gu élon, E., Guseva, E., Boudrant, J. (2011). Effect of surfactants, dispersion and temperature on solubility and biodegradation of phenanthrene in aqueous media. *Chemosphere*, 83(1), 29-33.
- Park, J. Y., Choi, Y. J., Moon, S., Shin, D. Y., Nam, K. (2009). Microbubble suspension as a carrier of oxygen and acclimated bacteria for phenanthrene biodegradation. *Journal of hazardous materials*, 163(2-3), 761-767.
- Parker, J. (1989). Multiphase flow and transport in porous media. *Reviews of Geophysics*, 27(3), 311-328.
- Parker, J., Van Genuchten, M. T. (1984). Determining transport parameters from laboratory and field tracer experiments. *Bulletin/Virginia Agricultural Experiment Station (USA)*. no. 84-3.
- Paul, D., Pandey, G., Pandey, J., Jain, R. K. (2005). Accessing microbial diversity for bioremediation and environmental restoration. *TRENDS in Biotechnology*, 23(3), 135-142.
- Perni, S., Preedy, E. C., Prokopovich, P. (2014). Success and failure of colloidal approaches in adhesion of microorganisms to surfaces. *Advances in colloid and interface science*, 206, 265-274.
- Philp, J. C., Bamforth, S. M., Singleton, I., Atlas, R. M. (2005). Environmental pollution and restoration: a role for bioremediation. *Bioremediation*. ASM Press, Washington, DC. USA, 1-48.
- Pinyakong, O., Habe, H., Supaka, N., Pinpanichkarn, P., Juntongjin, K., Yoshida, T., Furihata, K., Nojiri, H., Yamane, H., Omori, T. (2000). Identification of novel metabolites in the degradation of phenanthrene by *Sphingomonas* sp. strain P2. *FEMS Microbiology Letters*, 191(1), 115-121.
- Prescott, L. M., Harley, J., Klein, D. (2005). Microbiology, 6th. *McGrawHill Higher Education*.
- Rabaey, K., Verstraete, W. (2005). Microbial fuel cells: novel biotechnology for energy generation. *TRENDS in Biotechnology*, 23(6), 291-298.
- Rebello, S., Asok, A. K., Mundayoor, S., Jisha, M. S. (2014). Surfactants: toxicity, remediation and green surfactants. *Environmental Chemistry Letters*, 12(2), 275-287. doi: 10.1007/s10311-014-0466-2
- Reddy, K. R., Saichek, R. E. (2003). Effect of soil type on electrokinetic removal of phenanthrene using surfactants and cosolvents. *Journal of Environmental Engineering*, 129(4), 336-346.

## Bibliography

- Ripley, M., Harrison, A., Betts, W., Dart, R. (2002). Mechanisms for enhanced biodegradation of petroleum hydrocarbons by a microbe - colonized gas-liquid foam. *Journal of applied microbiology*, 92(1), 22-31.
- Ripley, M. B., Harrison, A. B., Betts, W. B., Dart, R. K. (2002). Mechanisms for enhanced biodegradation of petroleum hydrocarbons by a microbe-colonized gas-liquid foam. *Journal of Applied Microbiology*, 92, 22-31.
- Ripley, M. B., Harrison, A. B., Betts, W. B., Dart, R. K., Wilson, A. J. (2000). Enhanced degradation of a model oil compound in soil using a liquid foam-microbe formulation. *Environmental science & technology*, 34(3), 489-496.
- Romantschuk, M., Sarand, I., Pet änen, T., Peltola, R., Jonsson-Vihanne, M., Koivula, T., Yrj ä ä K., Haahtela, K. (2000). Means to improve the effect of in situ bioremediation of contaminated soil: an overview of novel approaches. *Environmental pollution*, 107(2), 179-185.
- Ron, E. Z. (2007). Biosensing environmental pollution. *Current Opinion in Biotechnology*, 18(3), 252-256.
- Rosenberg, M. (1984). Bacterial adherence to hydrocarbons: a useful technique for studying cell surface hydrophobicity. *FEMS Microbiology Letters*, 22(3), 289-295.
- Rothmel, R. K., Peters, R. W., St. Martin, E., DeFlaun, M. F. (1998). Surfactant foam/bioaugmentation technology for in situ treatment of TCE-DNAPLs. *Environmental science & technology*, 32(11), 1667-1675.
- Roy, D., Kommalapati, R. R., Valsaraj, K. T., Constant, W. D. (1995). Soil flushing of residual transmission fluid: application of colloidal gas aphron suspensions and conventional surfactant solutions. *Water Research*, 29(2), 589-595.
- Roy, D., Kongara, S., Valsaraj, K. T. (1995). Application of surfactant solutions and colloidal gas aphron suspensions in flushing naphthalene from a contaminated soil matrix. *Journal of hazardous materials*, 42(3), 247-263.
- Roy, D., Valsaraj, K., Constant, W., Darji, M. (1994). Removal of hazardous oily waste from a soil matrix using surfactants and colloidal gas aphron suspensions under different flow conditions. *Journal of hazardous materials*, 38(1), 127-144.
- Sakthivadivel, R. (1968). Theory and mechanism of filtration of non-colloidal fines through a porous medium.
- Sakthivadivel, R. (1969). *Clogging of a granular porous medium by sediment*: Hydraulic Engineering Laboratory, College of Engineering, University of California.
- Save, S. V., Pangarkar, V. G. (1994). Characterisation of colloidal gas aphrons. *Chemical Engineering Communications*, 127(1), 35-54.
- Scullion, J. (2006). Remediating polluted soils. *Naturwissenschaften*, 93(2), 51-65.
- Sebba, F. (1971). Microfoams—an unexploited colloid system. *Journal of Colloid and Interface Science*, 35(4), 643-646.
- Sebba, F. (1985). Separations using aphrons. *Separation and Purification Methods*, 14(1), 127-148.
- Sebba, F. (1987). *Foams and biliquid foams-aphrons*: Wiley New York.
- Semple, K. T., Doick, K. J., Jones, K. C., Burauel, P., Craven, A., Harms, H. (2004). Peer reviewed: defining bioavailability and bioaccessibility of contaminated soil and sediment is complicated: ACS Publications.
- Semple, K. T., Doick, K. J., Wick, L. Y., Harms, H. (2007). Microbial interactions with organic contaminants in soil: definitions, processes and measurement. *Environmental pollution*, 150(1), 166-176.
- Shaner, N. C., Steinbach, P. A., Tsien, R. Y. (2005). A guide to choosing fluorescent proteins. *Nature methods*, 2(12), 905-909.
- Sharma, P., Hanumantha Rao, K. (2002). Analysis of different approaches for evaluation of surface energy of microbial cells by contact angle goniometry. *Advances in colloid and interface science*, 98(3), 341-463.

## Bibliography

- Shen, X., Zhao, L., Ding, Y., Liu, B., Zeng, H., Zhong, L., Li, X. (2011). Foam, a promising vehicle to deliver nanoparticles for vadose zone remediation. *Journal of hazardous materials*, 186(2), 1773-1780.
- Shin, K.-H., Kim, K.-W., Kim, J.-Y., Lee, K.-E., Han, S.-S. (2008). Rhamnolipid morphology and phenanthrene solubility at different pH values. *Journal of Environmental Quality*, 37(2), 509-514.
- Shin, K. H., Kim, K. W., Seagren, E. A. (2004). Combined effects of pH and biosurfactant addition on solubilization and biodegradation of phenanthrene. *Applied microbiology and biotechnology*, 65(3), 336-343. doi: DOI 10.1007/s00253-004-1561-2
- Singh, A., Ward, O. P. (2004). Biotechnology and bioremediation—an overview *Biodegradation and Bioremediation* (pp. 1-17): Springer.
- Skorokhod, V., Get'man, O., Zuev, A., Rakitin, S. (1988). Correlation between the particle size, pore size, and porous structure of sintered tungsten. *Soviet powder metallurgy and metal ceramics*, 27(12), 941-947.
- Soberón-Chávez, G., Lépine, F., Déziel, E. (2005). Production of rhamnolipids by *Pseudomonas aeruginosa*. *Applied microbiology and biotechnology*, 68(6), 718-725.
- Spasojević, J. M., Maletić, S. P., Rončević, S. D., Radnović, D. V., Čučak, D. I., Tričković, J. S., Dalmacija, B. D. (2015). Using chemical desorption of PAHs from sediment to model biodegradation during bioavailability assessment. *Journal of hazardous materials*, 283, 60-69.
- Stringfellow, W. T., Aitken, M. D. (1995). Competitive metabolism of naphthalene, methylnaphthalenes, and fluorene by phenanthrene-degrading pseudomonads. *Applied and environmental microbiology*, 61(1), 357-362.
- Stringfellow, W. T., Alvarez-Cohen, L. (1999). Evaluating the relationship between the sorption of PAHs to bacterial biomass and biodegradation. *Water Research*, 33(11), 2535-2544.
- Su, Y., Zhao, Y. S., Li, L. L., Qin, C. Y., Wu, F., Geng, N. N., Lei, J. S. (2014). Transport characteristics of nanoscale zero-valent iron carried by three different “vehicles” in porous media. *Journal of Environmental Science and Health, Part A*, 49(14), 1639-1652.
- Subramani, A., Hoek, E. M. (2008). Direct observation of initial microbial deposition onto reverse osmosis and nanofiltration membranes. *Journal of Membrane Science*, 319(1), 111-125.
- Subramaniam, M. B., Blakebrough, N., Hashim, M. A. (1990). Clarification of suspensions by colloidal gas aphrons. *Journal of Chemical Technology and Biotechnology*, 48(1), 41-60.
- Tai, D. C., Hooks, D. A., Harvey, J. D., Smaill, B. H., Soeller, C. (2007). Illumination and fluorescence collection volumes for fiber optic probes in tissue. *Journal of biomedical optics*, 12(3), 034033.
- Thévenot, D. R., Toth, K., Durst, R. A., Wilson, G. S. (2001). Electrochemical biosensors: recommended definitions and classification. *Biosensors and Bioelectronics*, 16(1), 121-131.
- Tian, L., Ma, P., Zhong, J.-J. (2003). Impact of the presence of salicylate or glucose on enzyme activity and phenanthrene degradation by *Pseudomonas mendocina*. *Process Biochemistry*, 38(8), 1125-1132.
- Tiehm, A. (1994). Degradation of polycyclic aromatic hydrocarbons in the presence of synthetic surfactants. *Applied and environmental microbiology*, 60(1), 258-263.
- Tong, M., Long, G., Jiang, X., Kim, H. N. (2010). Contribution of extracellular polymeric substances on representative gram negative and gram positive bacterial deposition in porous media. *Environmental science & technology*, 44(7), 2393-2399.
- Trzesicka-Mlynarz, D., Ward, O. (1995). Degradation of polycyclic aromatic hydrocarbons (PAHs) by a mixed culture and its component pure cultures, obtained from PAH-contaminated soil. *Canadian journal of microbiology*, 41(6), 470-476.
- Tsuneda, S., Aikawa, H., Hayashi, H., Yuasa, A., Hirata, A. (2003). Extracellular polymeric substances responsible for bacterial adhesion onto solid surface. *FEMS Microbiology Letters*, 223(2), 287-292.
- Unc, A., Goss, M. J. (2003). Movement of faecal bacteria through the vadose zone. *Water, Air, & Soil Pollution*, 149(1), 327-337.

## Bibliography

- Urgun-Demirtas, M., Stark, B., Pagilla, K. (2006). Use of genetically engineered microorganisms (GEMs) for the bioremediation of contaminants. *Critical reviews in biotechnology*, 26(3), 145-164.
- USACE. (1997). *USACE Engineering Manual: In situ Air Sparging*. EM 1110-4005.
- Ussawarujikulchai, A., Laha, S., Tansel, B. (2008). Synergistic Effects of Organic Contaminants and Soil Organic Matter on the Soil-Water Partitioning and Effectiveness of a Nonionic Surfactant (Triton X-100). *Bioremediation Journal*, 12(2), 88-97.
- Van der Mei, H., Bos, R., Busscher, H. (1998). A reference guide to microbial cell surface hydrophobicity based on contact angles. *Colloids and Surfaces B: Biointerfaces*, 11(4), 213-221.
- Van Genuchten, M. T., Alves, W. (1982). Analytical solutions of the one-dimensional convective-dispersive solute transport equation. *Technical Bulletin No. 1661*, 2-3.
- Van Genuchten, T., ALVES, W. J. (1982). Analytical Solutions of the Convective-dispersive Solute Transport Equation. . *U.S. Department of Agriculture, Technical Bulletin No. 1601*.
- Van Hamme, J. D. (2004). Bioavailability and Biodegradation of Organic Pollutants—A Microbial Perspective *Biodegradation and Bioremediation* (pp. 37-56): Springer.
- van Loosdrecht, M. C., Lyklema, J., Norde, W., Zehnder, A. J. (1989). Bacterial adhesion: a physicochemical approach. *Microbial Ecology*, 17(1), 1-15.
- Van Oss, C. (1995). Hydrophobicity of biosurfaces—origin, quantitative determination and interaction energies. *Colloids and Surfaces B: Biointerfaces*, 5(3), 91-110.
- Van Oss, C., Good, R., Chaudhury, M. (1986). The role of van der Waals forces and hydrogen bonds in “hydrophobic interactions” between biopolymers and low energy surfaces. *Journal of Colloid and Interface Science*, 111(2), 378-390.
- Van Oss, C. J. (2006). *Interfacial forces in aqueous media*: CRC press.
- Vidali, M. (2001). Bioremediation. An overview. *Pure and Applied Chemistry*, 73(7), 1163-1172.
- Volkering, F., Breure, A. M., van Andel, J. G., Rulkens, W. H. (1995). Influence of nonionic surfactants on bioavailability and biodegradation of polycyclic aromatic hydrocarbons. *Applied and environmental microbiology*, 61(5), 1699-1705.
- Vu, K., Yang, G., Wang, B., Tawfiq, K., Chen, G. (2015). Bacterial interactions and transport in geological formation of alumino-silica clays. *Colloids and Surfaces B: Biointerfaces*, 125, 45-50.
- Wan, J., Veerapaneni, S., Gadelle, F., Tokunaga, T. K. (2001). Generation of stable microbubbles and their transport through porous media. *Water Resources Research*, 37(5), 1173-1182.
- Wan, J., Wilson, J. L. (1994). Visualization of the role of the gas - water interface on the fate and transport of colloids in porous media. *Water Resources Research*, 30(1), 11-23.
- Wan, J., Wilson, J. L., Kieft, T. L. (1994). Influence of the gas-water interface on transport of microorganisms through unsaturated porous media. *Applied and environmental microbiology*, 60(2), 509-516.
- Wang, Y., Tian, Z., Zhu, H., Cheng, Z., Kang, M., Luo, C., Li, J., Zhang, G. (2012). Polycyclic aromatic hydrocarbons (PAHs) in soils and vegetation near an e-waste recycling site in South China: concentration, distribution, source, and risk assessment. *Science of the Total Environment*, 439, 187-193.
- Werway, E., Overbeek, J. T. G. (1948). *Theory of Stability of Lyophobic Colloids* Elsevier. Amsterdam-New York, 34.
- Xiao-Hong, P., Xin-Hua, Z., Shi-Mei, W., Yu-Suo, L., Li-Xiang, Z. (2010). Effects of a biosurfactant and a synthetic surfactant on phenanthrene degradation by a *Sphingomonas* strain. *Pedosphere*, 20(6), 771-779.
- Yagi, K. (2007). Applications of whole-cell bacterial sensors in biotechnology and environmental science. *Applied microbiology and biotechnology*, 73(6), 1251-1258.
- Yang, H.-Y., Jia, R.-B., Chen, B., Li, L. (2014). Degradation of recalcitrant aliphatic and aromatic hydrocarbons by a dioxin-degrader *Rhodococcus* sp. strain p52. *Environmental Science and Pollution Research*, 21(18), 11086-11093.

## Bibliography

- Yolcubal, I., Piatt, J. J., Pierce, S. A., Brusseau, M. L., Maier, R. M. (2000). Fiber optic detection of in situ *lux* reporter gene activity in porous media: system design and performance. *Analytica chimica acta*, 422(2), 121-130.
- Yuan, X., Ren, F., Zeng, G., Zhong, H., Fu, H., Liu, J., Xu, X. (2007). Adsorption of surfactants on a *Pseudomonas aeruginosa* strain and the effect on cell surface hydrophobic property. *Applied microbiology and biotechnology*, 76(5), 1189-1198.
- Zhang, Y., Maier, W. J., Miller, R. M. (1997). Effect of rhamnolipids on the dissolution, bioavailability, and biodegradation of phenanthrene. *Environmental science & technology*, 31(8), 2211-2217.
- Zhang, Y., Miller, R. M. (1992). Enhanced octadecane dispersion and biodegradation by a *Pseudomonas* rhamnolipid surfactant (biosurfactant). *Applied and environmental microbiology*, 58(10), 3276-3282.
- Zhao, H.-P., Wu, Q.-S., Wang, L., Zhao, X.-T., Gao, H.-W. (2009). Degradation of phenanthrene by bacterial strain isolated from soil in oil refinery fields in Shanghai China. *Journal of hazardous materials*, 164(2), 863-869.
- Zhong, H., Liu, G., Jiang, Y., Brusseau, M. L., Liu, Z., Liu, Y., Zeng, G. (2016). Effect of low-concentration rhamnolipid on transport of *Pseudomonas aeruginosa* ATCC 9027 in an ideal porous medium with hydrophilic or hydrophobic surfaces. *Colloids and Surfaces B: Biointerfaces*, 139, 244-248.
- Zhu, S., Liang, S., You, X. (2013). *Effect of Rhamnolipid Biosurfactant on Solubilization and Biodegradation of Polycyclic Aromatic Hydrocarbons*. Paper presented at the Proceedings of the 2013 Third International Conference on Intelligent System Design and Engineering Applications.